

bromide has been found to work well in an iron reactive medium when a retardation factor of 1.2 is incorporated (Sivavec, 1996). During preliminary site characterization, the levels of tracer in the native groundwater should be measured. Elevated levels in the native groundwater would make the tracer test more difficult, because a larger concentration of injected tracer would be required. At high concentrations, the tracer may be subject to a density gradient as it travels through the aquifer or reactive cell. The resulting path of the tracer, then, may not be the same as that of the natural groundwater. One advantage of a tracer (such as bromide) is its ability to be continuously monitored using downhole, ion-selective electrodes. Continuous monitoring with such probes increases the probability of capturing the tracer peak and reduces labor costs. Ion-selective probes are expensive, but their cost could be justified by reduced labor requirements and increased chances of success. Field application of tracer tests for evaluating PRBs has not been very successful in the past for a variety of reasons (Focht et al., 1997). In particular, difficulties in ensuring the success of tracer tests occur as a result of the high cost involved in obtaining adequate sampling density (number of monitoring wells and frequency of sampling) and of the limitations of monitoring instruments. However, tracer tests within the PRB are more likely to be successful than those conducted in the aquifer for capture zone delineation, because the possible flowpaths in the PRB are relatively constrained by sheet piled on two sides.

An example tracer test in a PRB took place at the former NAS Moffett Field PRB site (Battelle, 1998). In this case, tracer was injected in a well in the upgradient pea gravel zone. It was observed that the tracer spreads laterally within the pretreatment zone before moving into the reactive zone (Figure 8-7), because the conductivity of the pea gravel in the pretreatment zone was greater than that of the reactive media. At this site, the tracer test showed that the flow was moving in the expected downgradient direction. It also showed that the actual flow through the reactive cell was highly heterogeneous. However, despite very extensive monitoring, it was not possible to achieve an acceptable mass balance for the tracer. Therefore, the presence of other pathways for flow could not be ruled out. Other examples of tracer testing for performance assessment at PRB sites are presented in Piana et al. (1999) for Fry Canyon, UT, and Devlin and Barker (1999) for monitoring of flushing through a PRB at the Borden site in Ontario, Canada.

8.3 Geochemical Performance Monitoring Strategy

Generally, monitoring the geochemical performance of a PRB is a secondary consideration, with contaminant degradation and hydraulic performance being the key short-term concerns. In the long term, however, site managers may want to evaluate how long the reactive medium will continue to provide the desired performance. Also, site managers may wish to determine how well the field PRB system matches the predictions of the geochemical evaluation done during the design stage (based on site characterization and column test information as described in Section 6.4).

There are three main methods available for monitoring the geochemistry of the PRB, and these range in cost and complexity:

- ❑ Groundwater monitoring for inorganic species
- ❑ Geochemical modeling
- ❑ Core extraction and analysis.

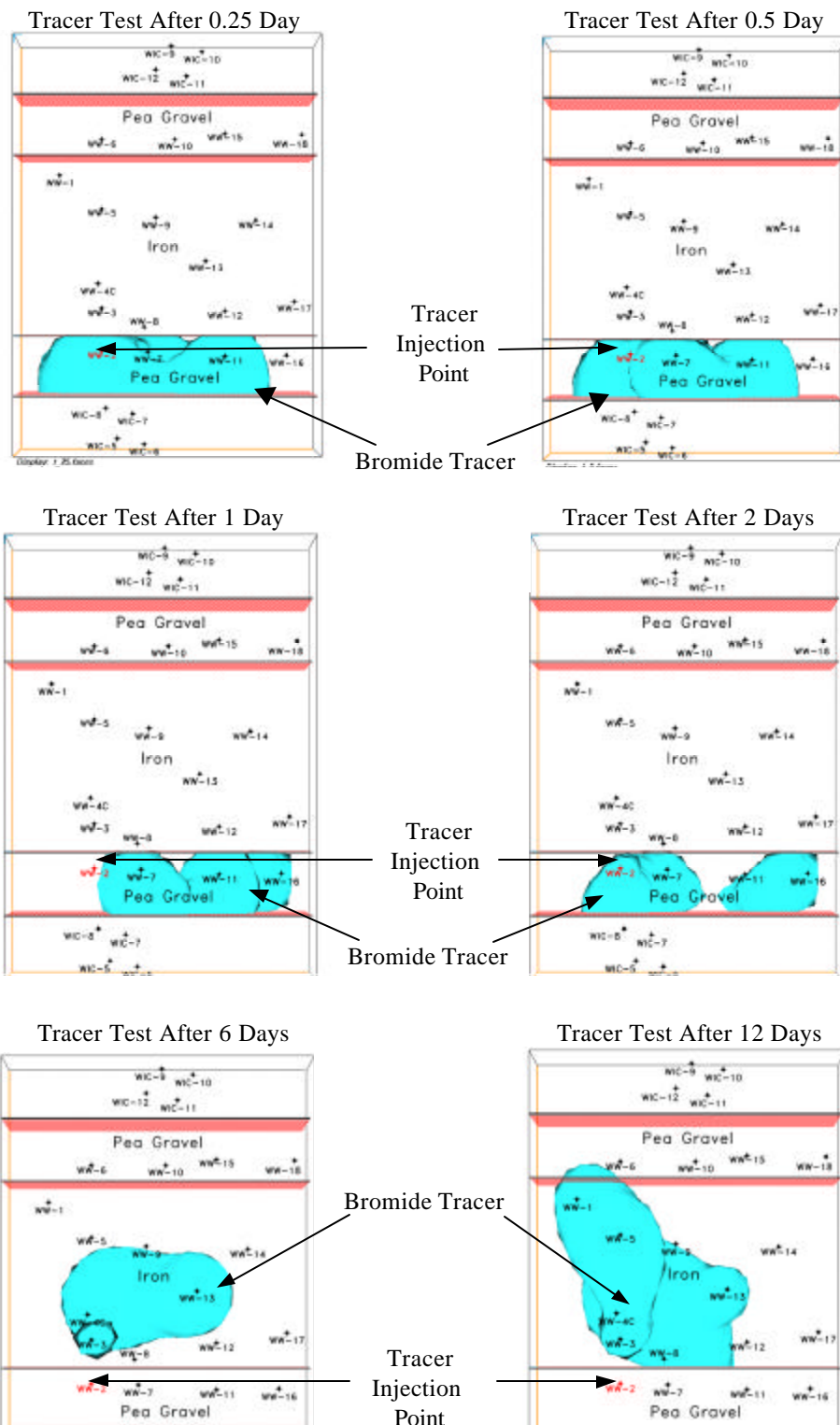


Figure 8-7. Movement of Bromide Tracer Plume through the PRB at Former NAS Moffett Field (Battelle, 1998)

Monitoring groundwater within the PRB for inorganic species is essential for understanding geochemical conditions and is a prerequisite for geochemical modeling. Inorganic analysis need not be performed as often as VOC sampling, but a comprehensive round of analyses could be done every one to two years. At this frequency of data collection it should be possible to detect any significant changes taking place within the barrier and have sufficient time to correct them before the barrier fails to meet compliance requirements. Generally, groundwater monitoring and data analysis is sufficient at most sites for evaluating geochemical interactions. Geochemical modeling and reactive medium core collection and analysis are specialized methods that could be undertaken for technology development purposes or for more detailed evaluation of the site geochemistry, if groundwater monitoring reveals any unusual patterns that could affect PRB performance.

Geochemical modeling requires high-quality measurements of field parameters and elemental concentrations that typically would be obtained during groundwater monitoring. Reliance on raw groundwater data alone is limited in two ways. First, subtle changes in groundwater chemistry may be overlooked in raw data; and second, there is no reference with which to compare raw data. However, with geochemical monitoring, subtle changes in groundwater chemistry may be more apparent in the modeling results; also, geochemical modeling results can be compared to theoretical equilibrium calculations, which would provide an important reference point for understanding the geochemical system through the monitoring data. It is important to note that the input data must include all parameters that relate to interactions in the barrier for geochemical modeling to produce meaningful results.

Finally, core sampling of the iron and surrounding media offers a direct way to observe geochemical behavior within these media. Core sampling is much more invasive than groundwater sampling and should only be performed at critical times. For example, if the performance of the barrier has degraded over time and this behavior seems to be related to either hydraulic factors (e.g., plume bypass) or a decline in reactivity (e.g., plume breakthrough), core sampling could provide important information about conditions within the barrier. If an opportunity arises to take core samples at an earlier stage (i.e., before any threat to the performance of the barrier is detected), the analysis data could serve as a baseline with which to compare observations at a later date. In addition, it is also a good idea to save some of the unused iron for comparison with core samples collected at a later time. The unused iron should be stored in an airtight container, preferably inside a desiccator.

8.3.1 Evaluating Geochemical Performance with Groundwater Monitoring

To monitor the processes taking place within a barrier, the following geochemical information should be collected on a routine basis (monitoring events could be incorporated into the compliance monitoring schedule):

- ❑ On-site field parameter measurements
- ❑ Inorganic chemical analysis of groundwater samples.

The primary purpose of taking field parameter measurements and analyzing groundwater samples for inorganic constituents is to ensure that the PRB maintains its ability to degrade halogenated contaminants or immobilize target metals. Another purpose may be to confirm that DO

is being scrubbed within a pretreatment zone, so that water entering the reactive cell is anoxic. On-site field parameter measurements should be used to track parameters such as DO, ORP, pH, conductivity, and temperature. Typical levels of DO in an aerobic aquifer can be measured using a DO probe. Usually, DO probes are effective when oxygen levels are between 0.5 mg/L and saturation (about 8 mg/L). They tend to give spurious readings when oxygen levels are below 0.5 mg/L and therefore are not suitable for measuring conditions within the reactive cell.

The strength of the reducing environment inside a reactive cell must be measured using a combination or pair of electrodes, consisting of a working electrode (usually a platinum wire) and a reference electrode (typically a AgCl/Ag cell). A more universal expression of ORP is the Eh, which refers to the standard hydrogen electrode (SHE) as the reference potential. ORP is easily converted to Eh by subtracting the reference cell potential. Redox measurements are often expressed in volt (V) or millivolt (mV) units. Another scale that can be used is the pe scale, which is related by $pe = Eh \text{ (mV)} / 59.2$ at 25°C. Thus, for both scales, a zero value refers to the same potential, and the signs stay the same. ORP, Eh, and pe become more negative in reducing environments and more positive in oxidizing environments. Because other factors, including pH, affect redox measurements, there are no absolute values that indicate oxidizing or reducing conditions only, or serve as a divider between the two.

In most situations, field parameter measurements can be taken using probes that are either configured for downhole submersion or coupled to a flowthrough cell for aboveground use. Whichever type is used, it is important to record the readings after the probe has stabilized. Also, the water inside the probes must be protected against contact with ambient air, particularly so that DO and ORP readings are not biased. Downhole probes more easily assure that air contamination does not occur.

If all groundwater sampling is to be conducted during one event, the samples for volatile organic analytes should be collected before those for inorganic analytes in order to obtain the most representative samples for VOC analysis, as explained in Section 8.1.2. It is preferable to collect all samples for VOCs first, and then repeat the sampling schedule to collect samples for inorganic analysis. Analytical laboratories require different containers and preservation methods for metals and anion analysis. Recommended inorganic analytical requirements for groundwater samples are given in Table 8-1. Added to the list would be any substances that are either treated by the barrier (such as Cr), or substances that may have some indirect effect on the barrier (such as high concentrations of phosphate). Samples for metals analysis should be filtered in the field using 0.45- μm or smaller pore-size membranes immediately after collection. Filtering helps to exclude colloidal material and suspended iron fines from being collected with the water sample, which would be subsequently acid-digested and analyzed. Elimination of colloidal material from the sample is necessary because only the concentrations of dissolved species rather than total metals have bearing on mineral precipitation. Iron and manganese are the most problematic metals to analyze, due to their tendencies to absorb onto colloidal material. If turbidity is very low, it may not be necessary to filter for main group metals, such as Na, K, Mg, and Ca. However, it is advisable to verify whether filtering should take place by taking filtered and unfiltered samples during one event and comparing the results. If metal concentrations are significantly higher in the unfiltered samples, then filtering should be considered necessary.

Table 8-1. Recommended Inorganic Analytical Requirements for Groundwater Samples

Analytes	Analysis Method	Sample Volume	Storage Container	Preservation Method	Sample Holding Time
<i>Cations</i>					
Na, Ca, Mg, Fe, and Mn	EPA 200.7	100 mL	Polyethylene	Filter, 4°C, pH<2 (HNO ₃)	180 days
<i>Anions</i>					
NO ₃ , SO ₄ , and Cl	EPA 300.0	100 mL	Polyethylene	4°C	28 days ^(a)
Alkalinity	EPA 310.1	100 mL	Polyethylene	4°C	14 days ^(b)
<i>Neutrals</i>					
Dissolved silica	EPA 6010	250 mL	Polyethylene	None	28 days
TDS	EPA 160.1	100 mL	Polyethylene	4°C	7 days

(a) Holding time for nitrate is 48 hours when unpreserved; holding time can be extended to 28 days when preserved with sulfuric acid.

(b) Determination of alkalinity in the field using a titration method is preferred whenever there is concern over precipitation in the sample container during storage.

In addition, anions including nitrate, sulfate, chloride, and alkalinity should be analyzed because of their electroactivity (nitrate and sulfate), potential for precipitation (alkalinity and sulfide), and conservative reference (chloride). Other analytes that should be measured include dissolved silica, because of concern over iron passivation, and TDS, which can be correlated with conductivity and helps confirm that all major dissolved species have been analyzed.

Ionic charge balance should be calculated to provide a measure of inorganic data quality independent of routine analytical quality assurance/quality control (QA/QC). Charge balance is calculated as the percent difference in cation and anion milliequivalents (meq), as shown in the following equation:

$$\text{Charge balance} = 100 \times \frac{\text{meq cations} - \text{meq anions}}{\text{meq cations} + \text{meq anions}} \quad (8-1)$$

Electrolyte solutions are electrically neutral, so any charge balance calculated to be more or less than zero represents cumulative errors in analysis of the ionic species. Solutions that are within 10% cation-anion balance are considered adequately balanced for subsequent uses such as geochemical modeling. Figure 8-8 shows charge balance results from sampling at Dover AFB in June 1999. In this figure, the data are distributed near the charge balance line (heavy line), and most points fall within the $\pm 10\%$ envelope. This figure also illustrates that water in Gate 2 had a higher ionic concentration than water in Gate 1.

Analysis of the groundwater monitoring data is similar to the evaluation of inorganic parameter data from column tests, as described in Section 6.4.2. In addition to conducting a qualitative evaluation of the types of precipitates that may be expected, a quantitative evaluation can be conducted by comparing the groundwater influent and effluent levels of inorganic parameters (e.g., Ca, Mg, and alkalinity). Tables 6-2 and 6-3 in Section 6.4 show how differences between the influent and effluent concentrations can be used to estimate the groundwater losses of these

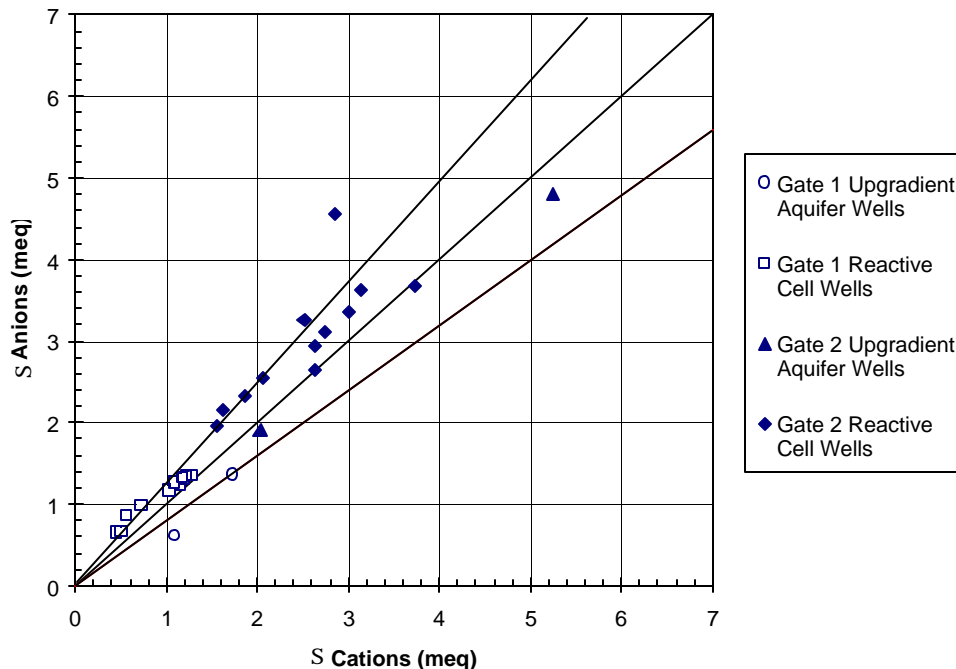


Figure 8-8. Ionic Charge Balance for Selected Wells at the PRB at Dover AFB (June 1999)

parameters due to precipitation. However, as also mentioned in that section, the difficulty in linking groundwater losses of these constituents to any losses in the reactive and hydraulic performance of the PRB lies with the inability to link mass of precipitate to loss of reactive surface sites. Currently, it is unclear how these precipitates account for a loss in reactive sites on the reactive medium. For example, if the precipitates form a thin mono-layer on the reactive medium surface, very little precipitate mass may be needed to consume all available reactive sites; on the other hand, it is not clear whether or not the precipitates occupy the same reactive sites as the contaminants. Also, if the precipitates either tend to form multiple layers on the reactive medium surface, settle in bulk at the bottom of the reactive cell, or are transported out of the reactive cell as colloidal particles, the PRB could sustain a considerable mass of precipitate before reactive and/or hydraulic performance starts declining. Evaluating the longevity of a PRB is an area requiring further research, especially given its potential influence on PRB performance and economics.

8.3.2 Evaluating Geochemical Performance with Geochemical Modeling

Geochemical modeling can be used to simulate reactions between a native groundwater and the reactive medium, such as iron. This modeling can be useful for understanding the mechanisms of various kinds of precipitates that can form. Two types of computer models are commonly used for this purpose: equilibrium models and inverse models. Both are described in Appendix D and contain examples from PRB sites.

8.3.3 Evaluating Geochemical Performance with Reactive Medium Core Sampling

Reactive medium core sampling and analysis are specialized techniques that may not be required at most PRB field sites. However, core analysis provides important geochemical information for

evaluating the longevity of the reactive medium. If problems with field PRB performance relating either to hydraulics or to degradation of contaminants of concern are detected, it may be desirable to investigate the cause by examining the reactive medium directly. This can be done by collecting core samples of the reactive medium and analyzing them for the following:

- ❑ Evidence of chemical and mineralogical changes
- ❑ Signs of any unusual microbial activity (aquifer soil samples should be analyzed too).

When performing core sampling, possible changes in the reactive medium near the interfaces with the adjoining sections are of particular interest, because these interfacial regions are the places where plugging could be most pronounced. The upgradient interface also is very important because this is where the most sudden change in chemical environments occurs. To examine these interfaces, vertical core samples of medium should be taken as close as possible to the adjoining upgradient section (i.e., pea gravel or aquifer). If possible, angled cores also should be placed into the upgradient interface of the medium. Vertical cores are easily taken by various kinds of direct push equipment. Taking angled cores, on the other hand, requires more versatile equipment. Angled cores can be very useful because they expose greater surface area and can cut across the interface of the medium and aquifer or pretreatment zone. Core samples of granular iron medium have been collected from some existing PRBs and examined for signs of the corrosion and precipitation as predicted by the groundwater analysis and geochemical modeling. Figure 8-9 shows a vertical core being extracted at the Dover AFB PRB site, and Figure 8-10 shows an angled core being taken at the former NAS Moffett Field PRB.

Coring locations should be chosen to provide specimens over a large area of the permeable barrier and also to include aquifer samples both upgradient and downgradient of the permeable barrier for microbiological analysis. However, precedence should be given to the upgradient



Figure 8-9. Core Sampler Extracting Vertical Core at Dover AFB



Figure 8-10. Enviro-Core™ Sampler Extracting Angled Core at Former NAS Moffett Field

portion of the reactive cell, where more precipitation is likely to occur. At least three cores should be taken in the reactive cell so that spatial information about the iron is available.

The sampler itself should be designed for coring at discrete depth intervals, so that depth information can be incorporated into the analysis. Core barrels are typically fitted with several short (6-inch-long) stainless steel or brass sleeves, or one long clear plastic sleeve. Multiple sleeves allow shipment of samples from a comparable depth interval to be shipped to various locations without the need for sub-sampling.

After sample sleeves are removed from the core barrel, the sleeves should be fitted with tight-fitting plastic caps to contain the sample and restrict air. It is important to minimize air contact with the samples after they are collected. Several storage approaches have been reported in the literature, as summarized in Table 8-2. The approach used at Dover AFB and former Lowry AFB has been to place the sample sleeves into Tedlar™ bags that contain packets of oxygen scavenging material, as shown in Figure 8-11. The bags then are purged with nitrogen gas, as shown in Figure 8-12, and refrigerated until they are shipped to an analytical laboratory. Samples for microbiological analysis should be shipped in an airtight container to the designated laboratory. Samples for inorganic analysis should be vacuum-dried using a vacuum oven without heat. Core samples then should be placed in a nitrogen-filled chamber for sub-sampling and storage until needed.

Table 8-2. Survey of Core Sampling and Preparation Methods

Location	Sampling/Drilling^(a)	Storage/Shipping^(a)	Sample Processing^(a)
Former NAS Moffett Field, CA; and former Lowry AFB, CO	<p>Enviro-core dual-tube sampling, vibrated into the ground. Poor core recovery at former Lowry AFB (with a “catcher.”)</p> <p>Polybutyrate liners used initially because they were denser; currently use three 6-inch-long stainless steel sleeves inside 18-inch-long barrel. Obtain three subsamples per barrel. Sleeves are placed in a Tedlar™ bag that has previously been purged with inert gas. Oxygen scrubber is put on the bag. Samples are shipped cold.</p> <p>Interface between reactive iron and pea gravel difficult to distinguish due to clogging of the sampling system when the pea gravel was encountered.</p>	Refrigerated immediately and shipped on blue ice to an off-site laboratory where samples were placed in a glove box and purged with ultrapure nitrogen.	<p>Sleeves were transferred to a heated vacuum dessicator. The tape was removed but it was unnecessary to remove the caps. Vacuum drying was conducted at 125°F and required up to 72 hrs. Core samples then were returned to the glove box.</p> <p>Sleeve end caps were removed from the dried core while inside the nitrogen glove box and 1 inch of material on each end was discarded. The remaining sample was put into glass jars and mixed to homogenize. Subsamples were prepared in small glass vials and sealed in nitrogen.</p>
Dover AFB	A direct-push CPT sampler was used for vertical core collection. Three 6-inch-long stainless steel sleeves were fitted into the core barrel for each push. Recovery of iron was less than 50%.	Refrigerated immediately and shipped on blue ice to an off-site laboratory where samples were placed in a glove box and purged with ultrapure nitrogen.	<p>Sleeves were transferred to a heated vacuum dessicator. The tape was removed but it was unnecessary to remove the caps. Vacuum drying was conducted at 125°F and required up to 72 hrs. Core samples then were returned to the glove box.</p> <p>Sleeve end caps were removed from the dried core while inside the nitrogen glove box and 1 inch of material on each end was discarded. The remaining sample was put into glass jars and mixed to homogenize. Subsamples were prepared in small glass vials and sealed in nitrogen.</p>
Somersworth landfill site, NH	Geoprobe® was used; there was a problem of pea gravel mixing with the Fe and biasing carbonate results.	<p>Shipped on ice</p> <p>Shipped overnight</p>	<p>XRD and SEM/EDS performed. Iron grains were gently washed with nitrogen-purged acetone in a nitrogen glove box. Grains were filtered, washed repeatedly with additional acetone, and then vacuum-dried in a dessicator.^(b)</p> <p>A single acetone rinse is insufficient, multiple rinses are needed.</p>

Table 8-2. Survey of Core Sampling and Preparation Methods (Continued)

Location	Sampling/Drilling	Storage/Shipping	Sample Processing
ORNL, TN	Geoprobe [®] used for angle coring, samples collected in polyurethane tubes. Attempted to obtain 4 ft samples but only retrieved ~2 ft because of compaction and spillage.	After removal, cores purged with argon and sealed with rubber stoppers. During the period between sampling and preparation (2-3 weeks), the storage tubes were purged with nitrogen twice per week. Other samples preserved with acetone.	Representative samples were washed with acetone prior to mineralogical analysis. Remainder of sample was air-dried, ground and mixed.
Kansas City Plant, KS; and Fry Canyon, UT	Geoprobe [®] used for angle coring, samples collected in PTEG sleeves. No problems obtaining complete core with intact interface.	After removal, cores purged with argon and sealed with rubber stoppers. During the period between sampling and preparation (2-3 weeks), the storage tubes were purged with nitrogen twice per week. Other samples preserved with acetone.	Kansas City Plant: Samples frozen, awaiting processing. Fry Canyon: USGS processing/no information available.
Elizabeth City, NC	Geoprobe [®] used.	Polycarbonate sleeves, cut and seal the sleeves with plastic electrical tape and quick freeze with liquid nitrogen in the field. Ship overnight on dry ice for processing in glove boxes. Also performing acetone treatment in field.	Geochemical analyses: replaced pore water with acetone to eliminate oxidative effects. Microbiology “freeze dry and store” frozen until analysis.
Others	Collected at Kansas City Plant and Fry Canyon sites.	Samples packed in ice with 50% ethanol in one set and a 2% solution of gluteraldehyde (stored anaerobically).	Microbiological analyses only.

(a) Sources: Korte, 1999; Battelle, 1998 and 2000.

(b) Comparison testing demonstrated that vacuum dried samples had additional oxidation relative to samples processed with acetone.

USGS = United States Geological Survey.

Samples should be analyzed by a laboratory that can perform the kinds of analyses recommended in Table 8-3. Many materials science or geology laboratories have instruments for inorganic non-biological analysis. Microbiological samples should be sent to a laboratory equipped to perform heterotrophic plate counts and phospholipid fatty acid (PLFA) profiles of microbial



Table 8-3. Recommended Characterization Techniques for Coring Samples

Analysis Method	Description
Total Carbon Analysis Combustion furnace used to quantify total organic and inorganic (carbonate) carbon	Quantitative determination of total carbon. Useful for determining fraction of carbonates in core profile.
Raman Spectroscopy Confocal imaging Raman microprobe	Semiquantitative characterization of amorphous and crystalline phases. Suitable for identifying iron oxides and hydroxides, sulfides, and carbonates.
Fourier Transform Infrared Spectroscopy (FTIR) FTIR coupled with auto-image microscopy	Attenuated total internal reflection (ATR) spectra were collected using a germanium internal reflection element.
Scanning Electron Microscopy Secondary electron images (SEI) Energy-dispersive spectroscopy (EDS)	High-resolution visual and elemental characterization of amorphous and crystalline phases. Useful for identifying morphology and composition of precipitates and corrosion materials.
X-Ray Diffraction (XRD) Powder diffraction	Qualitative determination of crystalline phases. Useful for identifying minerals such as carbonates, magnetite, and goethite.
Microbiological Analysis Heterotrophic plate count PLFA profiling	Identification of microbial population within the cored material. Useful for determining the presence or absence of iron-oxidizing or sulfate-reducing bacteria.

strains. The main intent of the non-biological analysis is to determine physical and chemical changes that have taken place in the iron due to exposure to site groundwater. The microbiological analysis is intended to determine if microbiological activity is occurring in the iron or downgradient aquifer, because buildup of and fouling by biomass is a potential concern.

9.0 PRB Economics

The potential long-term economic benefit of PRBs has been an important driving force behind the interest in this technology. At sites with groundwater contaminants, such as chlorinated solvents, that could persist for several years or decades, a passive technology (namely, PRB) that has no recurring operating labor or energy requirement beyond quarterly monitoring has a potential long-term cost advantage over a conventional P&T system. Key variables that affect PRB economics are the length of time that a given installed reactive medium will retain its reactive and hydraulic performance and, consequently, the type and frequency of the maintenance required to replace and/or regenerate the reactive medium. Because the PRB technology has undergone field application only in the last five years or so, there is no historical experience or data which can be relied on to make a clear judgement about the longevity of a PRB, and any cost evaluation should take this uncertainty into account.

Because PRB application costs need to be evaluated in the context of a competing technology, PRB and P&T costs are used to illustrate the costs evaluation in this section. Other alternatives to P&T, such as air sparging or bioremediation, also may be used as the competing technology with a similar evaluation approach.

The two main categories of costs for any technology are capital investment and O&M costs. These two categories of costs are addressed in this section for the PRB and P&T technologies. For long-term applications, O&M costs are spread over several years or decades. A PV analysis that takes into account the time value of money is described in this section to evaluate PRB and P&T costs. Finally, the intangible costs and benefits of the competing technologies (both PRB and P&T) are taken into account for a final economic decision on whether to implement a PRB at a given site. Appendix B provides an example of a cost evaluation conducted for a full-scale PRB application for a CVOC plume at Dover AFB, based on a pilot project completed recently (Battelle, 2000). Another useful reference for cost analysis of long-term projects is the document titled "Standard Life-Cycle Cost-Savings Analysis Methodology for Deployment of Innovative Technologies," published by the DOE Office of Environmental Management (DOE, 1998).

The cost evaluation described in this section can be conducted to varying degrees at two stages in the design of a PRB. First, a preliminary cost evaluation may be conducted during the preliminary assessment to determine the suitability of a site for PRB application. This evaluation would compare the cost of a PRB application at the site to the cost of using a competing technology, such as P&T. Although a detailed cost evaluation may not be possible at the preliminary assessment stage, rough estimates for capital investment and O&M costs for the two options (PRB and P&T) may be developed during initial discussions with reactive medium suppliers and construction contractors. This early process of contacting construction contractors also helps to identify the most cost-effective PRB construction technique for a given aquitard depth and other site features involved. If the preliminary cost evaluation turns out to be favorable for the PRB, site managers could proceed to additional site characterization, laboratory testing, modeling and engineering design, and monitoring plan preparation, as described in Section 2.0. Once the draft

design is ready, reactive medium suppliers and construction contractors can be contacted again, this time to obtain detailed cost estimates, and a detailed cost analysis then can be conducted.

At both stages of the cost evaluation, a major uncertainty in the cost evaluation is the longevity of the reactive medium (i.e., the period of time over which the reactive medium can sustain the desired reactive and hydraulic performance). The longevity of the reactive medium determines the frequency at which the reactive medium may need to be regenerated or replaced, and therefore determines the long-term O&M costs of the PRB. In the absence of a reasonably accurate prediction of the longevity of the PRB, the methodology of developing multiple longevity scenarios described in Section 9.3 is suggested. These longevity scenarios indicate the minimum life expectancy of the reactive medium that will make the PRB a cost-effective investment.

9.1 Capital Investment

Capital investment in a technology refers to the funds required to cover the initial non-recurring cost involved in acquiring and installing the technology to the point where it is ready for its intended use. Using the PRB installed at Dover AFB as an example, Table 9-1 illustrates the items that constitute the capital investment in a PRB. The capital investment for installing a PRB includes the following major items:

- ❑ Preconstruction costs
- ❑ Materials and construction costs.

Most sites with PRBs so far have reported materials and construction costs only as the total cost of a PRB, probably because materials and construction costs are easier to identify, track, and estimate than are preconstruction costs. However, preconstruction costs are generally significant enough that they should be considered for the economic evaluation. Appendix B contains an illustration of the capital investment requirements estimated for a PRB at Dover AFB, as well as the capital investment estimated for an equivalent P&T system for comparison. An equivalent P&T system is one capable of capturing the same amount of water as the PRB.

9.1.1 Preconstruction Costs

Preconstruction costs are those incurred for the activities leading up to initiation of PRB construction at the site. This category includes items such as preliminary site assessment, site characterization, laboratory testing, PRB modeling and design, procurement of materials and construction contractors, and regulatory review. Preconstruction costs are not inconsequential and can constitute as much as 50% of the total capital investment in the PRB.

Site characterization is usually the largest component of preconstruction costs, whether for a PRB or a P&T system. Given the fact that the PRB is a more or less permanent structure that is difficult to expand and/or modify, adequate site characterization is all the more important for understanding the local contaminant and groundwater flow features of the site on the scale of the planned PRB. The degree of site characterization required at a site may vary depending on the complexity of the contaminant distribution and/or hydrogeologic environment and on the amount of existing information available from previous RFI or RI/FS studies.

Table 9-1. Illustration for Estimating Capital Investment Based on the Projections for Operating a Full-Scale PRB at Dover AFB

Item	Description	Basis	Cost
<i>Phase 1: Preconstruction Activities</i>			
Preliminary site assessment	Historical site data evaluation	RI/FS, other reports procurement and evaluation; site meeting	\$15,000
Site characterization	Characterization Plan, fieldwork, laboratory analysis	CPT pushes for geologic mapping and temporary wells; analysis of water samples for CVOCs; select samples for geotechnical analysis; slug tests; ground-penetrating radar survey ^(a)	\$200,000
Column tests	Two column tests; Area 5 groundwater	Column tests ^(a) and laboratory analysis of water samples; report	\$50,000
Design, procurement of subcontractors, and regulatory review	Data evaluation, modeling, engineering design, Design Plan; procurement of subcontractors; interactions with regulators	Characterization/column test data evaluation; hydrogeologic modeling; geochemical evaluation; engineering design; report; procurement process; regulatory interactions	\$100,000
Subtotal			\$365,000
<i>Phase 2: PRB Construction Activities</i>			
Site preparation	Utilities clearances; arrangements for equipment/media storage and debris disposal	Coordination with regulators and Base facilities staff	\$10,000
Reactive media procurement	Connelly iron, shipping	Iron: 108 tons @ \$360/ton Shipping: \$9,000	\$48,000
PRB Construction	Mobilization/demobilization; Installation of four 8-ft-diameter caisson gates to 40-ft depth; 120-ft-long sheet pile funnel; asphalt parking lot restoration	Mob./demob.: \$60,000 Gates: \$266,000 Monitoring wells: \$25,000 Funnel: \$102,000 Surface restoration: \$34,000	\$487,000
Monitoring system construction	Thirty-four PVC aquifer wells installed for monitoring the pilot-scale PRB	Aquifer wells: \$37,000	\$37,000
Subtotal			\$582,000
TOTAL			\$947,000

(a) All cost items may not be necessary or applicable at other sites. A lower level of these activities may be sufficient at some sites.

Design and modeling, procurement of materials and construction contractors, and regulatory review are important preconstruction activities that may require some effort and cost. Design and modeling generally include the analysis conducted to interpret the laboratory test data and site characterization data in order to determine the location, orientation, configuration, and dimensions of the PRB.

Selection and procurement of a suitable reactive medium also may require some effort, especially if a medium other than the more common variety of granular iron is used. Procurement of a suitable construction contractor is a key activity that may take a few weeks, especially if

construction techniques other than standard backhoe excavation are needed. Most contractors are capable of conducting backhoe excavation (for the gate or for a continuous reactive barrier) and slurry wall construction (for the funnel, if required). Any other construction technique may involve a limited number of contractors, and extensive review both of different construction options offered by different vendors, and of the technical suitability and cost of these options for a given site. Generally, relatively deep aquifers (more than 30 ft deep) require evaluation of special alternative methods of construction (see Section 7.0). Even for relatively shallow aquifers, new technologies such as the continuous trencher (Section 7.1.4) should be considered as a way of reducing costs, if technically feasible. A site visit should be arranged before receiving final bids to provide interested construction contractors an opportunity to see the site and talk to site personnel. Construction contractors may identify unusual site features (e.g., site access or overhead utilities) that could make construction more difficult and affect the cost of implementing their particular technologies. Once the construction contractor has been selected, a preconstruction meeting generally is required to discuss preparations and arrangements for construction. Site managers have to provide sufficient storage and working space around the PRB location, arrange for traffic diversion during construction, and/or arrange for the disposal of spoils/groundwater removed from the ground during construction.

9.1.2 PRB Materials and Construction Costs

Table 9-1 illustrates the materials and construction components of capital investment required for a PRB. The reactive medium itself can be a significant cost item. The unit cost of the reactive medium depends on the type of medium selected. Granular iron is the cheapest and most well-understood of the currently available reactive metal media, and therefore has been preferred for most PRB applications so far. Although initial field applications are reported to have paid up to \$650/ton for the granular iron, identification of additional sources has reduced the unit cost of iron available to approximately \$300-350/ton. At least three suppliers of granular iron in the desired form are available. If the selected reactive medium is patented, licensing costs may be involved.

The total cost of the reactive medium is driven not only by the unit cost of the reactive metal, but also by the amount of reactive metal required. The amount of reactive metal required depends on the following site-specific factors:

- ❑ **Type and Concentrations of the Chlorinated Contaminants.** Contaminants that have longer half-lives require a larger flowthrough thickness of the reactive cell, and therefore higher cost.
- ❑ **Regulatory Treatment Criteria.** The more stringent the treatment criteria that the PRB has to meet, the greater is the required residence time; and the greater the residence time, the greater is the required thickness of the reactive cell, which increases the cost accordingly.
- ❑ **Groundwater Velocity.** The higher the groundwater velocity, the greater the thickness of the reactive cell required to obtain a certain residence time, which increases the cost accordingly.

- ❑ **Groundwater Flow and Contaminant Distribution.** At sites where the distribution of groundwater flow or contaminants is very heterogeneous, a continuous reactive barrier of uniform thickness and extent can lead to an inefficient use of reactive medium. Construction of the reactive cell in zones of higher permeability or the use of funnel-and-gate configurations and pea gravel-lined cells are some of the ways in which the contaminant loading on the reactive medium may be made more homogeneous. On the other hand, continuous reactive barriers are easier to design and build, and they generate less complex hydraulic flow patterns.

The unit costs of construction depend on the type of technique selected, which, in turn, depends on the depth of the installation. Table 7-1 (in Section 7.0) summarizes the construction techniques available, the maximum depth possible for each technique, and some representative unit costs obtained from several geotechnical contractors. Although some variability in the cost of each technique represents differences in vendors, the range of unit costs is more likely driven by depth. The total cost of construction is based on three main factors:

- ❑ **Plume and Aquifer Depth.** For a given construction technique, the upper part of the cost range generally applies to the greater depths in its range.
- ❑ **Plume Width.** The greater the width of the plume, the wider the PRB is required to be in order to capture it.
- ❑ **Geotechnical Considerations.** The presence of rocks or highly consolidated sediments, underground/overhead utilities, or other structures in the vicinity may make it harder to drive the construction equipment (e.g., sheet piles or caissons) into the ground.

Given the cost difference between the construction techniques for a funnel versus those for a reactive cell in Table 7-1 (Section 7.0), there may be a cost trade-off between selecting a funnel-and-gate system versus a continuous reactive barrier. Disposal of spoils generated during construction is another cost that may vary based on the construction technique selected. For example, construction of slurry walls generates more spoils than does construction of sheet pile barriers. Disposal of spoils could be more costly if the barrier must be located within the plume, in which case the spoils may have to be disposed of as hazardous waste. Restoration of the site surface may include returning it to grade or repaving the surface for built-up sites.

Monitoring wells are a cost component for both PRB and P&T options. The number and distribution of monitoring wells generally is determined by regulatory guidance and the need to collect performance data (see Section 8.0 on monitoring).

9.1.3 Capital Investment for an Equivalent P&T System

The materials and construction components required for a P&T system generally include extraction wells, pumps, piping and instrumentation, an air stripper (for VOCs) or ion exchange unit (for metallic contaminants), a carbon polishing unit for the liquid effluent, and an air treatment unit (if the air discharge from the stripper exceeds local regulatory limits for a point source). In recent years, low-profile (tray type) air strippers have been used as a cheaper and less space-consuming (higher capacity) alternative to bulkier packed towers for VOC treatment. In

general, a P&T system comparable to the PRB described in this subsection would have to capture the same volume of groundwater as the full-scale PRB. Because of possible capture inefficiencies with extraction wells, the P&T system may generally be designed to capture groundwater from an aquifer region larger than the extent of the plume.

9.2 Operating and Maintenance Costs

The O&M costs of a technology are the recurring or periodic costs incurred during the operating life of the system. Using the PRB at Dover AFB as an example, the O&M cost components of a PRB are illustrated in Table 9-2.

Table 9-2. Illustration for Estimating O&M Costs Based on the Projections for Operating a Full-Scale PRB at Dover AFB

Item	Description	Basis	Cost
<i>Annual Monitoring Activities</i>			
Groundwater sampling	Quarterly, labor, materials, travel	40 wells	\$80,000
CVOC analysis	Quarterly, 40 wells	44 per quarter @ \$120/sample	\$20,000
Inorganic analysis	Annual, 20 wells	22 @ \$200/sample	\$4,000
Water-level survey	Quarterly, labor	40 wells per quarter	\$4,000
Data analysis; report; regulatory review	Quarterly, labor	4 times per year	\$40,000
Annual operating cost			\$148,000
<i>Maintenance Activities (once every 10 years assumed)</i>			
Site preparation	Permitting, clearances	Labor	\$10,000
Reactive media procurement	Connelly iron, shipping	Iron: 108 tons @ \$360/ton Shipping: \$9,000	\$48,000
Removal/replace-ment of gates	Mobilization/demobilization; installation of four 8-ft-diameter caisson gates to 39-ft depth; asphalt parking lot restoration	Mob./demob.: \$38,000 Gates: \$266,000 Monitoring wells: \$25,000 Surface restoration: \$34,000	\$363,000
Periodic maintenance cost (once every 10 years assumed)			\$421,000

- ❑ **Contaminant Monitoring Costs.** These costs may vary from site to site depending on regulatory requirements, number of monitoring wells, and frequency of sampling. These costs include sampling, laboratory analysis, and reporting.
- ❑ **Performance Monitoring Costs.** If additional monitoring is desired by site managers to achieve other performance evaluation objectives (see Section 8.2), additional monitoring costs may be incurred. These costs will vary depending on the objectives of site managers at a given site.
- ❑ **Periodic Maintenance Costs.** Maintenance may be required if inorganic precipitates build up to a point where either the reactivity or the hydraulic conductivity of the reactive cell is significantly affected. The reactive medium may have to be regenerated or replaced. Table 9-2 assumes that the reactive medium in the gates will be

removed and replaced every 30 years. Another alternative that has been mentioned is to install a second PRB near the first one after the reactive medium in the first PRB is exhausted. Any of these regeneration/replacement options are likely to be relatively expensive and the expectation from the PRB technology is that such maintenance will be infrequent. Although various rules-of-thumb have been proposed in the past, the best approach may be to develop multiple economic scenarios, as described in Section 9.3, to assess the impact of the longevity of the reactive medium on the economic suitability of the PRB.

The O&M costs of a P&T system include operating labor, energy, and maintenance. The labor and energy requirements for operating the P&T system are a major driver of O&M cost. In addition to this recurring operating cost, a P&T system often requires frequent maintenance to replace moving parts, replace the carbon in a carbon polishing unit, or replace the catalyst in a catalytic oxidation unit. Appendix B contains an example of the O&M costs estimated for a PRB and a P&T system for a CVOC plume at Dover AFB.

9.3 Present Value Analysis

Although this may not be the case at every site, the P&T system at Dover AFB (see Appendix B) was estimated to require a lower initial capital investment as compared to the PRB. On the other hand, the P&T system has higher O&M costs, primarily because of the recurring annual labor and energy requirements to operate the P&T system (Battelle, 2000). The P&T system requires more frequent routine maintenance (e.g., replacement of pumps and seals) and periodic maintenance in the form of carbon and catalyst replacement. Because the PRB and P&T system require maintenance at different points in time and because the contamination (and the associated operating/monitoring costs) is expected to last for several years or decades, a PV analysis is required to consolidate the capital investment and long-term O&M costs into a total long-term cost in today's dollars.

Typically, PV or discounted cashflow analysis is used to determine the life cycle cost of a technology. PV cost represents the amount of money that would have to be set aside today to cover all the capital investment and O&M costs occurring in the present and future.

$$PV_{\text{technology}} = \text{Capital Investment} + PV_{\text{annual O\&M costs over life of the new technology}} \quad (9-1)$$

In the above equation, capital investment does not have to be discounted back to the present because this investment occurs immediately (time $t=0$). The term $PV_{\text{annual O\&M costs over life of the new technology}}$ represents the annual O&M costs (and savings realized, if any) over several years of operation, adjusted for the time value of money. This adjustment is done by dividing each year's O&M costs by a factor that incorporates a discount rate (r), as shown in Equations 9-2 and 9-3. The discount rate incorporates the combined effect of inflation, productivity, and risk. In other words, the discount rate accounts for the fact that any cost postponed into future years frees up money which can be put to productive use and which provides a rate of return equal to the discount rate (r).

$$PV_{\text{annual O\&M costs}} = \sum \frac{\text{O \& M cost in Year } t}{(1 + r)^t} \quad (9-2)$$

$$PV_{\text{annual O\&M costs}} = \frac{\text{O \& M cost in Year 1}}{(1+r)^1} + \frac{\text{O \& M cost in Year 2}}{(1+r)^2} + \dots + \frac{\text{O \& M cost in Year n}}{(1+r)^n} \quad (9-3)$$

Another way of interpreting Equation 9-3 is that, because O&M costs are incurred gradually over several years, a smaller amount of money can be set aside today (for example, in a bank deposit that provides a rate of return, r) to cover future O&M costs. The further into the future (i.e., the greater the t), the greater is the denominator for the relevant t , and the lesser is the PV of that year's O&M cost. That is, fewer dollars must be set aside today (in a separate investment that provides a rate of return, r) to cover the O&M costs of the future. Herein lies the potential advantage of a PRB over a P&T system: whereas P&T systems incur a continuous O&M cost for labor, maintenance, and energy requirements, O&M costs for a PRB are postponed until the reactive medium performance starts declining. Indications from existing PRBs are that these PRBs could operate without any O&M costs for several years. Note that both P&T systems and PRBs require routine monitoring to verify regulatory compliance; this is the only recurring annual cost for the PRB.

A total time period of 30 years ($n = 30$) typically is used for the long-term evaluation of remediation costs. A real discount rate of 2.9% is currently recommended in the PV analysis, as per the 1999 update to the U.S. EPA Office of Management and Budget (OMB) circular (U.S. EPA, 1993).

Table 9-3 illustrates the PV analysis based on the projections for a full-scale PRB at Dover AFB (Battelle, 2000) and the estimated cost for an equivalent P&T system, over a 30-year period (see Appendix B for details). In this illustration, it is assumed that the PRB will maintain its reactivity and hydraulic performance over 10 years of operation, after which time the reactive medium in the four gates will have to be removed and replaced. An initial capital investment of \$947,000 is estimated for the PRB and \$502,000 for an equivalent P&T system to capture and treat a 100-ft-wide CVOC plume. The O&M cost of the PRB in Year 10 includes the annual monitoring cost of \$148,000, plus the reactive medium replacement cost of \$421,000 (cost to remove and re-install four gates containing iron). The P&T system incurs an annual O&M cost of \$214,000, except in years that require periodic maintenance to replace the polishing carbon and/or the catalyst in the effluent air oxidizer. The PVs of the capital investment and annual O&M costs are listed in columns 2 and 5 of Table 9-3 (for the PRB and P&T system, respectively), and indicate that the further back in time that the cost occurs, the lower is its PV. Columns 3 and 6 list the cumulative PV at the end of each year; the cumulative PV includes the capital investment and the PV of all the O&M costs up to that year. The year in which the cumulative PV cost of the PRB is equal to or below cumulative PV cost of the P&T system is the payback period or break-even point for the PRB.

As shown in Table 9-3, there are two potential break-even times for the PRB (indicated by the shaded cells in the table). In Year 8, the cumulative or total PV cost of the PRB is lower than the PV cost of the P&T system, indicating the first potential break-even point. However, in Year 10, the nonroutine maintenance cost of replacing the iron in the four gates is incurred, which makes the total cost of the PRB slightly higher again than the P&T system. In Year 14, the total PV cost of the PRB again becomes lower, and this is the true break-even point. In other words, over

**Table 9-3. Illustration of a PV Analysis of PRB and P&T Systems for Dover AFB
Assuming 10-Year Life of PRB**

Year	PRB			P&T System		
	Annual Cost ^(a)	PV of Annual Cost ^(b)	Cumulative PV of Annual Cost ^(c)	Annual Cost ^(a)	PV of Annual Cost ^(b)	Cumulative PV of Annual Cost ^(c)
0	\$947,000 ^(d)	\$947,000	\$947,000	\$502,000 ^(d)	\$502,000	\$502,000
1	\$148,000 ^(e)	\$143,829	\$1,090,829	\$214,000 ^(e)	\$207,969	\$709,969
2	\$148,000	\$139,775	\$1,230,604	\$214,000	\$202,108	\$912,077
3	\$148,000	\$135,836	\$1,366,441	\$214,000	\$196,412	\$1,108,489
4	\$148,000	\$132,008	\$1,498,449	\$214,000	\$190,876	\$1,299,365
5	\$148,000	\$128,288	\$1,626,736	\$235,000	\$203,700	\$1,503,065
6	\$148,000	\$124,672	\$1,751,408	\$214,000	\$180,269	\$1,683,334
7	\$148,000	\$121,159	\$1,872,567	\$214,000	\$175,189	\$1,858,523
8	\$148,000	\$117,744	\$1,990,311	\$214,000	\$170,251	\$2,028,774
9	\$148,000	\$114,426	\$2,104,737	\$214,000	\$165,453	\$2,194,228
10	\$569,000^(f)	\$427,522	\$2,532,259	\$242,000	\$181,828	\$2,376,056
11	\$148,000	\$108,067	\$2,640,326	\$214,000	\$156,259	\$2,532,315
12	\$148,000	\$105,021	\$2,745,347	\$214,000	\$151,855	\$2,684,170
13	\$148,000	\$102,061	\$2,847,408	\$214,000	\$147,575	\$2,831,745
14	\$148,000	\$99,185	\$2,946,593	\$214,000	\$143,416	\$2,975,162
15	\$148,000	\$96,390	\$3,042,983	\$235,000	\$153,051	\$3,128,213
16	\$148,000	\$93,673	\$3,136,656	\$214,000	\$135,446	\$3,263,659
17	\$148,000	\$91,033	\$3,227,690	\$214,000	\$131,629	\$3,395,289
18	\$148,000	\$88,468	\$3,316,158	\$214,000	\$127,920	\$3,523,208
19	\$148,000	\$85,974	\$3,402,132	\$214,000	\$124,314	\$3,647,523
20	\$569,000^(f)	\$321,222	\$3,723,354	\$242,000	\$136,618	\$3,784,141
21	\$148,000	\$81,197	\$3,804,550	\$242,000	\$132,768	\$3,916,908
22	\$148,000	\$78,908	\$3,883,459	\$214,000	\$114,097	\$4,031,006
23	\$148,000	\$76,685	\$3,960,143	\$214,000	\$110,882	\$4,141,887
24	\$148,000	\$74,523	\$4,034,667	\$214,000	\$107,757	\$4,249,644
25	\$148,000	\$72,423	\$4,107,090	\$235,000	\$114,996	\$4,364,641
26	\$148,000	\$70,382	\$4,177,472	\$214,000	\$101,769	\$4,466,409
27	\$148,000	\$68,399	\$4,245,871	\$214,000	\$98,901	\$4,565,310
28	\$148,000	\$66,471	\$4,312,341	\$214,000	\$96,113	\$4,661,423
29	\$148,000	\$64,598	\$4,376,939	\$214,000	\$93,405	\$4,754,827
30	\$569,000^(f)	\$241,352	\$4,618,291	\$242,000	\$102,649	\$4,857,476

(a) Annual cost is equal to the capital investment in Year 0 and the O&M cost in subsequent years.

(b) PV cost is the annual cost divided by a discount factor term based on a 2.9% discount rate.

(c) Cumulative PV cost is the sum of annual PV costs in each year and previous years.

(d) Initial capital investment.

(e) Annual O&M cost.

(f) Annual monitoring cost of \$148,000, plus maintenance/replacement of gates for \$421,000.

14 years, the lower annual operating cost (passive operation) of this PRB makes it a worthwhile investment. At the end of the analysis period of 30 years, the PV of the total savings from implementing a PRB versus a P&T system in this illustration is \$239,000 (that is, the difference between the cumulative costs of \$4,618,291 and \$4,857,476 for the PRB and P&T system at the

end of 30 years). If the plume persists for 50 or more years, the estimated savings will be even greater, as seen in Table 9-4.

Because the break-even point is sensitive to the assumption on the life of the PRB, the PV analysis shown in Table 9-3 can be repeated assuming that the life of the reactive medium is 5, 10, 20, and 30 years (see Tables B-8 to B-11 in Appendix B). Table 9-4 summarizes the results of running these longevity scenarios. The same longevity scenarios can be represented pictorially as shown in Figure 9-1. As seen in Table 9-4 and Figure 9-1, if the reactive medium lasts only 5 years, and the gates must be replaced every 5 years, then the P&T system is less expensive (i.e., there is no break-even point because the PV cost of the PRB is always higher than the PV cost of the P&T system). If the PRB lasts at least 10 years, it is less expensive than a P&T system. The longer the reactive medium performance lasts, the greater are the savings at the end of 30+ years. The longer the duration of the project (that is, the longer the plume persists at the site), the greater are the potential savings. In Table 9-4, when the project duration increases to 50 years, the potential savings realized are greater than \$1 million (see Table B-12 in Appendix B).

Table 9-4. Illustration of the Break-Even Point and Savings by Using a PRB Instead of a P&T System at Dover AFB

Life of Reactive Medium	Break-Even Point	PV of Savings Over the Duration of the Project	Duration of Project
5	None	-\$603,000	30 years
10 years	14 years	\$239,000	30 years
20 years	8 years	\$734,000	30 years
30 years	8 years	\$793,000	30 years
30 years	8 years	\$1,251,000	50 years

These same simulations are described graphically in Figure 9-1. In this figure, the break-even point is the point at which the two lines (solid line for PRB cost and dashed line for P&T cost) intersect. When periodic maintenance (replacement of iron) is required every 5 years, the PRB cost is always greater than the P&T cost, as indicated by the fact that the two lines do not intersect. If the reactive medium lasts 10 years or longer without replacement, there is a break-even point.

The estimated saving or cost advantage of using a PRB at Dover AFB, although substantial over a long period of time, is not as great as that reported at some other sites. One reason for the cost difference is that in many previous studies, higher discount rates (8 to 15%) have been used. For example, using a discount rate of 8%, the PV of the savings for the PRB at former NAS Moffett Field was estimated at \$14 million after 30 years (Battelle, 1998). However, the PV estimate for the PRB at Dover AFB is calculated with a much lower discount rate of 2.9%, which is based on the most recent (1999) update to the U.S. EPA guidance (U.S. EPA, 1993). This year's low discount rate reflects the current low-inflation environment of the U.S. economy. In a low-inflation (low-discount rate) environment, future savings appear to be less attractive than in a high-inflation (high-discount rate) environment.

At many sites, a continuous reactive barrier (no funnel) may be more economical than a funnel-and-gate system, especially for relatively shallow PRBs that can be installed with cost-effective techniques such as continuous trenching. Innovative construction techniques, such as jetting and hydrofracturing, offer the potential for additional cost reduction in deeper aquifers.

In the absence of reasonably accurate predictions of the life of the reactive medium, the multiple longevity scenarios shown in Table 9-4 provide a way of understanding the performance expectations of the reactive medium. In the example in Table 9-4, indications are that the PRB at this site would have to retain its reactive and hydraulic performance for at least 10 years, before the long-term O&M savings realized are large enough to offset the higher initial capital invested in the PRB (as compared to a P&T system). At other sites, the break-even point for the PRB may occur in earlier or later years, depending on the differences in capital investment and O&M costs between a PRB and a competing technology (such as P&T).

9.4 Cost-Benefit Evaluation

The cost analysis in Section 9.3 takes into account only the more tangible costs (and savings) of the two groundwater treatment options (PRB and P&T system). An economic decision on which of the two technologies to adopt should be based on a cost-benefit analysis that includes less tangible and/or intangible costs and benefits of the two technologies. An example of a less tangible benefit of the PRB is continued productive use of the PRB site because of the absence of above-ground structures (as in a P&T system). For example, at Dover AFB and former NAS Moffett Field, the sites are still being used as parking lots. It is difficult to assign a dollar value to this benefit; however, it is a benefit that adds to the savings realized by implementing a PRB instead of a P&T system. At the private Intersil site in California, site owners were able to lease the property to a new tenant because of the absence of aboveground structures and lack of O&M requirements besides monitoring (Yamane et al., 1995). In addition, PRBs are not prone to the high down time and labor/maintenance/waste disposal requirements of a P&T system.

9.5 Computerized Cost Models

The Remedial Action Cost Engineering and Requirements (RACER) System is an environmental costing program developed by the U.S. Air Force. It can estimate costs for various phases of a remediation project:

- ☐ Site characterization studies
- ☐ Remedial action (including O&M activities)
- ☐ Site work and utilities.

The program's framework is based on actual engineering solutions gathered from historical project information, construction management companies, government laboratories, vendors, and contractors. It is designed to factor in specific project conditions and requirements based on minimal user input in order to generate a cost estimate. RACER Version 3.2 has a cost database created mostly from the U.S. Army Corps of Engineers' Unit Price Book and supplemented by vendor and contractor quotes. Version 3.2 has been adapted especially for PRB applications.

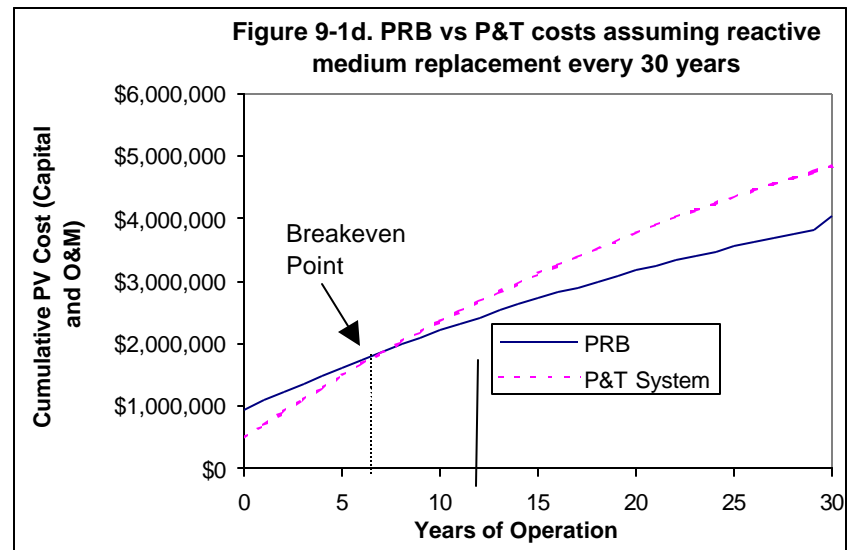
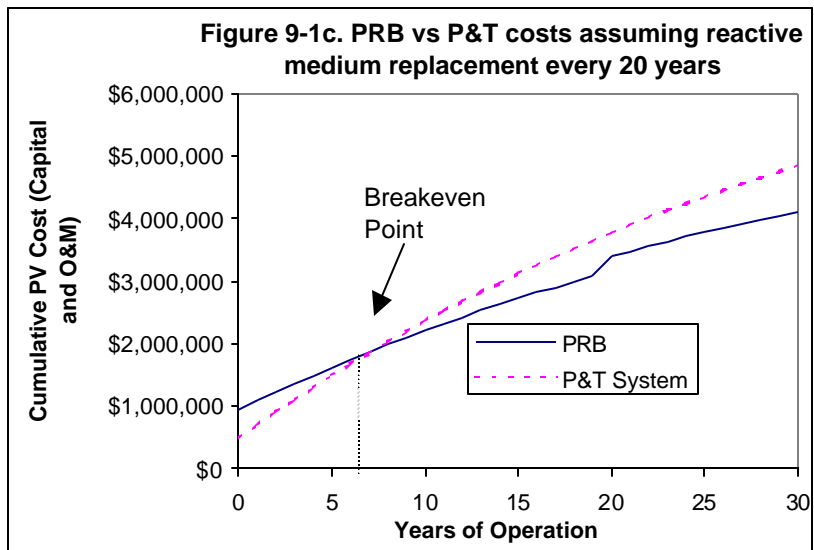
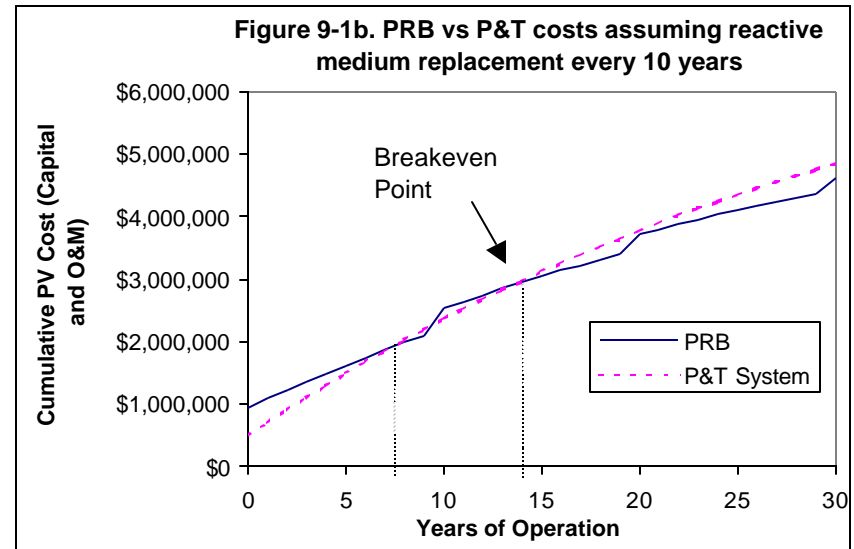
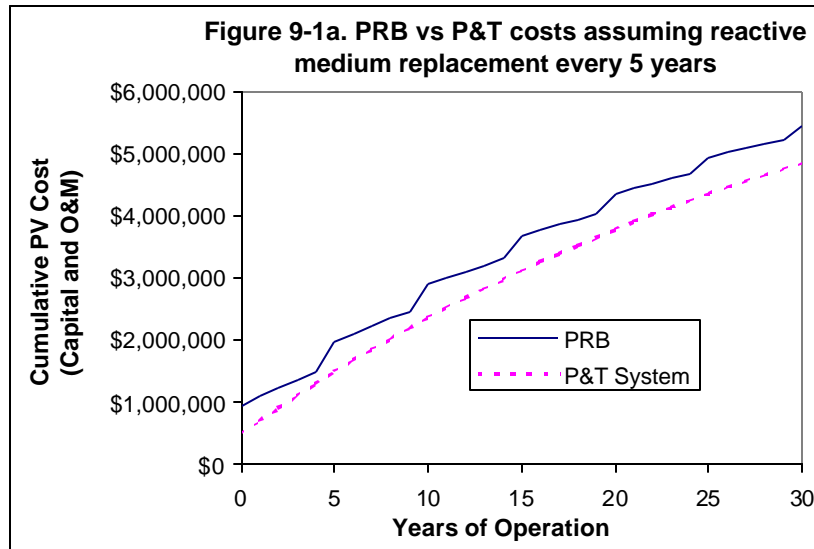


Figure 9-1. Illustration of How Break-Even Point or Payback Period Varies with Expected Life of the Reactive Medium

10.0 Current Status of the PRB Technology

This section reviews the technical, economic, and regulatory experience at various sites where the PRB technology has been applied.

10.1 Existing PRB Applications

Tables 10-1 and 10-2 (which appear at the end of this section) summarize the site characteristics, PRB features, and monitoring updates at the sites where PRBs have been applied. Although the lists are not exhaustive, these sites offer a good distribution of contaminants, reactive media, hydrogeologic characteristics, PRB configurations and dimensions, construction methods, and costs. Some noteworthy trends in these applications are listed below:

- ❑ To date, most of the PRBs have used granular iron medium and have been applied to address CVOC contaminants. CVOC degradation by iron has been demonstrated at several sites. The tendency of CVOCs to persist in the environment for several years or decades makes them an obvious target for a passive technology.
- ❑ Metals amenable to precipitation, under the reducing conditions created by the common iron medium, have been the next most common targets. Examples of these metals include hexavalent chromium and uranium. One concern is that, unlike CVOCs, metals do not degrade but instead accumulate in the reactive medium. At some point in time, the reactive medium (containing the precipitated metals) may have to be removed and disposed of. With CVOCs, even after the PRB performance has declined, it is possible that the reactive medium can just be left in the ground.
- ❑ Although many initial applications were pilot-scale PRBs, most recent applications have been full scale, indicating that confidence in this technology has grown.
- ❑ At many sites, the target cleanup levels have been MCLs. At some sites, state/local regulations have required more stringent cleanup levels for some contaminants, such as VC.
- ❑ At sites where target cleanup levels have not been achieved in the downgradient aquifer, the reason has generally been the inability of the PRB to achieve the designed plume capture or residence time, rather than the inability of the reactive medium to replicate laboratory-measured reactivity (contaminant half-lives) in the field. Inadequate hydraulic capture and/or inadequate residence time has been observed at some sites with either funnel-and-gate systems (Denver Federal Center and former NAS Alameda) or continuous reactive barriers (DOE Kansas City Plant). At one site (former NAS Alameda), plume heterogeneities appear to have contributed to higher-than-expected contaminant concentrations at the influent to and effluent from the reactive cell (Einarson et al., 2000).

- ❑ PRBs have been applied at sites with groundwater velocities (in the aquifer) reported at 0.0003 to 2.8 ft/day. No monitoring data are available for the two sites that represent the extreme ends of the range. Although 2.8 ft/day is a velocity that could be handled with a reasonable thickness of the reactive cell, it is unclear how efficiently the groundwater moving at 0.0003 ft/day would passively contact the reactive medium.
- ❑ Although most PRB applications used iron as the reactive medium during the initial use of this technology, the use of other innovative media has been investigated in recent years at some sites.
- ❑ More of the recent applications have been configured as continuous reactive barriers rather than funnel-and-gate systems. One reason for this is that the unit cost of iron medium has declined from \$650/ton to about \$300/ton, plus shipping and handling. Although, in theory, the same amount of iron should be required for a given mass of plume contaminants, the heterogeneous distribution of the contaminant concentrations in the plume makes the amount of iron required in a uniformly thick continuous reactive barrier somewhat inefficient. However, the lower cost of iron and other benefits make continuous reactive barriers more attractive. Benefits of continuous reactive barriers include easier design and construction, and a propensity to generate less complex flow patterns.
- ❑ Although initial use of this technology involved conventional construction techniques (such as backhoe excavation, sheet pile, and/or slurry wall), innovative construction techniques (such as caissons, continuous trenching, jetting, and hydrofracturing) are being explored at more recent PRB sites. These techniques offer the potential to access greater depths with lower construction costs.

Additional information and updates on some of these PRB sites can be obtained from the RTDF Web site at www.rtdf.com.

10.2 Guidance from Government Agencies

In an effort to promote more regular consideration of newer, less costly, and more effective technologies to address the problems associated with hazardous waste sites, the U.S. EPA has published six In Situ Remediation Technology Status Reports, one of which deals with PRBs (U.S. EPA, 1995). This Technology Status Report briefly describes demonstrations, field applications, and research on PRBs. A more detailed report by the U.S. EPA on PRB technology application also is available (U.S. EPA, 1998). As shown in Table 10-2, federal drinking water standards or MCLs have been the cleanup targets at many sites. However, at some sites, state environmental agencies have imposed more stringent cleanup goals for individual compounds, such as VC.

In addition to these federal government efforts, individual states have formed the ITRC group to build a consensus among the states on regulatory issues surrounding innovative remediation technologies. The ITRC has formed a PRBs subgroup. This subgroup first convened at a meeting in Philadelphia on September 25, 1996, and includes members from environmental regulatory agencies in 29 states, as well as other interested parties such as environmental groups, the

U.S. military, industry, and environmental consulting firms. The subgroup has developed consensus documents for the states that enhance the regulatory acceptance of the PRB technology and provide guidance on compliance monitoring requirements (ITRC, 1997 and 1999). Although these documents represent a general regulatory consensus on PRBs, individual states may decide to add on their own specific requirements.

At many existing PRB sites to date, regulatory requirements for design, construction, and monitoring have been determined on a case-by-case basis, under the general guidance of the ITRC documents. Regulatory agencies suggest that for a prospective site there should be (1) compelling reasons why a PRB is the best choice for that site and (2) data to show why the PRB is expected to work as planned. As field data from a growing number of PRB applications becomes available, acceptance of this technology by regulators is expected to increase.

Intersil, the site in Sunnyvale, CA that implemented the first full-scale PRB application, was in many ways an ideal situation from a technical feasibility and regulatory viewpoint. It was an underutilized property, was run by a cooperative potentially responsible party (PRP), and posed no excessive human health threat. Furthermore, it had shallow groundwater, poor (brackish) water quality, a competent aquitard, and a relatively shallow aquifer. A pilot study conducted at the site showed that the PRB would work and that the total cost was estimated as half that of a P&T system over 30 years (Kilfe, 1996). The cost analysis for this site assumed that the iron medium would not require replacement and included the benefit of being able to lease the property, an option that was enabled by the passive long-term nature of the technology. Although the plume had moved off the property at Intersil, regulators allowed placement of the PRB within property lines based on indications that natural attenuation of the chlorinated contaminants, which was occurring downgradient, would take care of the off-site portion of the plume.

Other sites may be more difficult from an application viewpoint. At one potential site where a full-scale PRB was being considered, the approval process was made difficult by the fact that there is already a ROD with 30 signatories (PRPs) in place for installing a P&T system to clean up a regional plume. Obtaining a consensus for modifying the ROD with 30 PRPs proved difficult. Another difficulty that could be encountered is if the plume has moved off the property and the PRB needs to be installed outside the property boundaries; obtaining site access when the prospective site is beyond the property boundary may be difficult.

One important trend is that regulators are increasingly open to discussion of cleanup costs. There is a growing willingness in the regulatory community to consider cost an important factor in selecting alternatives for cleanup. If a significant benefit-to-cost ratio can be shown for the PRB versus a P&T system (or any other competing technology), it would be a considerable factor in favor of a PRB. It is recommended that site managers confer with regulators as early as possible in the design stage to promote better understanding of the technical, cost, and regulatory concerns of all stakeholders.

10.3 Future Challenges for the PRB Technology

As shown in Table 10-2, for many CVOC contaminants, the most common target for PRB applications so far, the ability of granular iron medium to degrade the contaminants to MCLs has been adequately demonstrated at several different sites (Battelle, 1998 and 2000; Blowes et al., 1997;

Yamane et al., 1995; U.S. EPA, 1998). Demonstrating the reactive capabilities of granular iron with CVOC plumes is now a fairly routine matter that can be addressed by suitable column tests. As common reactive media (e.g., granular iron) are increasingly standardized by various suppliers, and these media are applied at multiple sites for common contaminants (such as TCE), it may be possible to forgo many features of treatability testing (column tests) in favor of published contaminant half-life values with appropriate safety factors. Proceeding with PRB application without site-specific treatability tests for some common contaminants would have to be approved by the concerned regulators. In general, site-specific treatability tests are helpful, especially if the groundwater exhibits unusual geochemistry (e.g., high levels of DOC, nitrate, or alkalinity) or the construction method involves mixing of the reactive medium with another material (e.g., biodegradable slurry).

Three key technical factors – plume capture, residence time, and geochemistry (longevity) – are the main challenges that need to be addressed in designing a PRB. A PRB should be designed to provide the required plume capture and sufficient residence time in the reactive medium to degrade the contaminants to target levels at a particular site. Also, on a long-term basis, the reactive medium-groundwater geochemistry should be suitable for sustaining the reactive and hydraulic performance of the PRB over long periods of time. For non-CVOC contaminants (e.g., RCRA metals and/or radionuclides) and reactive media other than the commonly-used granular iron, demonstrating the reactive capabilities of the PRB-groundwater system with treatability tests on a site-specific basis is still important because of the limited history of PRBs.

There are two reasons why hydraulic issues (plume capture and residence time) pose a design challenge. First, site characterization conducted at some sites may not be adequate to obtain a good understanding of the hydraulic flow characteristics of the site. Second, even at sites which have undergone substantial characterization, hydrogeologic heterogeneities (variability in gradients and conductivities), plume heterogeneities (variability in contaminant concentrations), and seasonal variability in flow magnitude and direction can pose a challenge for PRB design. To address these hydraulic issues, the authors of this document recommend that technology users conduct adequate site characterization, simulate multiple groundwater flow scenarios, and incorporate adequate safety factors in the design dimensions and orientation of the PRB.

Assessing longevity, or the ability of the reactive medium to sustain the reactive and hydraulic performance of the PRB over time, also is a challenge. Although much progress has been made at several sites in using inorganic analysis of groundwater, iron coring, and geochemical modeling to evaluate precipitation potential in the reactive medium, predicting the life of the reactive medium has proved difficult. In the absence of reasonable estimates of the life of the reactive medium, the authors of this document recommend the use of multiple longevity scenarios (see Section 9.3) to evaluate the cost/savings expectations from a PRB application.

An interagency initiative supported by several government agencies, including DoD, DOE, U.S. EPA, and ITRC, is making an effort to address the three issues of plume capture, residence time, and longevity (Battelle, 1999). The DoD effort, funded by Strategic Environmental Research and Development Program/Environmental Security Technology Certification Program (SERDP/ESTCP), is being led by the Naval Facilities Engineering Service Center (NFESC) and Battelle, with AFRL, ITRC, the U.S. Army Corps of Engineers, and the U.S. Air Force Center for

Environmental Excellence as partners. Field data from several PRBs at DoD sites are being reviewed and supplemented with additional focused monitoring, where required, to address the three important issues discussed above. ORNL (for U.S. DOE) and the U.S. EPA are conducting similar efforts with the PRBs at DOE and U.S. EPA sites.

Innovative PRB construction techniques that do not involve trenching (e.g., jetting and hydraulic fracturing) are being demonstrated at various sites. As more field data from these demonstrations are published, and as the ability of these techniques to ensure the desired continuity and thickness of the reactive cell is verified, depth may no longer be a significant limitation for the PRB technology. This improvement is expected to increase the applicability of the technology.

Table 10-1. Update on Design, Construction, and Cost of PRBs

PRB Site	PRB Type	Depth to Aquitard (ft bgs)	Reactive Cell Thickness (ft)	Amount of Reactive Medium (tons)	Gate or CRB Width (ft)	Funnel Width (ft)	Gate or CRB Construction Method	Funnel Construction Method	PRB Cost
Elizabeth City, NJ	CRB	25 ^(a)	2	450	150		Continuous trenching		\$500,000 total
DOE facility, Kansas City, MO	CRB	30	6	666	130		Cofferdam		\$1,300,000 total installation
Watervliet Arsenal, NY	CRB with 2 trenches	10-15	2.5	166	Trench A 205; Trench B 83		Trench box		\$257,000 total
Former manufacturing site, NJ	CRB	15-23	5	720	127		Cofferdam		\$725,000 installation
Seneca Army depot activity, NY	CRB	8 to 10	1	203	650		Continuous trenching		\$250,000 iron and construction
Industrial site, SC	CRB		1	400	325		Continuous trenching		\$350,000 installation
Caldwell Trucking, NJ	CRB with 2 trenches		0.25	250	150 and 90		Vertical hydraulic fracturing technique		\$670,000 for 90 ft and \$450,000 for 150 ft
Private electronics firm, Mountainview, CA	CRB			90					\$80,000-\$100,000 total
Dry cleaning site, Germany	CRB			69 iron 85 iron sponge	74 (33 granular iron & 41 iron sponge)		Overlapping boreholes		\$93,000 total
Bardowie Farm, Cambridge, NZ	CRB		5		115		Continuous trenching		
Massachusetts military reservation	CRB		0.28	44	48		Vertical hydraulic fracturing technique		\$160,000 installation

Table 10-1. Update on Design, Construction, and Cost of PRBs (Continued)

PRB Site	PRB Type	Depth to Aquitard (ft bgs)	Reactive Cell Thickness (ft)	Amount of Reactive Medium (tons)	Gate or CRB Width (ft)	Funnel Width (ft)	Gate or CRB Construction Method	Funnel Construction Method	PRB Cost
Belfast, Northern Ireland	Funnel-and-gate					80 to 100	In situ reaction vessel	Bentonite cement slurry walls	\$20,000 iron \$350,000 construction
Industrial facility, NY	Funnel-and-gate	20	3.5	45	12	15	Cofferdam	Sheet piling	\$30,000 iron \$250,000 construction
Industrial facility, NY	CRB (2 walls)	18	1	742	Trench A = 120 ft; trench B = 370 ft		Continuous trenching		\$797,000 installation
Intersil, Sunnyvale, CA	Funnel-and-gate		4	220	36	535 (300 and 235 gates)	Cofferdam	Cement-bentonite slurry wall	\$170,000 iron \$720,000 construction
Canadian Forces Base, Borden, Canada	CRB	20	5		5		Clamshell excavation, sheet pile box for shoring		\$25,000- \$30,000 total
Denver Federal Center	Funnel-and-gate (with 4 gates)	23-30	2 to 6		160 (40 ft × 4)	1,040	Cofferdam	Sealable-joint sheet piling	\$1,000,000 total
Former NAS Moffett Field	Funnel-and-gate	25	6	75	10	40 (20 × 2)	Backhoe excavation, sheet pile box for shoring	Sealable-joint sheet piling	\$323,000 installation
Somersworth Sanitary Landfill Superfund Site	Funnel-and-gate	40	4			30	Caisson	Bentonite slurry walls	\$175,000 total construction
Somersworth Sanitary Landfill Superfund Site	CRB	40	2.3	100	21		Bioslurry trench		\$175,000 construction
Former Lowry AFB, CO	Funnel-and-gate with angled funnel	17	5		10	28 (14 × 2)	Cofferdam	Sealable-joint sheet piling	\$530,000 installation

Table 10-1. Update on Design, Construction, and Cost of PRBs (Continued)

PRB Site	PRB Type	Depth to Aquitard (ft bgs)	Reactive Cell Thickness (ft)	Amount of Reactive Medium (tons)	Gate or CRB Width (ft)	Funnel Width (ft)	Gate or CRB Construction Method	Funnel Construction Method	PRB Cost
Portsmouth gaseous diffusion plant, OH	Above ground	32							\$4,000,000 total
ORNL, TN	Funnel-and-gate						Concrete treatment canisters		\$1,000,000 for both barriers
ORNL, TN	CRB		2	80	26	225	Continuous trenching, guar gum slurry for shoring		\$1,000,000 for both barriers
East Garrington gas plant, Canada	Trench with 2 gates				6	290 (145 × 2)	Vertical culverts	Trench sealed with liner	\$67,200 construction
Fry Canyon site, UT	Funnel-and-gate with 3 barriers		3		7				\$140,000 installation \$30,000 design
Private site, Tifton, GA	Funnel-and-gate					400		Vibrating beam	\$520,000 construction and reactive media
Former NAS Alameda, CA	Funnel-and-gate; compound gate with 2 reactive cells in series		10		15	20 (10 × 2)	Trench with concrete pad on bottom		\$400,000 construction
Public school, Ontario, Canada	Funnel-and-gate		6		6	32 (16 × 2)		Sealable sheet pilings	\$5,000 construction
Tonolli Superfund Site, PA	Groundwater trench		3		1,100		Continuous trench		

Table 10-1. Update on Design, Construction, and Cost of PRBs (Continued)

PRB Site	PRB Type	Depth to Aquitard (ft bgs)	Reactive Cell Thickness (ft)	Amount of Reactive Medium (tons)	Gate or CRB Width (ft)	Funnel Width (ft)	Gate or CRB Construction Method	Funnel Construction Method	PRB Cost
Nickel Rim Mine, Canada	Funnel-and-gate		12		50		Cut-and-fill Technique	Coarse sand buffer zone	\$30,000 total cost
Aircraft maintenance facility, OR	Funnel-and-gate with 2 gates	24	1.5' gate 1 and 3' gate 2		Gate 1, 50 ft and gate 2, 50 ft	650	Continuous trencher and trackhoe and drag box	Soil-bentonite slurry	\$600,000 construction
Industrial site, KS	Funnel-and-gate	30	3	70	20	980 (490 × 2)	Cofferdam	Soil bentonite slurry	\$400,000 installation
Cape Canaveral Air Station, FL	CRB (2 walls)	43	1 ft (mandrel)	98 (mandrel) 107 JAG	70	100.5 (51.5 and 49 barriers)	Mandrel and JAG emplacement		\$279,000 mandrel system \$238,000 JAG system
Dover AFB, DE	Funnel-and-gate with 2 gates	40-45	4	54 iron 5 pyrite	8 (2 gates, 4 ft each)	60	Caissons	Sealable sheet piles	\$22,000 iron \$25,000 pyrite \$327,000 construction
Rocky Flats, Golden, CO	Collection and treatment system	5 to 16				230	Gravity-fed reaction vessel	Collection trenches	
Manufactured gas plant, Germany	Funnel-and-gate with 2 gates	49			79				
Wood-treating facility, NH	Funnel-and-gate				30	650		Sealable sheet piles	
100D Area, Hanford site, WA	In situ redox manipulation	85	50		150		Injecting sodium dithionite into existing wells		\$480,000 construction
Savannah River site, Aiken, SC	Geosiphon cell								\$26,400 iron \$119,115 total costs

Table 10-1. Update on Design, Construction, and Cost of PRBs (Continued)

PRB Site	PRB Type	Depth to Aquitard (ft bgs)	Reactive Cell Thickness (ft)	Amount of Reactive Medium (tons)	Gate or CRB Width (ft)	Funnel Width (ft)	Gate or CRB Construction Method	Funnel Construction Method	PRB Cost
DoD facility, SC	CRB	NA	1		275 (4 parallel walls 275 ft wide)		Continuous trenching		\$400,000 total
Industrial facility, LA	CRB	23	1	616.5	720		Continuous trenching		\$260,000 total
DoD facility, Warren, AFB	CRB	28-38	4	1680	565		Trench box		\$1,000,000 total
DoD facility, Pease AFB, NH	CRB	33	2.5		150		Bioslurry trench		\$300,000 total
Industrial facility, MA	CRB	17	2.5		180		Sheet pile "box"		\$420,000 total
Industrial facility, OH	CRB	20	1	72	200		Open trench excavation		\$70,000 total
DoD facility, Travis AFB, CA	CRB	50	4-5	300	80		Jetting		\$360,000 construction
NASA facility, LA	Granular iron placed around leaking manhole			22.5			Sheet pile box		
Maxwell AFB, AL	CRB	75	0.08-0.3	40			Vertical hydraulic fracturing technique		

(a) PRB is not keyed in to aquitard.

CRB = Continuous reactive barrier.

JAG = Jet-assisted grouting.

Table 10-2. Update on PRB Site Characteristics and Monitoring

PRB Site (Installation Date)	Scale of PRB	Target Contaminants	Reactive Medium	Target Cleanup Levels	Groundwater Velocity in Aquifer (ft/day)	Monitoring Update and Remarks
Elizabeth City, NC (June 1996)	Full ^(a)	Cr ⁺⁶ (3,430 ug/L) TCE (4,320 ug/L) <i>cis</i> -DCE (12 mg/L) VC (0.1 mg/L)	Granular iron	MCLs: Cr (50 µg/L) TCE (5 µg/L)		MCLs met in reactive cell; plume migration below hanging PRB possible. ^(a)
DOE facility, Kansas City, MO (April 1998)	Full	<i>cis</i> -DCE (1,500 µg/L) VC (291 µg/L)	Granular iron	MCLs: <i>cis</i> -DCE (70 µg/L) VC (2 µg/L)	0.025 in clay zone; 1.13 in gravel zone	Possible plume bypass around south end of PRB. MCLs met in reactive cell.
Watervliet Arsenal, NY (October 1998)	Full	PCE (1,100 µg/L) TCE (1,500 µg/L) <i>cis</i> -DCE (4,200 µg/L) <i>trans</i> -DCE (11 µg/L) VC (1,700 µg/L)	Granular iron and sand mixture	PCE, TCE, <i>cis</i> -DCE, <i>trans</i> -DCE (5 µg/L) VC (2 µg/L)	0.15	
Former manufacturing site, NJ (September 1998)	Full	1,1,1-TCA (1,200 ppb) PCE (19 ppb) TCE (110 ppb)	Granular iron and sand mixture	PCE, TCE (1 µg/L) 1,1,1-TCA (30 µg/L) VC (5 µg/L)	0.6	
Seneca Army depot activity, NY (December 1998)	Full	TCE (4 to 190 µg/L) DCE (43 to 150 µg/L)	Granular iron and sand mixture	TCE, <i>cis</i> -DCE (5 µg/L) VC (2 µg/L)	0.17	
Industrial site, SC (November 1997)	Full	TCE (25 mg/L) <i>cis</i> -DCE (3.5 mg/L) VC (0.9 mg/L)	Granular iron and sand mixture	MCLs: TCE (5 µg/L) <i>cis</i> -DCE (70 µg/L) VC (2 µg/L)	0.14	
Caldwell Trucking, NJ (April 1998)	Full	TCE (6,000-8,000 µg/L)	Granular iron	50 µg/L TCE	1.1	
Private electronics firm, Mountainview, CA	Pilot	<i>cis</i> -DCE (5-10 mg/L) TCE (1 mg/L) VC (5-50 mg/L)	Granular iron			
Drycleaning site, Germany	Full	PCE (20 mg/L) <i>cis</i> -DCE (0.5 mg/L)	Granular iron and iron sponge		2.8	
Bardowie Farm, Cambridge, NZ	Full	Nitrate (50 mg/L)	Native soil and sawdust			

Table 10-2. Update on PRB Site Characteristics and Monitoring (Continued)

PRB Site (Installation Date)	Scale of PRB	Target Contaminants	Reactive Medium	Target Cleanup Levels	Groundwater Velocity in Aquifer (ft/day)	Monitoring Update and Remarks
Massachusetts military reservation (June 1998)	Pilot	TCE (15 µg/L) PCE (300 µg/L)	Granular iron suspended in a guar gum slurry	MCLs: PCE, TCE (5 µg/L)	1	
Belfast, Northern Ireland (December 1995)	Full	TCE (390 mg/L)	Granular Iron	TCE (500 µg/L)		99.7% reduction in TCE and <i>cis</i> -DCE. Low levels (<100 µg/L) of <i>cis</i> -DCE have been detected. VC has not been detected.
Industrial facility, NY (May 1995)	Pilot	TCE (300 µg/L) <i>cis</i> -DCE (500 µg/L) VC (80 µg/L)	Granular iron	MCLs: TCE (5 µg/L) <i>cis</i> -DCE (70 µg/L) VC (2 µg/L)	1	MCLs met within 1.5 ft of travel through the reactive media
Industrial facility, NY (December 1997)	Full	TCE (200-1,280 µg/L) <i>cis</i> -DCE (300-1,800 µg/L) VC (26-53 µg/L)	Granular iron	MCLs: TCE, DCE (5 µg/L) VC (2 µg/L)	0.6	Wall constructed over top of pilot system. MCLs met in iron zone. Relic VOCs in down- gradient aquifer wells.
Intersil, Sunnyvale, CA (February 1995)	Full	TCE (50-200 µg/L) <i>cis</i> -DCE (450-1,000 µg/L) VC (500 µg/L) Freon® 113 (60 µg/L)	Granular iron	TCE (5 µg/L) <i>cis</i> -DCE (6 µg/L) VC (0.5 µg/L) Freon® (1,200 µg/L)	1	MCLs being met after 5 years of operation.
Canadian Forces Base, Borden, Canada	Pilot	PCE (43 mg/L) TCE (250 mg/L)	Granular iron and sand mixture	MCLs: PCE, TCE (5 µg/L)	0.3	90% TCE removed and 88% PCE removed. MCLs not met.

Table 10-2. Update on PRB Site Characteristics and Monitoring (Continued)

PRB Site (Installation Date)	Scale of PRB	Target Contaminants	Reactive Medium	Target Cleanup Levels	Groundwater Velocity in Aquifer (ft/day)	Monitoring Update and Remarks
Denver Federal Center (October 1996)	Full	TCE (600 µg/L) TCA (200 µg/L) <i>cis</i> -DCE (470 µg/L) 1,1-DCE (230 µg/L) VC (15 µg/L)	Granular iron	TCA (200 µg/L) TCE (5 µg/L) <i>cis</i> -DCE (70 µg/L) 1,1-DCE (7 µg/L) VC (2 µg/L) 1,1-DCA (5 µg/L)	0.5	Cleanup targets met in iron, except 1,1-DCA (8 µg/L) in gate effluent. Upgradient mounding may be causing plume bypass over or around the PRB. CVOC concentrations increasing in the groundwater flowing around the south end of barrier. Also, plume potentially may be moving under the barrier.
Former NAS Moffett Field (April 1996)	Pilot ^(a)	TCE (1,300 µg/L) <i>cis</i> -DCE (230 µg/L)	Granular iron	MCLs: TCE (5 µg/L) <i>cis</i> -DCE (70 µg/L)	0.2-0.5	MCLs met in reactive cell. Plume underflow possible through intentional gap between thin aquitard and base of PRB. ^(a)
Somersworth Sanitary Landfill Superfund Site (November 1996)	Pilot	TCE, <i>cis</i> -DCE, VC (<300 µg/L)	Granular iron and sand mixture	MCLs: TCE (5 µg/L) <i>cis</i> -DCE (70 µg/L) VC (2 µg/L)	0.5 to 2.0	Constructability test using bioslurry trench completed in October 1999, prior to full-scale application.

Table 10-2. Update on PRB Site Characteristics and Monitoring (Continued)

PRB Site (Installation Date)	Scale of PRB	Target Contaminants	Reactive Medium	Target Cleanup Levels	Groundwater Velocity in Aquifer (ft/day)	Monitoring Update and Remarks
Former Lowry AFB, CO (December 1995)	Pilot	TCE (1,400 µg/L)	Granular iron	MCLs: TCE (5 µg/L) <i>cis</i> -DCE (70 µg/L)	1	MCLs met
Portsmouth gaseous diffusion plant, OH	Pilot	TCE (70-150 µg/L)	Granular iron in canisters	MCL (5 µg/L)		MCLs met
ORNL, TN	Full	HNO ₃ , uranium, technetium	Granular iron			
East Garrington gas plant, Canada	Pilot	BTEX (12 mg/L)	None			
Fry Canyon Site, UT	Full	Uranium (20,700 µg/L)	Bone char phosphate, foamed zero-valent iron, and amorphous ferric oxide		1.5	
Private Site, Tifton, GA	Full	Pesticides and VOCs	Activated carbon			
Former NAS Alameda, CA (December 1996)	Pilot	<i>cis</i> -DCE (250 mg/L) VC (70,000 mg/L) Toluene (9 mg/L)	Granular iron in first reactive cell; biosparging in following cell		0.42-1.25	Breakthrough of CVOCs due to higher-than-expected CVOC concentrations in gate influent. Residence time in iron reactive cell inadequate.
Public school, Ontario, Canada	Pilot	Phosphate (1.0 mg/L) Nitrate (23 to 82 mg/L)	6% iron and Ca-oxides, 9% Ca limestone, and 85% sand		0.9	
Tonolli Superfund Site, PA	Full	Pb (328 ppb) Cd (77 ppb) As (313 ppb) Zn (1,130 ppb) Cu (140 ppb)	Limestone			

Table 10-2. Update on PRB Site Characteristics and Monitoring (Continued)

PRB Site (Installation Date)	Scale of PRB	Target Contaminants	Reactive Medium	Target Cleanup Levels	Groundwater Velocity in Aquifer (ft/day)	Monitoring Update and Remarks
Nickel Rim Mine, Canada	Full	Sulfate (2,400-3,800 mg/L) Fe (740-1,000 mg/L) Ni (10 mg/L)	Municipal compost, leaf compost, and wood chips		0.13	
Aircraft maintenance facility, OR (March 1998)	Full	VOCs (500 µg/L)	Granular iron		3.0	MCLs met in iron zone.
Industrial Site, KS (January 1996)	Full	TCE (400 µg/L) 1,1,1-TCA (100 µg/L)	Granular iron		0.2	Two additional gates and 3,200 ft of slurry wall were added to system in November 1999.
Cape Canaveral Air Station, FL (November 1997)	Pilot	TCE (90 mg/L) DCE (170 mg/L) VC (7 mg/L)	Granular iron		0.1 to 0.5	
Dover AFB, DE (January 1998)	Pilot	PCE (5,617 µg/L) TCE (549 µg/L) <i>cis</i> -DCE (529 µg/L)	Granular iron (pretreatment zones containing iron-sand or iron-pyrite mixtures)	MCLs: PCE, TCE (5 µg/L) <i>cis</i> -1,2-DCE (70 µg/L) VC (2 µg/L)	0.06-0.3	MCLs met.
Rocky Flats, Golden, CO (July 1998)	Full	PCE (528,000 µg/L) TCE (18,000 µg/L)	Granular iron		0.5 to 2	
Manufactured gas plant, Germany	Full	PAHs (>100 µg/L)	Granular activated carbon			
Wood-treating facility, NH	Pilot	Nonaqueous-phase liquid				
100D Area, Hanford site, WA	Full	Chromate (2 mg/L)	Chemical reducing agent			
Savannah River site, Aiken, SC (July 1997)	Pilot	TCE (200-250 µg/L) <i>cis</i> -DCE (20-50 µg/L) NO ₃ (10-70 mg/L)	Granular iron	MCLs: PCE, TCE (5 µg/L) <i>cis</i> -1,2-DCE (70 µg/L) VC (2 µg/L)	Controlled flowrate	MCLs met in iron zone of Geosiphon.

Table 10-2. Update on PRB Site Characteristics and Monitoring (Continued)

PRB Site (Installation Date)	Scale of PRB	Target Contaminants	Reactive Medium	Target Cleanup Levels	Groundwater Velocity in Aquifer (ft/day)	Monitoring Update and Remarks
DoD facility, SC (November 1998)	Full	1,1,1-TCE (6,000 µg/L) 1,1-DCA (10,000 µg/L) <i>cis</i> -DCE (1,400 µg/L) 1,1-DCE (450 µg/L) VC (240 µg/L)	Granular iron	MCLs: 1,1,1-TCE (200µg/L) 1,1-DCE (7 µg/L) <i>cis</i> -DCE (70 µg/L) VC (2 µg/L)	1.5	Thin iron zones, desorption of VOCs from aquifer strongly influenced results.
Industrial facility, LA (November 1998)	Full	TCE (10,000 µg/L) PCE (260,000 µg/L) <i>cis</i> -DCE (66,000 µg/L) VC (32,000 µg/L) TCE (5,000 µg/L)	Granular iron	PCE (25µg/L) TCE (210 µg/L) <i>cis</i> -DCE (116,000 µg/L) VC (358 µg/L)	0.0003	Very low flow velocity.
DoD facility, WY (August 1999)	Full	TCE (21,000) <i>cis</i> -DCE (560) VC (120)	One segment granular iron; two segments granular iron sand mixture	MCLs: TCE (5 µg/L) <i>cis</i> -DCE (70 µg/L) VC (2 µg/L)	1.33	
DoD facility, NH (August 1999)	Full	TCE (4,700 µg/L) <i>cis</i> -DCE (10,000 µg/L) VC (1,700 µg/L)	Granular iron and sand mixture	MCLs: TCE (5 µg/L) <i>cis</i> -DCE (70 µg/L) VC (2 µg/L)	0.03	
Industrial facility, MA (August, 1999)	Full	PCE (17,000 µg/L) TCE (100 µg/L) <i>cis</i> -DCE (100 µg/L) VC (20 µg/L)	Granular iron	MCLs: TCE (5 µg/L) <i>cis</i> -DCE (70 µg/L) VC (2 µg/L)		
Industrial facility, OH (November, 1999)	Full	TCE (8,000 µg/L) <i>cis</i> -DCE (50 µg/L) <i>trans</i> -DCE (50 µg/L) VC (30 µg/L)	Granular iron and sand mixture	MCLs: TCE, PCE (5 µg/L) <i>cis</i> -DCE (70 µg/L) VC (2 µg/L) 1,1-DCE (7 µg/L)	0.01	

Table 10-2. Update on PRB Site Characteristics and Monitoring (Continued)

PRB Site (Installation Date)	Scale of PRB	Target Contaminants	Reactive Medium	Target Cleanup Levels	Groundwater Velocity in Aquifer (ft/day)	Monitoring Update and Remarks
DoD facility, Travis AFB, CA (July 1999)	Pilot	TCE (10,000 µg/L) <i>cis</i> -DCE (300 µg/L) 1,1-DCE (700 µg/L) <i>cis</i> -DCE (23,200 µg/L)	Fine grained granular iron mixed with aquifer material	MCLs: TCE, PCE (5 µg/L) <i>cis</i> -DCE (70 µg/L) VC (2 µg/L) 1,1-DCE (7 µg/L)	0.2	
NASA Facility, LA (August 1999)	Pilot	TCE (22,500 µg/L) VC (6,810 µg/L) <i>cis</i> -DCE (23,200 µg/L)	Granular iron	TCE (2,600 µg/L) VC (4,500 µg/L) <i>cis</i> -DCE (70,300 µg/L)		
Maxwell AFB, AL (July 1998)	Pilot	TCE (720 µg/L) PCE (<1 µg/L)	Granular iron suspended in a guar gum slurry		0.07-0.2	

(a) PRB is not keyed in to aquitard.

11.0 References

- Agrawal, A., and P.G. Tratnyek. 1994. "Abiotic Remediation of Nitro-Aromatic Groundwater Contaminants by Zero-Valent Iron." *Proceedings of the 207th ACS National Meeting, San Diego, CA*, 34(1): 492-494.
- Agrawal, A., and P.G. Tratnyek. 1996. "Reduction of Nitro Aromatic Compounds by Zero-Valent Iron Metal." *Environ. Sci. Technol.*, 30(1): 153-160.
- Appleton, E.L. 1996. "A Nickel-Iron Wall Against Contaminated Groundwater." *Environmental Science and Technology*, 30(12): 536A-539A.
- Ballard, S. 1996. "The In-Situ Permeable Flow Sensor: A Ground-Water Flow Velocity Meter." *Ground Water*, 34(2): 231-240.
- Battelle. 1997a. *Design Guidance for Application of Permeable Barriers to Remediate Dissolved Chlorinated Solvents*. Prepared for AFRL, Tyndall AFB. February.
- Battelle. 1997b. *Design/Test Plan: Permeable Barrier Demonstration at Area 5, Dover AFB*. Prepared for Air Force Research Laboratory, Tyndall AFB. November 14.
- Battelle. 1998. *Performance Evaluation of a Pilot-Scale Permeable Reactive Barrier at Former Naval Air Station Moffett Field, Mountain View, California*. Prepared for Naval Facilities Engineering Service Center, Port Hueneme, CA. November 20.
- Battelle. 1999. *Final Permeable Reactive Barriers (PRBs) Survey Report*. Prepared for the Naval Facilities Engineering Service Center, Port Hueneme, CA. November 19.
- Battelle. 2000. *Design, Construction, and Monitoring of the Permeable Reactive Barrier in Area 5 at Dover Air Force Base*. Final. Prepared for Tyndall Air Force Base, FL. March 31.
- Benner, S.G., D.W. Blowes, and C.J. Ptacek. 1997. "A Full-Scale Porous Reactive Wall for Prevention of Acid Mine Drainage." *Ground Water Monitor Remediation*, 17(4): 99-108.
- Blowes, D.W., R.W. Puls, T.A. Bennett, R.W. Gillham, C.J. Hanton-Fong, and C.J. Ptacek. 1997. "In-Situ Porous Reactive Wall for Treatment of Cr(VI) and Trichloroethylene in Groundwater." *Proceedings of the International Containment Technology Conference*. St. Petersburg, FL. February 9-12. pp. 851-857.
- Blowes, D.W., C.J. Ptacek, S.G. Benner, C.W.T. McRae, and R.W. Puls. 1998. In International Association of Hydrological Sciences (Publication No. 250), *Groundwater Quality: Remediation*

and Protection. pp. 483-490. Proceedings of the Groundwater Quality Conference, Tubingen, Germany, September 1998.

Borden, R.C., R.T. Goin, and C.-M. Kao. 1997. "Control of BTEX Migration Using a Biologically Enhanced Permeable Barrier." *Ground Water Monitor Remediation*, 17(1): 70-81.

Boronina, T., K.J. Klabunde, and G. Sergeev. 1995. "Destruction of Organohalides in Water Using Metal Particles: Carbon Tetrachloride/Water Reactions with Magnesium, Tin and Zinc." *Environ. Sci. Technol.*, 29: 1511-1517.

Bostick, W.D., R.J. Jarabek, W.A. Slover, J.N. Fiedor, J. Farrell, and R. Heferich. 1996. *Zero-Valent Iron and Metal Oxides for the Removal of Soluble Regulated Metals in Contaminated Groundwater at a DOE Site, K/TSO-35-P*. Lockheed Martin Energy Systems, Inc., Oak Ridge, TN.

Breaux, B. 1996. Personal communication from B. Breaux of Envirowall, Belle Chase, LA, with Battelle.

Burke, G.K. 1996. Personal communication from G.K. Burke of Hayward Baker, Inc., Odneton, MD with Battelle.

Burris, D.R., T.J. Campbell, and V.S. Manoranjan. 1995. "Sorption of Trichloroethylene and Tetrachloroethylene in a Batch Reactive Metallic Iron-Water System." *Environ. Sci. Technol.* 29(11): 2850-2855.

Cantrell, K.J., and Kaplan, D.I. 1996. "Zero-Valent Iron Colloid Construction in Sand Columns." *J. Environ. Eng.* (In press).

Cantrell, K.J., Kaplan, D.I., and Gilmore, T.J. 1997. "Injection of Colloidal Fe⁰ Particles in Sand Columns with Shearthinning Fluids." *J. Environ. Eng.* (Submitted).

Carlson, L. and U. Schwertmann. 1987. "Iron and Manganese Oxides in Finnish Ground Water Treatment Plants." *Water Research*, 21: 165-170.

Cavalli, N.J. 1992. "Composite Barrier Slurry Wall." In D.B. Paul, R.R. Davidson, and N.J. Cavalli (Eds.), *Slurry Walls: Design, Construction and Quality Control, ASTM STP 1129*. American Society for Testing and Materials, Philadelphia, PA.

Chapelle, F.H. 1993. *Ground-Water Microbiology & Geochemistry*. John Wiley & Sons, New York.

Chiu, P.C., and D.K. Cha. 2000. "Characterizing a Culture that Dechlorinates TCE with Fe(0)." Abstract for *Remediation of Chlorinated and Recalcitrant Compounds: The Second International Conference*. Monterey, CA. May 22-25, 2000.

- Clark, D.K., D.F. Darling, T.L. Hineline, and P.H. Hayden. 1997. "Field Trial of the Biowall Technology at a Former Manufactured Gas Plant Site." In *Proceedings of the Mid-Atlantic Industrial Waste Conference*. Technomic Publishing Co., Lancaster, PA. pp. 397-403.
- Czekalla, C., W. Mevius, and H. Hanna. 1985. "Quantitative Removal of Iron and Manganese by Microorganisms in Rapid Sand Filters (In Situ Investigations)." *Water Supply*, 3: 111-123.
- Day, S. 1996. Personal Communication with S. Day of Geo-Con, Inc., Denver, CO.
- Day, S.R., S.F. O'Hannesin, and L. Marsden. 1999. "Geotechnical Techniques for the Construction of Reactive Barriers." *Journ. Haz. Mat.*, 67: 285-297.
- Deng, B., T.J. Campbell, and D.R. Burris. 1997. "Hydrocarbon Formation in Metallic Iron/Water Systems." *Environ. Sci. Technol.*, 31(4): 1185-1190.
- Devlin, J.F. and J.F. Barker. 1999. Field Demonstration of Permeable Wall Flushing for Biostimulation of a Shallow Sandy Aquifer. *Groundwater Monitoring and Remediation*, 19(1): 75-83.
- DOE, see United States Department of Energy.
- Domenico, P.A., and F. W. Schwartz. 1990. *Physical and Chemical Hydrogeology*. John Wiley & Sons, Inc., New York.
- Einarson, M.D., R.L. Langdon, and J.F. Barker. 2000. *Draft Hydraulic Performance of a Funnel-and-Gate Treatment System in a Shallow Tidally-Affected Aquifer: Site 1, Alameda Point, Alameda, California*. Prepared for Naval Facilities Engineering Command under Contract No. N47408-98-C-2210. January.
- EnviroMetal Technologies, Inc. 1996. Personal communication from J. Vogan, EnviroMetal Technologies, Inc., Guelph, Ontario, Canada, with Battelle.
- EnviroMetal Technologies, Inc. 1997. Personal communication from J. Vogan and S. O'Hannesin, EnviroMetal Technologies, Inc., Guelph, Ontario, Canada, with Battelle.
- EnviroMetal Technologies, Inc. 1999. Personal communication from J. Vogan, EnviroMetal Technologies, Inc., Waterloo, Ontario, Canada, with Battelle. November.
- ETI, see EnviroMetal Technologies, Inc.
- Fetter, C.W. 1994. *Applied Hydrogeology*, 3rd ed. Merrill Publishing Company: Columbus, OH.

Focht, R.M. 1994. "Bench-Scale Treatability Testing to Evaluate the Applicability of Metallic Iron for Above-Ground Remediation of 1,2,3-Trichloropropane Contaminated Groundwater." M.Sc. Thesis, Department of Earth Sciences, University of Waterloo, Ontario, Canada. p. 58.

Focht, R.M., J.L. Vogan, and S.F. O'Hannesin. 1997. "Hydraulic Studies of In-Situ PRBs." Unpublished paper, University of Waterloo, Ontario, Canada.

Fruchter, J.S., C.R. Cole, M.D. Williams, V.R. Vermeul, S.S. Teel, J.E. Amonette, J.E. Szecsody, and S.B. Yabusaki. 1997. "Creation of a Subsurface Permeable Reactive Barrier Using In Situ Redox Manipulation." *Proceedings of International Containment Technology Conference and Exhibition*. St. Petersburg, FL, February 9-12. pp. 704-710.

Gavaskar, A.R., B.M. Sass, E. Drescher, L. Cumming, D. Giammar, and N. Gupta. 1998. "Enhancing the Reactivity of Permeable Barrier Media." In G.B. Wickramanayake and R.E. Hinchey (Eds.), *Designing and Applying Treatment Technologies: Remediation of Chlorinated and Recalcitrant Compounds*, vol. C1-6. Proceedings of the First International Conference on Remediation of Chlorinated and Recalcitrant Compounds, Battelle Press.

Gavaskar, A.R. 1999. "Design and Construction Techniques for Permeable Reactive Barriers." *Journ. Haz. Mat.*, 68: 41-71.

Gillham, R.W. 1993. Cleaning Halogenated Contaminants from Groundwater. U.S. Patent No. 5,266,213. November 30.

Gillham, R.W. 1996. "In Situ Treatment of Groundwater: Metal-Enhanced Degradation of Chlorinated Organic Contaminants." In M.M. Aral (Ed.), *Advances in Groundwater Pollution Control and Remediation*, pp. 249-274. Kluwer Academic Publishers, New York, NY.

Gillham, R.W., D.W. Blowes, C.J. Ptacek, and S.F. O'Hannesin. 1994. "Use of Zero-Valent Metals in In-Situ Remediation of Contaminated Ground Water." In G.W. Gee and N.R. Wing (Eds.), *In-Situ Remediation: Scientific Basis for Current and Future Technologies*. Battelle Press, Columbus, OH. pp. 913-930.

Gillham, R.W., and S.F. O'Hannesin. 1992. "Metal-Catalyzed Abiotic Degradation of Halogenated Organic Compounds." *IAH Conference: Modern Trends in Hydrogeology*. Hamilton, Ontario, May 10-13. pp. 94-103.

Gillham, R.W., and S.F. O'Hannesin. 1994. "Enhanced Degradation of Halogenated Aliphatics by Zero-Valent Iron." *Ground Water*, 32: 958-967.

Gillham, R.W., S.F. O'Hannesin, and W.S. Orth. 1993. "Metal Enhanced Abiotic Degradation of Halogenated Aliphatics: Laboratory Tests and Field Trials." Paper presented on March 9-11, HazMat Central Conference, Chicago, IL.

- Hardy, L.I., and R.W. Gillham. 1996. "Formation of Hydrocarbons from the Reduction of Aqueous CO₂ by Zero-Valent Iron." *Environ. Sci. Technol.*, 30(1): 57-65.
- Hayes, J.J., and D.L. Marcus. 1997. "Design of a Permeable Reactive Barrier In Situ Remediation System, Vermont Site." In *Proceedings of the In Situ Remediation of the Geoenvironment Conference*, 12: 56-67. American Society of Civil Engineers, Minneapolis, MN, October 5-8.
- Herbert, R.B., S.G. Benner, and D.W. Blowes. 1998. "Reactive Barrier Treatment of Groundwater Contaminated by Acid Mine Drainage: Sulphur Accumulation and Sulphide Formation." In International Association of Hydrological Sciences (Publication No. 250), *Groundwater Quality: Remediation and Protection*. pp. 451-457. Proceedings of the Groundwater Quality Conference, Tübingen, Germany, September 1998.
- Hocking, G., S.L. Wells, and R.I. Ospina. 1998. "Design and Construction of Vertical Hydraulic Fracture Placed Iron Reactive Walls." *Proceedings of the First International Conference on Remediation of Chlorinated and Recalcitrant Compounds*, vol. C1-6. Battelle Press. Monterey, CA. May 18-21. pp. 103-108.
- Holser, R.A., S.C. McCutcheon, and N.L. Wolfe. 1995. "Mass Transfer Effects on the Dehalogenation of Trichloroethene by Iron/Pyrite Mixtures." *Extended Abstracts from the 209th ACS National Meeting, Anaheim, Cal.*, 35(1): 788-791. Anaheim, CA. Div. Of Environ. Chem., Am. Chem. Soc., Washington, D.C.
- Hubble, D.W., R.W. Gillham, and J.A. Cherry. 1997. "Emplacement of Zero-Valent Metal for Remediation of Deep Contaminant Plumes." *Proceedings of the International Containment Technology Conference*. St. Petersburg, FL. February 9-12. pp. 872-878.
- Interstate Technology and Regulatory Cooperation Working Group. 1997. *Regulatory Guidance for Permeable Barrier Walls Designed to Remediate Dissolved Chlorinated Solvents*. Prepared by ITRC Work Group Permeable Barriers Work Team.
- Interstate Technology and Regulatory Cooperation Working Group. 1999. *Regulatory Guidance for Permeable Reactive Barriers Designed to Remediate Inorganic and Radionuclide Contamination*. Draft. Prepared by ITRC Work Group Permeable Barrier Walls Work Team. January 29.
- ITRC, see Interstate Technology and Regulatory Cooperation Working Group.
- Jeffers, P.M., L.M. Ward, L.M. Woytowitch, and N.L. Wolfe. 1989. "Homogeneous Hydrolysis Rate Constants for Selected Chlorinated Methanes, Ethanes, Ethenes and Propanes." *Environ. Sci. Technol.*, 23(8): 965-969.
- Kaplan, D.I., K.J. Cantrell, T.W. Wietsma, and M.A. Potter. 1996. "Formation of a Chemical Barrier with Zero-Valent Iron Colloids for Groundwater Remediation." *J. Environ. Qual.*, 25: 1086-1094.

Kearl, P.M. 1997. "Observations of Particle Movement in a Monitoring Well Using the Colloidal Borescope." *Journal of Hydrology* (200): 323-344.

Kearl, P.M., N.E. Korte, M. Stites, and J. Baker. 1994. "Field Comparison of Micropurging vs. Traditional Ground Water Sampling." *Ground Water Monitoring and Remediation*, 14(4): 183-190.

Kershaw, D.S., and S. Pamukcu. 1997. "Ground Rubber: Reactive Permeable Barrier Sorption Media." In *Proceedings of the American Society of Civil Engineers Conference on In Situ Remediation of the Geoenvironment*: 26-40.

Kilfe, H. 1996. Personal communication from H. Kilfe, Water Resources Control Engineer, California Regional Water Quality Control Board, with Battelle.

Korte, N.E. 1999. Personal communication from N.E. Korte, Oak Ridge National Laboratory, Grand Junction, CO, with Battelle. October.

Korte, N.E., L. Liang, and J. Clausen. 1995. "The Use of Palladized Iron as a Means of Treating Chlorinated Contaminants." *Emerging Technologies in Hazardous Waste Management VII, Extended Abstracts for the Special Symposium*. Atlanta, GA. pp. 42-45.

Kriegman-King, M.R., and M. Reinhard. 1991. "Reduction of Hexachloroethane and Carbon Tetrachloride at Surfaces of Biotite, Vermiculite, Pyrite, and Marcasite." In R.A. Baker (Ed.), *Organic Substances and Sediments in Water*, Vol. 2. Lewis Publishers, Chelsea, MI.

Kriegman-King, M.R., and M. Reinhard. 1994. "Transformation of Carbon Tetrachloride by Pyrite in Aqueous Solution." *Environ. Sci. Technol.*, 28: 692-700.

Kruseman, G.P., and N.A. de Ridder. 1991. *Analysis and Evaluation of Pumping Test Data*, 2nd ed. (completely revised). International Institute for Land Reclamation and Improvement, Wageningen, The Netherlands, Publication 47.

Landis, R. 1998. "Potential Use of Jetting to Emplace Permeable Reactive Barriers." Presentation Materials for the *RTDF Permeable Reactive Barriers Action Team Meeting*. Beaverton, OR. April 15-16. pp. 51.

Lipczynska-Kochany, E., S. Harms, R. Milburn, G. Sprah, and N. Nadarajah. 1994. "Degradation of Carbon Tetrachloride in the Presence of Iron and Sulphur Containing Compounds." *Chemosphere*, 29: 1477-1489.

Lütters-Czekalla, S. 1990. "Lithoautotrophic Growth of the Iron Bacterium *Gallionella ferruginea* with Thiosulfate or Sulfide as Energy Source." *Archives of Microbiology*, 154: 417-421.

Mackenzie, P.D., S.S. Baghel, G.R. Eykholt, D.P. Horney, J.J. Salvo, and T.M. Sivavec. 1995. "Pilot-Scale Demonstration of Reductive Dechlorination of Chlorinated Ethenes by Iron Metal." Presented at the 209th ACS National Meeting, Anaheim, CA, April 2-6.

Mackenzie, P.D., D.P. Horney, and T.M. Sivavec. 1999. "Mineral Precipitation and Porosity Losses in Granular Iron Columns." *Journal of Hazardous Materials*, 68: 1-17.

Marchand, E.G., P.A. Shirley, K.A. McNelis, and T.L. Fiorillo. 1998. "New Installation Techniques in Side-by-Side Demonstrations at Cape Canaveral Air Station." Presentation Materials for the *RTDF Permeable Reactive Barriers Action Team Meeting*. Beaverton, OR. April 15-16. pp. 23-24.

Matheson, L.J., and P.G. Tratnyek. 1994. "Reductive Dehalogenation of Chlorinated Methanes by Iron Metal." *Environ. Sci. Technol.*, 28: 2045-2053.

Morkin, M., J. Barker, R. Devlin, and M. McMaster. 1998. "In Situ Sequential Treatment of a Mixed Organic Plume Using Granular Iron, O₂, and CO₂ Sparging." In G.B. Wickramanayake and R.E. Hinchee (Eds.), *Proceedings of the First International Conference on Remediation of Chlorinated and Recalcitrant Compounds: Designing and Applying Treatment Technologies* (Vol C1-6). Battelle Press, Columbus, OH. Conference held in Monterey, CA, May 18-21, 1998.

Muftikian, R., Q. Fernando, and N. Korte. 1995. "A Method for the Rapid Dechlorination of Low Molecular Weight Chlorinated Hydrocarbons in Water." *Water Res.*, 29: 2434.

Myller, B. 1996. Personal communication from B. Myller of Dames and Moore, with Battelle.

National Research Council. 1994. *Alternatives for Ground Water Clean Up*. National Academy Press, Washington, DC.

O'Hannesin, S.F. 1993. A Field Demonstration of a Permeable Reaction Wall for the In Situ Abiotic Degradation of Halogenated Aliphatic Organic Compounds. Unpublished M.S. thesis, University of Waterloo, Ontario, Canada.

Orth, R.G., and D.E. McKenzie. 1995. "Reductive Dechlorination of Chlorinated Alkanes and Alkenes by Iron Metal and Metal Mixtures." *Extended Abstracts from the Special Symposium Emerging Technologies in Hazardous Waste Management VII*. American Chemical Society, Atlanta, GA. p. 50.

Orth, W.S., and R.W. Gillham. 1995. "Chloride and Carbon Mass Balances for Iron-Enhanced Degradation of Trichloroethene." Presented at the 209th ACS National Meeting, Anaheim, CA, April 2-6.

Orth, W.S., and R.W. Gillham. 1996. "Dechlorination of Trichloroethene in Aqueous Solution Using Fe(0)." *Environ. Sci. Technol.*, 30(1): 66-71.

Owaidat, L. 1996. Personal communication from L. Owaidat of Geo. Con., Inc., Rancho Cordova, CA, with Battelle.

Piana, M.J., G.W. Freethey, D.L. Naftz, C.C. Fuller, and J.A. Davis. 1999. "Investigation of Flow Through a Permeable Reactive Barrier Using Ionic Tracers and Groundwater Modeling." *Eos, Transactions, AGU*, 80(46): F325. November 16.

Powell, R.M. and R.W. Puls, 1997. "Hitting the Bull's-Eye in Groundwater Sampling." *Pollution Engineering*, June: 51-54.

PRC, see PRC Environmental Management, Inc.

PRC Environmental Management, Inc. 1996. *Naval Air Station Moffett Field, California, Iron Curtain Area Groundwater Flow Model*. June.

Puls, R.W., R.M. Powell, and C.J. Paul. 1995. "In Situ Remediation of Ground Water Contaminated with Chromate and Chlorinated Solvents Using Zero-Valent Iron: A Field Study." *Extended Abstracts from the 209th ACS National Meeting Anaheim, CA*, 35(1): 788-791. Anaheim, CA. Div. of Environ. Chem., Am. Chem. Soc., Washington, DC.

Reardon, E.J. 1995. "Anaerobic Corrosion of Granular Iron: Measurement and Interpretation of Hydrogen Evolution Rates." *Environ. Sci. Technol.*, 29(12): 2936-2945.

Reynolds, G.W., J.T. Hoff, and R.W. Gillham. 1990. "Sampling Bias Caused by Materials Used to Monitor Halocarbons in Groundwater." *Environ. Sci. Technol.*, 24(1): 135-142.

Roberts, A.L., L.A. Totten, W.A. Arnold, D.R. Burris, and T.J. Campbell. 1996. "Reductive Elimination of Chlorinated Ethylenes by Zero-Valent Metals." *Environ. Sci. Technol.*, 30(8): 2654-2659.

Rocky Mountain Remediation Services. 1999. Draft Mound Site Plume Project Completion Report, Fiscal Year 1998. January.

Schmithorst, B. 1996. Personal communication from B. Schmithorst of Parsons Engineering Science, with Battelle.

Schreier, C.G., and M. Reinhard. 1994. "Transformation of Chlorinated Organic Compounds by Iron and Manganese Powders in Buffered Water and in Landfill Leachate." *Chemosphere*, 29: 1743-1753.

Senzaki, T. 1988. "Removal of Chlorinated Organic Compounds from Wastewater by Reduction Process: III. Treatment of Tetrachloroethane with Iron Powder II." *Kogyo Yosui*, 391: 29-35 (in Japanese).

Senzaki, T., and Y. Kumagai. 1988a. "Removal of Chlorinated Organic Compounds from Wastewater by Reduction Process: Treatment of 1,1,2,2-Tetrachloroethane with Iron Powder." *Kogyo Yosui*, 357: 2-7 (in Japanese).

Senzaki, T., and Y. Kumagai. 1988b. "Removal of Chlorinated Organic Compounds from Wastewater by Reduction Process: II. Treatment of Tetrachloroethane with Iron Powder." *Kogyo Yosui*, 369: 19-25 (in Japanese).

Shikaze, S. 1996. *3D Numerical Modeling of Groundwater Flow in the Vicinity of Funnel-and-Gate Systems*. ARA-TR-96-5286-1. Prepared by Applied Research Associates, Inc. for U.S. Air Force, Tyndall Air Force Base, April.

Sivavec, T.M. 1996. Personal communication from T.M. Sivavec, General Electric Corporate Research and Development, Schenectady, NY., with Battelle.

Sivavec, T.M. 1997. Personal communication from T.M. Sivavec, General Electric Corporate Research and Development, Schenectady, NY., with Battelle.

Sivavec, T.M. 1999. Personal communication from T.M. Sivavec, General Electric Corporate Research and Development, Schenectady, NY with Bruce Sass of Battelle.

Sivavec, T.M., and D.P. Horney. 1995. "Reductive Dechlorination of Chlorinated Ethenes by Iron Metal." Presented at the 209th ACS National Meeting, Anaheim, CA. April 2-6.

Sivavec, T.M., P.D. Mackenzie, D.P. Horney, and S.S. Baghel. "Redox-Active Media for Permeable Reactive Barriers." *Proceedings of the 1997 International Containment Technology Conference and Exhibition*, St. Petersburg, FL: 9-12.

Smith, D., J. Cherry, and R. Jowett. 1995. "Sealable Joint Steel Sheet Piling for Groundwater Pollution Control." In *Proceedings of ER '95: Committed to Results*. U.S. Department of Energy, Denver, CO.

Starr, R.C., and J.A. Cherry. 1994. "In Situ Remediation of Contaminated Ground Water: The Funnel-and-Gate System." *Ground Water*, 32(3): 465-476.

Su, C., and R.W. Puls. 1998. "Temperature Effect on Reductive Dechlorination of Trichloroethene by Zero-Valent Metals." In G.B. Wickramanayake and R.E. Hinchey (Eds.), *Proceedings of the First International Conference on Remediation of Chlorinated and Recalcitrant Compounds: Physical, Chemical, and Thermal Technologies* (Vol. C1-5). Battelle Press, Columbus, OH. Conference held in Monterey, CA, May 18-21, 1998.

Sweeny, K.H. 1981a. "The Reductive Treatment of Industrial Wastewaters: I. Process Description." In G.F. Bennett (Ed.), *American Institute of Chemical Engineers, Symposium Series, Water-1980*, 77(209): 67-71.

Sweeny, K.H. 1981b. "The Reductive Treatment of Industrial Wastewaters: II. Process Description." In G.F. Bennett (Ed.), *American Institute of Chemical Engineers, Symposium Series, Water-1980*, 77(209): 72-88.

Sweeny, K.H. 1983. Treatment of Reducible Halohydrocarbons Containing Aqueous Stream. U.S. Patent 4,382,865.

Sweeny, K.H., and J.R. Fischer. 1972. Reductive Degradation of Halogenated Pesticides. U.S. Patent No. 3,640,821. February 8.

Thombre, M.S., B.M. Thomson, and L.L. Barton. 1997. "Use of a Permeable Biological Reaction Barrier for Groundwater Remediation at a Uranium Mill Tailings Remedial Action (UMTRA) Site." In DOE's *Proceedings of the International Containment Technology Conference and Exhibition*. Conference held at St. Petersburg, FL, February 9-12, 1997.

Tuhela, L., L. Carlson, and O.H. Tuovinen. 1992. "Ferrihydrite in Well Water Samples and Bacterial Enrichment Cultures." *Water Research*, 26: 1159-1162.

Tuhela, L., S.A. Smith, and O.H. Tuovinen. 1993. "Microbiological Analysis of Iron-Related Biofouling in Water Wells and a Flow-Cell Apparatus for Field and Laboratory Investigations." *Ground Water*, 31: 982-988.

United States Department of Energy. 1998. *Standard Life-Cycle Cost-Savings Analysis Methodology for Deployment of Innovative Technologies*. DOE Office of Environmental Management, Federal Energy Technology Center. October 30.

United States Environmental Protection Agency. 1993. Revisions to OMB Circular A-94 on Guidelines and Discount Rates for Benefit-Cost Analysis. Revised annually at <http://www.whitehouse.gov/OMB/circulars/a094/a094.html#ap-c>.

United States Environmental Protection Agency. 1995. *In Situ Remediation Technology Status Report: Treatment Walls*. EPA 542-K-94-004. U.S. EPA, Office of Solid Waste and Emergency Response. April.

United States Environmental Protection Agency. 1997. Selection of Media for the Dover AFB Field Demonstration of Permeable Barriers to Treat Groundwater Contaminated with Chlorinated Solvents. Preliminary Report to U.S. Air Force for SERDP Project 107. August 4.

United States Environmental Protection Agency. 1998. *Permeable Reactive Barrier Technologies for Contaminant Remediation*. EPA 600-R-98-125.

U.S. EPA, see United States Environmental Protection Agency.

Venhuis, M., S. Lesage, K.R. Millar, and A.S. Crowe. 1999. "Evaluation of Polyalkastylene Absorbent Beads for the Remediation of PCE in Groundwater." *Water Quality Research Journal of Canada*, 34(3): 455-468.

Waybrant, K.R., D.W. Blowes, and C.J. Ptacek. 1998. "Selection of Reactive Mixtures for Use in Permeable Reactive Walls for Treatment of Mine Drainage." *Environ. Sci. Technol.*, 32(13): 1972-1979.

Werner, P. 1998. "Impact of Microbial Processes on the Efficiency of Reactive Walls." In International Association of Hydrological Sciences (Publication No. 250), *Groundwater Quality: Remediation and Protection*. pp. 497-500. Proceedings of the Groundwater Quality Conference, Tubingen, Germany, September 1998.

Westinghouse Savannah River Company. 1999. *GeoSiphon™ /GefLow™ Technology, Subsurface Contaminants Focus Area*. June.

WSRC, see Westinghouse Savannah River Company.

Yamane, C.L., S.D. Warner, J.D. Gallinati, F.S. Szerdy, T.A. Delfino, D.A. Hankins, and J.L. Vogan. 1995. "Installation of a Subsurface Groundwater Treatment Wall Composed of Granular Zero-Valent Iron." Preprinted of paper presented at the 209th ACS National Meeting, Anaheim, CA. April 2-7. *Proceedings*, 35(1): 793-795.

Appendix A

Points of Contact

Appendix A

Points of Contact

AFRL Project Officer

Alison Lightner
Air Force Research Laboratory (AFRL)
139 Barnes Drive, Suite 2
Tyndall AFB, FL 32403
Tel: (850) 283-6303
Fax: (850) 283-6064
E-Mail: alison.lightner@tyndall.af.mil

Technical Information Center
Tel: (850) 283-6285
E-Mail: andrew.poulis@tyndall.af.mil

Battelle Project Manager

Arun R. Gavaskar
Battelle
505 King Avenue
Columbus, OH 43201
Tel: (614) 424-3403
Fax: (614) 424-3667
E-Mail: gavaskar@battelle.org

SERDP Contact

Catherine Vogel
SERDP Program Office
901 North Stuart Street, Suite 303
Arlington, VA 22203
Tel: (703) 696-2118
Fax: (703) 696-2114
E-Mail: vogelc@acq.osd.mil

DoD Contact for Tri-Agency PRB Initiative

Charles Reeter
Naval Facilities Engineering Service Center (NFESC)
1100 23rd Street
Port Hueneme, CA 93043
Tel: (805) 982-4991
Fax: (805) 982-4304
E-Mail: reetercv@nfesc.navy.mil

Appendix B

Cost Evaluation of a PRB at Dover AFB

B.1 Capital Investment

B.2 Scaleup

B.3 Projected Operating and Maintenance Costs

B.4 Present Value Analysis of PRB and P&T Options

Appendix B

Cost Evaluation of a PRB at Dover AFB

The cost evaluation of the permeable reactive barrier (PRB) in Area 5 at Dover Air Force Base (AFB) includes the actual capital investment required for the pilot-scale PRB installed in December 1997 (Figure B-1) and the estimated capital investment for a proposed scaleup (Figure B-2). Also, annual operating and maintenance (O&M) costs are projected for the scaled-up PRB only. Finally, a present value (PV) analysis is provided which compares the long-term costs of a PRB and an equivalent pump-and-treat (P&T) system.

B.1 Capital Investment

Table B-1 lists the capital investment incurred in installing a pilot-scale PRB in Area 5. This PRB is a funnel-and-gate system with two gates. Each gate is 4 ft wide and is keyed into the aquitard at a depth of 39 ft. Each gate has a 4-ft thickness of iron and incorporates a pretreatment zone (PTZ) and an exit zone. The funnel is 60 ft wide, giving a total barrier width of 68 ft. The PRB is estimated to capture about 50-ft width of plume in an aquifer that is approximately 25 ft thick. The various items in Table B-1 include the costs incurred by Battelle and its construction subcontractor (C³ Environmental), as well as broad estimates of relevant costs incurred by Dover AFB staff for site arrangements and by the United States Environmental Protection Agency's National Exposure Research Laboratory (U.S. EPA-NERL) for the on-site column tests.

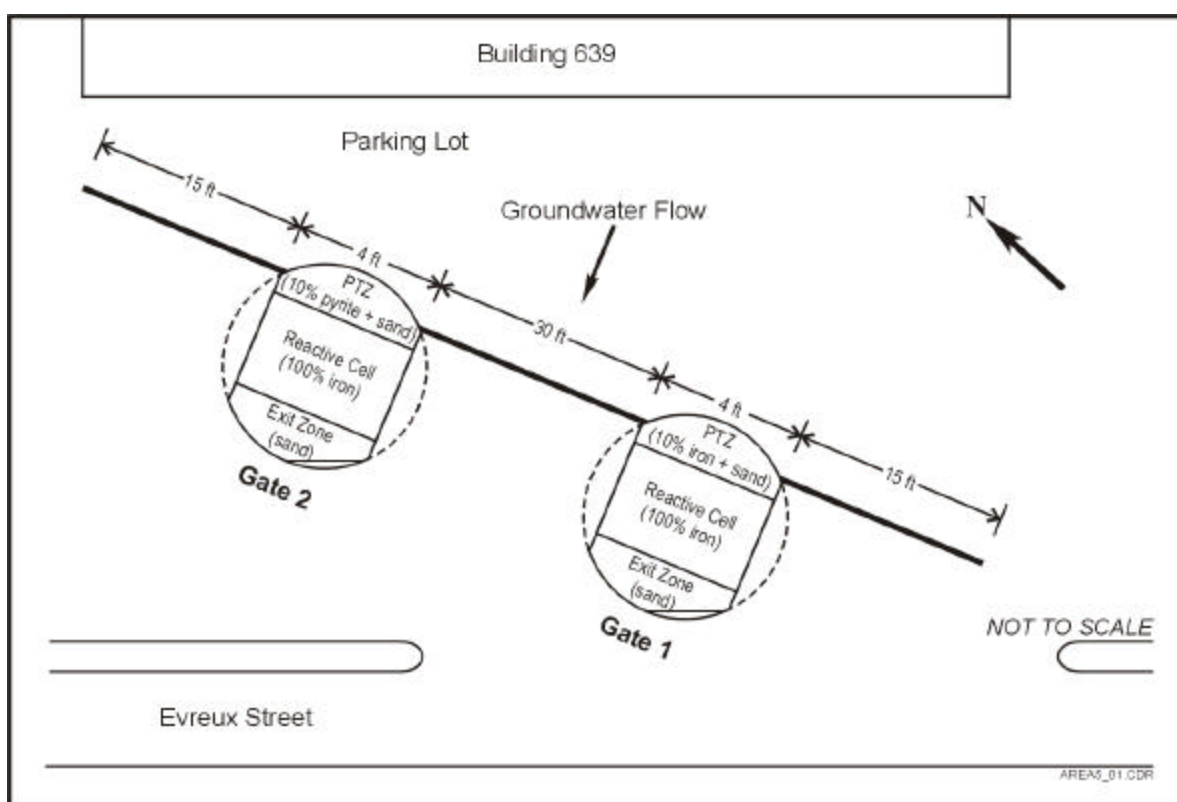


Figure B-1. Schematic of the Pilot-Scale PRB in Area 5 at Dover AFB

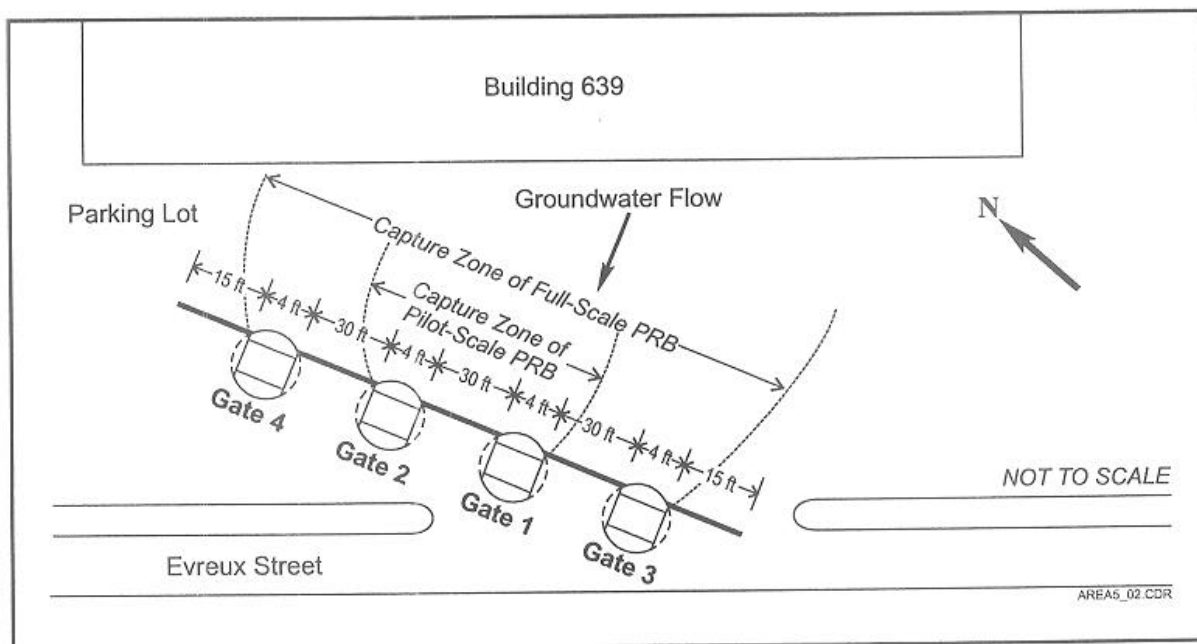


Figure B-2. Schematic of the Scaleup of the PRB

Table B-1 lists the capital investment costs for the pilot-scale PRB in two categories: preconstruction activities and PRB construction activities. Site characterization was a key cost driver in the preconstruction category. Because the PRB is an in situ structure, it is all the more important that the chlorinated volatile organic compound (CVOC) distribution and aquifer characteristics be well defined. In a P&T system, site characterization and design deficiencies can be corrected after system installation by adding additional wells or adjusting the aboveground treatment system. However, once a PRB has been installed, making system adjustments or expansions can be relatively expensive. Another factor driving the characterization cost at Area 5 was that the bulk of the plume was not in the area identified by data from regional wells as reported in the existing Remedial Investigation/Feasibility Study (RI/FS) documents. Characterization activities were redirected after data from temporary wells pushed during additional site characterization activities (June 1997) became available.

The column test costs in Table B-1 illustrate the type of long-term on-site tests conducted for the Dover AFB pilot-scale effort on reactive media selection and degradation rate estimation. For a full-scale application, much less rigorous column tests are required, with a concomitantly lower cost.

The design, procurement, and regulatory review costs include activities such as site characterization, data evaluation, hydrologic and geochemical modeling, draft and final design/test plan preparation, evaluation and procurement of reactive media suppliers and construction subcontractors, and regulatory review. Procurement of a commercial source of pyrite proved to be particularly challenging, because pyrite is no longer the primary source for sulfuric acid production in the chemical industry. Procuring a construction subcontractor involved solicitation of bids, arrangement of a site visit for prospective vendors, and selection of the best technical and cost

Table B-1. Capital Investment Incurred in Installing the Field Pilot-Scale PRB in Area 5

Item	Description	Basis	Cost^(a)
<i>Phase 1: Preconstruction Activities</i>			
Preliminary site assessment	Historical site data evaluation	RI/FS, other reports procurement and evaluation; site meeting	\$15,000
Site characterization	Characterization plan, fieldwork, laboratory analysis	Cone penetrometer test (CPT) pushes for geologic mapping and temporary wells; analysis of water samples for CVOCs; select samples for geotechnical analysis; slug tests; ground-penetrating radar survey ^(b)	\$150,000
Column tests	Two columns for two reactive media combinations; Area 5 groundwater	Three-month on-site test and laboratory analysis of water samples ^(b) ; report	\$100,000 ^(b)
Design; procurement; regulatory review	Data evaluation, modeling, engineering design, Design/Test Plan; construction subcontractor procurement; regulatory interactions	Characterization, column test data evaluation; hydrogeologic modeling; geochemical evaluation; engineering design; report; procurement process; regulatory approvals; preconstruction meeting	\$100,000
Subtotal			\$365,000
<i>Phase 2: PRB Construction Activities</i>			
Site preparation	Utilities clearances; arrangement for equipment/media storage and debris disposal	Coordination with Base facilities staff	\$10,000
Reactive media procurement	Connelly iron, shipping; pyrite source identification, procurement; pyrite chunks, crushing, sizing, shipping.	Iron: 54 tons @ \$360/ton Pyrite: 5 tons @ \$1,400/ton Pyrite preparation: \$12,000 Shipping: \$9,000	\$47,000
PRB Construction	Mobilization/demobilization; installation of two 8-ft-diameter caisson gates to 40-ft depth and one 60-ft-long sheet pile funnel; restoration of asphalt parking lot	Mob./demob.: \$38,000 Gates: \$133,000 Monitoring wells: \$25,000 Funnel: \$51,000 Surface restoration: \$17,000	\$264,000
Monitoring system construction	Thirty-four polyvinyl chloride (PVC) aquifer wells installed for monitoring the pilot-scale PRB (fewer wells would be required for a full-scale system); four in situ groundwater velocity sensors	Aquifer wells: \$37,000 Velocity sensors: \$16,000	\$53,000
Subtotal			\$374,000
TOTAL			\$739,000

(a) Includes costs incurred for labor and materials by Battelle and its construction subcontractor C³ Environmental, as well as broad estimates of relevant costs incurred by Dover AFB staff for site arrangements and by U.S. EPA-NERL for the on-site column tests. Some cost items in this table may not be applicable at other sites.

(b) This level of testing was done for demonstration purposes and may be excessive for full-scale application.

bid. The PRB design was finalized only after discussion of several alternative designs and construction techniques with various bidders and a preconstruction meeting with the winning bidder.

Site preparation involved acquisition of clearances from the Base utilities office, arrangements to receive reactive media and construction equipment shipments, and arrangements to dispose of the construction debris. On a per ton basis, the pyrite was costlier than iron, especially after pyrite processing costs were included. It is presumed that if pyrite use for PRB applications grow, less expensive sources of pyrite may become available over time.

PRB construction costs at this site were driven by the cost of installing the caisson gates. However, this method of installation was found to be less costly compared with other alternatives. Also, caisson gates were easier to install in the midst of multiple utility lines that crisscross Area 5. Note that the mobilization/demobilization costs at this site are probably lower than at other sites, because the construction subcontractor used a local partner in Dover, DE to supply most of the heavy equipment and operators, such as the 100-ton crane, 5-ft-diameter auger, and the pile driver. Having this equipment locally available also significantly minimized the time periods that this equipment had to be retained on site. Most of the heavy equipment and operators were requisitioned only on the days that the equipment was actually used. These advantages may not be available at other sites.

Because of the research needs of the demonstration, more monitoring wells were installed than would be required for full-scale application. The monitoring system also includes the installation of the four velocity sensors.

B.2 Scaleup

Although the PRB in Area 5 is considered pilot-scale, its relatively large size (68 ft wide and 39 ft deep) makes its economics easily scalable to a full-scale PRB. CVOC contamination at Area 5 of Dover AFB is fairly widespread, with elevated CVOC concentrations identified in wells on both the north and south sides of Building 639. During additional site characterization in June 1997, an effort was made to identify the most contaminated portion of the plume for this demonstration; however, the boundaries of the entire plume were not mapped. Also, CVOC concentrations at Area 5 tend to vary sharply in both horizontal and vertical planes, indicating the presence of multiple sources of contamination. Lastly, the aquifer region under Building 639 remains unsampled and the CVOC distribution in that region is unknown.

Dover AFB is considering expanding the current pilot-scale PRB to capture more of the plume. In that event, additional site characterization to delineate more of the plume would be required. Based on the CVOC data from monitoring points on the fringes of the demonstration area, it is suspected that the plume may be at least 100 ft wide. The local gradients that drive the movement of this larger plume would have to be evaluated during additional characterization. Local gradients, on the scale of the parking lot at Area 5, will determine whether an extended PRB would continue along a straight line along the current orientation or would be angled from the edges of the current funnel. Based on regulatory and cost considerations, a decision will have to be made as to how much of the larger plume would need to be captured and treated.

To capture a 100-ft width of the plume with the current configuration, two more gates would have to be added to double the capture zone, as the current pilot system captures a 40- to 50-ft-width of the plume. The two additional gates could be installed with caissons, and the funnel could be extended using additional sheet piles. The scaled-up system is shown in Figure B-2. The costs of this extended barrier are listed Table B-2. The costs have been estimated as if the full-scale barrier had been installed right at the beginning, instead of installing the pilot-scale barrier and then extending it.

In Table B-2, Phase 1 costs remain mostly the same as in Table B-1. One difference is that \$50,000 has been added to reflect the cost of additional site characterization to locate the

Table B-2. Capital Investment Projected for Installing a Full-Scale PRB at Dover AFB

Item	Description	Basis	Cost
<i>Phase 1: Preconstruction Activities</i>			
Preliminary site assessment	Historical site data evaluation	RI/FS, other reports procurement and evaluation; site meeting	\$15,000
Site characterization	Characterization Plan, fieldwork, laboratory analysis	CPT pushes for geologic mapping and temporary wells; analysis of water samples for CVOCs; select samples for geotechnical analysis; slug tests	\$200,000
Column tests	Two column tests; Area 5 groundwater	Column tests and laboratory analysis of water samples; report	\$50,000
Design, procurement of subcontractors, and regulatory review	Data evaluation, modeling, engineering design, Design Plan; procurement of subcontractors; interactions with regulators	Characterization, column test data evaluation; hydrogeologic modeling; geochemical evaluation; engineering design; report; procurement process; regulatory interactions	\$100,000
Subtotal			\$365,000
<i>Phase 2: PRB Construction Activities</i>			
Site preparation	Utilities clearances; arrangements for equipment/media storage and debris disposal	Coordination with regulators and Base facilities staff	\$10,000
Reactive media procurement	Connelly iron, shipping	Iron: 108 tons @ \$360/ton Shipping: \$9,000	\$48,000
PRB Construction	Mobilization/demobilization; Installation of four 8-ft-diameter caisson gates to 40-ft depth, and one 120-ft-long sheet pile funnel; restoration of asphalt parking lot	Mob./demob.: \$60,000 Gates: \$266,000 Monitoring wells: \$25,000 Funnel: \$102,000 Surface restoration: \$34,000	\$487,000
Monitoring system construction	Thirty-four PVC aquifer wells installed for monitoring the pilot-scale PRB	Aquifer wells: \$37,000	\$37,000
Subtotal			\$582,000
TOTAL			\$947,000

boundaries of the plume and assess the geology along a longer length. Another difference is that the column test costs have been reduced to reflect the less rigorous tests required for the full-scale application. In Phase 2, several of the items change. Assuming that only iron is used in the gates (no pyrite), the reactive media cost does not change significantly because the additional iron required costs much less than the small amounts of pyrite that it replaces.

In the category of PRB construction, mobilization/demobilization costs have been increased compared to the pilot system in order to reflect transportation of additional sheet piles and other materials. For a full-scale system, the same number of wells as currently installed for the pilot-scale system could be redistributed over the four gates; a higher number of wells was used for demonstration purposes for the pilot system. The costs for the gates, funnel, and surface restoration have been doubled to reflect the addition of two more gates and another 60 ft of funnel. The aquifer monitoring system cost was kept the same, based on the assumption that the same number of wells could be spread over a larger area. Also, the HydroTechnics velocity meters have been eliminated.

B.3 Projected Operating and Maintenance Costs

The expected O&M costs of the full-scale barrier over the next several years consist of:

- ❑ **Annual monitoring cost.** This item relates to the groundwater sampling and analysis and water-level measurements that would be required to verify acceptable capture and treatment of the plume.
- ❑ **Periodic maintenance cost.** Assuming that the reactivity and/or hydraulic performance of the reactive cell may decline before the plume (or the possible DNAPL source) dissipates, it is probable that some maintenance would be required to regenerate or replace the reactive medium.

It is presumed that groundwater sampling for CVOC analysis would have to be conducted on a quarterly basis, consistent with the regulatory sampling conducted on the rest of the Base. Water levels also could be measured on a quarterly basis to track seasonal flow conditions. Groundwater sampling for inorganic analysis may be required only once a year or once in two years to track the geochemical environment. Other measurements, such as iron core evaluation, may be considered only if required. Table B-3 provides the projected cost of such a monitoring schedule.

Estimating the maintenance cost of the PRB is more difficult. First, the frequency at which such maintenance would be required is unknown. PRBs are a fairly new technology; the longest-running PRB has been in the ground for about 5 years. Long-term column tests at accelerated flowrates have been conducted, but extrapolating the results to field conditions has proved difficult. A rule-of-thumb approximation has been proposed and used in the past at some sites to project the cost of long-term maintenance. This approximation suggests a maintenance requirement that 25% of the iron medium would have to be replaced every 5 or 10 years, depending on the level of dissolved solids (or potential for precipitation) in the groundwater. However, there are no data to really drive such projections.

Table B-3. O&M Costs Projected for Operating a Full-Scale PRB in Area 5

Item	Description	Basis	Cost
<i>Annual Monitoring Activities</i>			
Groundwater sampling	Quarterly, labor, materials, travel	40 wells	\$80,000
CVOC analysis	Quarterly, 40 wells	44 per quarter @ \$120/sample	\$20,000
Inorganic analysis	Annual, 20 wells	22 per year @ \$200/sample	\$4,000
Water-level survey	Quarterly, labor	40 wells per quarter	\$4,000
Data analysis; report; regulatory review	Quarterly, labor	4 times per year	\$40,000
Annual operating cost			\$148,000
<i>Periodic Maintenance Activities (once every 10 years)</i>			
Site preparation	Permitting, clearances	Labor	\$10,000
Reactive media procurement	Connelly iron, shipping	Iron: 108 tons @ \$360/ton Shipping: \$9,000	\$48,000
Removal/replacement of gates	Mobilization/demobilization; installation of four 8-ft-diameter caisson gates to 39-ft depth; restoration of asphalt parking lot	Mob./demob.: \$38,000 Gates: \$266,000 Monitoring wells: \$25,000 Surface restoration: \$34,000	\$363,000
Periodic maintenance cost (once every 10 years)			\$421,000

Also, it is unclear as to what physical means would be applied to remove and replace the reactive medium. Presumably, the contents of the gates could be removed with an auger after installing temporary sheet piles along the upgradient and downgradient edges of the reactive cells to retain the sides of the excavation. However, such removal activities may not be easy given that the shape of the reactive cell is square, and that augering probably would be impeded by the presence of monitoring wells. After gate removal, fresh iron then could be installed in a manner similar to that for the new installation. All the costs in the construction category in Table B-2 would be incurred, except for the funnel cost. This assumes that all reactive media in the gate is to be replaced; partial removal and replacement would be much more difficult.

Based on these assumptions for monitoring and maintenance, Table B-3 shows the projected O&M costs for the PRB over the long term. Table B-3 assumes that PRB maintenance will be required once every 10 years. Maintenance is assumed to involve replacement of all the iron in the gates. Maintenance costs are assumed to be similar to the construction costs of the original gates. The funnel cost and the aquifer monitoring system costs in Table B-2 have been dropped from Table B-3. Additional scenarios involving periodic maintenance requirements of every 5, 10, 20, or 30 years are discussed in Section B.4. Because the longevity of the reactive medium cannot be predicted with certainty, these multiple scenarios show the dependency of the economics of the PRB on the longevity of the reactive medium.

B.4 Present Value Analysis of PRB and P&T Options

The PRB technology is an innovative alternative to conventional P&T systems. As compared with a P&T system, a PRB offers the benefits of passive operation (no external energy input

required for operation) and absence of aboveground structures. A long-term comparison of these two technology options for Area 5 is presented in this section. For this comparison, the capital investment and O&M cost of an equivalent P&T system were estimated, and are summarized in Tables B-4 and B-5. The estimated P&T system costs for Area 5 are based on a similar system designed, built, and tested in a CVOC plume in a different area at Dover AFB (Battelle, 1994).

A comparable P&T system for plume migration control would have to capture the same volume of groundwater as the full-scale PRB with four gates. At the maximum flowrate of 4.1 ft/day through each gate, the PRB is expected to capture the equivalent of approximately 10 gallons per minute (gpm) of flow. Because of possible capture inefficiencies with extraction wells, the P&T system is designed to capture and treat twice as much, or 20 gpm. As described in Table B-4, the investment in the P&T system includes three extraction wells, an air stripper to transfer CVOCs to air, a catalytic oxidizer to treat the air effluent from the stripper, and polishing carbon to remove any residual CVOCs down to maximum contaminant levels (MCLs).

Projected O&M costs of the P&T system consist of an annual operating cost to keep the system running, an annual groundwater monitoring cost, and periodic maintenance costs. The periodic maintenance costs involve replacement of the carbon every 10 years and replacement of the catalyst every 5 years. Tables B-4 and B-5 indicate that the P&T system requires a lower initial capital investment as compared to the PRB, but incurs higher O&M costs, primarily because of the labor and energy requirements to operate the P&T system. The P&T system requires more frequent periodic maintenance in the form of carbon and catalyst replacement. Because the PRB and P&T system require maintenance at different points in time and because the CVOC plume is expected to last for several years or decades, a PV analysis is required to consolidate the capital investment and long-term O&M costs into a total (cumulative) cost in today's dollars.

Table B-6 shows the discounted cash flow (i.e., PV) analysis of the capital investment and O&M costs over 30 years for both PRB and P&T system options. A real discount rate of 2.9% is used in the analysis, as per the 1999 update to the U.S. EPA Office of Management and Budget's circular (U.S. EPA, 1993). It is assumed that the PRB will maintain its reactivity and hydraulic performance over 10 years of operation, after which all four gates will have to be removed and replaced (at an estimated total cost of \$421,000, as shown in Table B-3). The PVs of the capital investment and annual O&M costs are listed in columns 2 and 5 of Table B-6 (for the PRB and P&T system, respectively), and indicate that the further back in time that the cost occurs, the lower its PV. Columns 3 and 6 list the cumulative PV at the end of each year; the cumulative PV includes the capital investment and the PV of all O&M costs up to that year. The year in which the cumulative PV cost of the PRB is equal to or below cumulative PV cost of the P&T system is the payback period or break-even point for the PRB.

As shown in Table B-6, there are two potential break-even times for the PRB (indicated by the shaded cells in the table). In Year 8, the cumulative or total PV cost of the PRB is lower than the PV cost of the P&T system, indicating the first potential break-even point (see shaded cells in Table B-6). However, in Year 10, the nonroutine maintenance cost of replacing the iron in the four gates is incurred (see bold numbers in Table B-6), which makes the total cost of the PRB slightly higher again than the pump-and-treat system. In Year 14, the total PV cost of the PRB again becomes lower, and this is the true break-even point. In other words, over 14 years, the lower

Table B-4. Capital Investment Projected for Installing a P&T System at Dover AFB

Item	Description	Basis	Cost ^(a)
Phase 1: Preconstruction Activities			
Preliminary site assessment	Historical site data evaluation	RI/FS, other reports procurement and evaluation; site meeting	\$15,000
Site characterization	Characterization Plan, fieldwork, laboratory analysis	CPT pushes for geologic mapping and temporary wells; analysis of water samples for CVOCs and inorganics; slug tests in existing wells	\$200,000
Design; procurement; regulatory review	Data evaluation, modeling, engineering design, Design Plan; procurement; regulatory interactions	Characterization data analysis; hydrogeologic modeling; engineering design; report; procurement; regulatory review	\$100,000
Subtotal			\$315,000
Phase 2: P&T System Construction Activities			
Site preparation	Utilities clearances; arrangements for equipment storage	Coordination with regulators and Base facilities staff	\$10,000
P&T system construction	Installation of three 4-inch-diameter extraction wells; pumps; air stripper; catalytic oxidizer; polishing carbon; shed; piping	20-gpm groundwater extraction and treatment system	\$145,000
Monitoring system construction	Thirty PVC aquifer wells installed for monitoring plume movement	Aquifer wells: \$32,000	\$32,000
Subtotal			\$187,000
TOTAL			\$502,000

(a) Based on a similar P&T system designed, built, and tested for a CVOC plume in a different area at Dover AFB (Battelle, 1994). Details are in Section B.4.

Table B-5. O&M Costs Projected for Operating a P&T System at Dover AFB

Item	Description	Basis	Cost ^(a)
Annual System O&M (includes routine maintenance)			
System operation	Keeping P&T system operational	Labor, energy consumption, materials replacement, waste handling, routine maintenance/replacement of pumps	\$66,000
Groundwater monitoring	Quarterly, 40 wells; CVOC, inorganics, water levels	Labor, materials, analytical	\$148,000
Annual operating cost			\$214,000
Periodic Maintenance (once every 10 years)			
Carbon replacement	Polishing carbon for liquid	Used carbon disposal, new carbon installation	\$7,000
Periodic Maintenance (once every 5 years)			
Catalyst replacement	Oxidizer catalysts for effluent air treatment	Used catalyst disposal, new catalyst installation	\$21,000

(a) Based on a similar P&T system designed, built, and tested for a CVOC plume in a different area at Dover AFB (Battelle, 1994). Details are in Section B.4.

**Table B-6. Present Value Analysis of PRB and P&T Systems in Area 5 at Dover AFB
Assuming 10-Year Life of PRB**

Year	PRB			P&T System		
	Annual Cost ^(a)	PV of Annual Cost ^(b)	Cumulative PV of Annual Cost ^(c)	Annual Cost ^(a)	PV of Annual Cost ^(b)	Cumulative PV of Annual Cost ^(c)
0	\$947,000 ^(d)	\$947,000	\$947,000	\$502,000 ^(d)	\$502,000	\$502,000
1	\$148,000 ^(e)	\$143,829	\$1,090,829	\$214,000 ^(e)	\$207,969	\$709,969
2	\$148,000	\$139,775	\$1,230,604	\$214,000	\$202,108	\$912,077
3	\$148,000	\$135,836	\$1,366,441	\$214,000	\$196,412	\$1,108,489
4	\$148,000	\$132,008	\$1,498,449	\$214,000	\$190,876	\$1,299,365
5	\$148,000	\$128,288	\$1,626,736	\$235,000 ^(g)	\$203,700	\$1,503,065
6	\$148,000	\$124,672	\$1,751,408	\$214,000	\$180,269	\$1,683,334
7	\$148,000	\$121,159	\$1,872,567	\$214,000	\$175,189	\$1,858,523
8	\$148,000	\$117,744	\$1,990,311	\$214,000	\$170,251	\$2,028,774
9	\$148,000	\$114,426	\$2,104,737	\$214,000	\$165,453	\$2,194,228
10	\$569,000^(f)	\$427,522	\$2,532,259	\$242,000 ^(g)	\$181,828	\$2,376,056
11	\$148,000	\$108,067	\$2,640,326	\$214,000	\$156,259	\$2,532,315
12	\$148,000	\$105,021	\$2,745,347	\$214,000	\$151,855	\$2,684,170
13	\$148,000	\$102,061	\$2,847,408	\$214,000	\$147,575	\$2,831,745
14	\$148,000	\$99,185	\$2,946,593	\$214,000	\$143,416	\$2,975,162
15	\$148,000	\$96,390	\$3,042,983	\$235,000 ^(g)	\$153,051	\$3,128,213
16	\$148,000	\$93,673	\$3,136,656	\$214,000	\$135,446	\$3,263,659
17	\$148,000	\$91,033	\$3,227,690	\$214,000	\$131,629	\$3,395,289
18	\$148,000	\$88,468	\$3,316,158	\$214,000	\$127,920	\$3,523,208
19	\$148,000	\$85,974	\$3,402,132	\$214,000	\$124,314	\$3,647,523
20	\$569,000^(f)	\$321,222	\$3,723,354	\$242,000 ^(g)	\$136,618	\$3,784,141
21	\$148,000	\$81,197	\$3,804,550	\$242,000	\$132,768	\$3,916,908
22	\$148,000	\$78,908	\$3,883,459	\$214,000	\$114,097	\$4,031,006
23	\$148,000	\$76,685	\$3,960,143	\$214,000	\$110,882	\$4,141,887
24	\$148,000	\$74,523	\$4,034,667	\$214,000	\$107,757	\$4,249,644
25	\$148,000	\$72,423	\$4,107,090	\$235,000 ^(g)	\$114,996	\$4,364,641
26	\$148,000	\$70,382	\$4,177,472	\$214,000	\$101,769	\$4,466,409
27	\$148,000	\$68,399	\$4,245,871	\$214,000	\$98,901	\$4,565,310
28	\$148,000	\$66,471	\$4,312,341	\$214,000	\$96,113	\$4,661,423
29	\$148,000	\$64,598	\$4,376,939	\$214,000	\$93,405	\$4,754,827
30	\$569,000^(f)	\$241,352	\$4,618,291	\$242,000 ^(g)	\$102,649	\$4,857,476

(a) Annual cost is equal to the capital investment in Year 0 and the O&M cost in subsequent years.

(b) Present value cost is the annual cost divided by a discount factor term based on a 2.9% discount rate, as described in Section 9.3.

(c) Cumulative present value cost is the sum of annual present value costs in each year and previous years.

(d) Initial capital investment.

(e) Annual routine O&M cost.

(f) Annual monitoring cost of \$148,000, plus maintenance/replacement of gates for \$421,000, as described in Table B-3.

(g) Periodic (nonroutine) maintenance to replace catalyst and/or carbon, as described in Table B-5.

annual operating cost (passive operation) of the PRB makes it a worthwhile investment. At the end of the analysis period of 30 years, the PV of the total savings from implementing a PRB versus a P&T system in this illustration is \$239,000 (that is, the difference between the cumulative costs of \$4,618,291 and \$4,857,476 for the PRB and P&T system at the end of 30 years). Table B-7 shows the summarized results of additional scenarios. Because the break-even point is sensitive to the assumption on the life of the PRB, the PV analysis was repeated assuming that the life of the PRB is 5, 10, 20, and 30 years (see Tables B-8 to B-11). In addition, Table B-12 shows a similar scenario extended for a project duration of 50 years.

Table B-7. Break-Even Point and Savings by Using a PRB Instead of a P&T System in Area 5 at Dover AFB

Life of Reactive Medium	Break-Even Point	PV of Savings Over the Duration of the Project	Duration of Project
5 years	None	-\$603,000	30 years
10 years	14 years	\$239,000	30 years
20 years	8 years	\$734,000	30 years
30 years	8 years	\$793,000	30 years
30 years	8 years	\$1,251,000	50 years

Table B-7 summarizes the results of these economic scenarios. As seen in this table, if the PRB lasts only 5 years, and the gates have to be replaced every 5 years, the P&T system is less expensive. If the PRB lasts at least 10 years, it is less expensive than a P&T system. The longer the PRB lasts, the greater the savings at the end of 30 or 50 years. These same cost scenarios, which are discussed in Section 9.3, are depicted in Figure B-3.

Note that this PV cost analysis only takes into account the more tangible costs of the two options. A significant intangible benefit of using a PRB in Area 5 at Dover AFB is that there are no aboveground structures involved, and the site can still be used as a parking lot. With a P&T system, there would be some loss of space for housing the piping and aboveground treatment equipment. The ability of site owners to use, lease, or sell the space that would have been taken up by a P&T system, and to improve the attractiveness of the property as a whole, is a significant benefit of PRB technology. In addition, previous and/or new owners of the property would not have to deal with the high level of maintenance and waste handling during P&T operations.

**Table B-8. PV Analysis of PRB and P&T Systems for Area 5 at Dover AFB
Assuming 5-Year Life of PRB**

Year	PRB			P&T System		
	Annual Cost	PV of Annual Cost	Cumulative PV of Annual Cost	Annual Cost	PV of Annual Cost	Cumulative PV of Annual Cost
0	\$947,000	\$947,000	\$947,000	\$502,000	\$502,000	\$502,000
1	\$148,000	\$143,829	\$1,090,829	\$214,000	\$207,969	\$709,969
2	\$148,000	\$139,775	\$1,230,604	\$214,000	\$202,108	\$912,077
3	\$148,000	\$135,836	\$1,366,441	\$214,000	\$196,412	\$1,108,489
4	\$148,000	\$132,008	\$1,498,449	\$214,000	\$190,876	\$1,299,365
5	\$569,000	\$493,214	\$1,991,663	\$235,000	\$203,700	\$1,503,065
6	\$148,000	\$124,672	\$2,116,335	\$214,000	\$180,269	\$1,683,334
7	\$148,000	\$121,159	\$2,237,493	\$214,000	\$175,189	\$1,858,523
8	\$148,000	\$117,744	\$2,355,237	\$214,000	\$170,251	\$2,028,774
9	\$148,000	\$114,426	\$2,469,663	\$214,000	\$165,453	\$2,194,228
10	\$569,000	\$427,522	\$2,897,185	\$242,000	\$181,828	\$2,376,056
11	\$148,000	\$108,067	\$3,005,252	\$214,000	\$156,259	\$2,532,315
12	\$148,000	\$105,021	\$3,110,273	\$214,000	\$151,855	\$2,684,170
13	\$148,000	\$102,061	\$3,212,335	\$214,000	\$147,575	\$2,831,745
14	\$148,000	\$99,185	\$3,311,520	\$214,000	\$143,416	\$2,975,162
15	\$569,000	\$370,580	\$3,682,099	\$235,000	\$153,051	\$3,128,213
16	\$148,000	\$93,673	\$3,775,773	\$214,000	\$135,446	\$3,263,659
17	\$148,000	\$91,033	\$3,866,806	\$214,000	\$131,629	\$3,395,289
18	\$148,000	\$88,468	\$3,955,274	\$214,000	\$127,920	\$3,523,208
19	\$148,000	\$85,974	\$4,041,248	\$214,000	\$124,314	\$3,647,523
20	\$569,000	\$321,222	\$4,362,470	\$242,000	\$136,618	\$3,784,141
21	\$148,000	\$81,197	\$4,443,667	\$242,000	\$132,768	\$3,916,908
22	\$148,000	\$78,908	\$4,522,575	\$214,000	\$114,097	\$4,031,006
23	\$148,000	\$76,685	\$4,599,260	\$214,000	\$110,882	\$4,141,887
24	\$148,000	\$74,523	\$4,673,783	\$214,000	\$107,757	\$4,249,644
25	\$569,000	\$278,438	\$4,952,221	\$235,000	\$114,996	\$4,364,641
26	\$148,000	\$70,382	\$5,022,603	\$214,000	\$101,769	\$4,466,409
27	\$148,000	\$68,399	\$5,091,001	\$214,000	\$98,901	\$4,565,310
28	\$148,000	\$66,471	\$5,157,472	\$214,000	\$96,113	\$4,661,423
29	\$148,000	\$64,598	\$5,222,070	\$214,000	\$93,405	\$4,754,827
30	\$569,000	\$241,352	\$5,463,422	\$242,000	\$102,649	\$4,857,476

**Table B-9. PV Analysis of PRB and P&T Systems for Area 5 at Dover AFB
Assuming 10-Year Life of PRB**

Year	PRB			P&T System		
	Annual Cost	PV of Annual Cost	Cumulative PV of Annual Cost	Annual Cost	PV of Annual Cost	Cumulative PV of Annual Cost
0	\$947,000	\$947,000	\$947,000	\$502,000	\$502,000	\$502,000
1	\$148,000	\$143,829	\$1,090,829	\$214,000	\$207,969	\$709,969
2	\$148,000	\$139,775	\$1,230,604	\$214,000	\$202,108	\$912,077
3	\$148,000	\$135,836	\$1,366,441	\$214,000	\$196,412	\$1,108,489
4	\$148,000	\$132,008	\$1,498,449	\$214,000	\$190,876	\$1,299,365
5	\$148,000	\$128,288	\$1,626,736	\$235,000	\$203,700	\$1,503,065
6	\$148,000	\$124,672	\$1,751,408	\$214,000	\$180,269	\$1,683,334
7	\$148,000	\$121,159	\$1,872,567	\$214,000	\$175,189	\$1,858,523
8	\$148,000	\$117,744	\$1,990,311	\$214,000	\$170,251	\$2,028,774
9	\$148,000	\$114,426	\$2,104,737	\$214,000	\$165,453	\$2,194,228
10	\$569,000	\$427,522	\$2,532,259	\$242,000	\$181,828	\$2,376,056
11	\$148,000	\$108,067	\$2,640,326	\$214,000	\$156,259	\$2,532,315
12	\$148,000	\$105,021	\$2,745,347	\$214,000	\$151,855	\$2,684,170
13	\$148,000	\$102,061	\$2,847,408	\$214,000	\$147,575	\$2,831,745
14	\$148,000	\$99,185	\$2,946,593	\$214,000	\$143,416	\$2,975,162
15	\$148,000	\$96,390	\$3,042,983	\$235,000	\$153,051	\$3,128,213
16	\$148,000	\$93,673	\$3,136,656	\$214,000	\$135,446	\$3,263,659
17	\$148,000	\$91,033	\$3,227,690	\$214,000	\$131,629	\$3,395,289
18	\$148,000	\$88,468	\$3,316,158	\$214,000	\$127,920	\$3,523,208
19	\$148,000	\$85,974	\$3,402,132	\$214,000	\$124,314	\$3,647,523
20	\$569,000	\$321,222	\$3,723,354	\$242,000	\$136,618	\$3,784,141
21	\$148,000	\$81,197	\$3,804,550	\$242,000	\$132,768	\$3,916,908
22	\$148,000	\$78,908	\$3,883,459	\$214,000	\$114,097	\$4,031,006
23	\$148,000	\$76,685	\$3,960,143	\$214,000	\$110,882	\$4,141,887
24	\$148,000	\$74,523	\$4,034,667	\$214,000	\$107,757	\$4,249,644
25	\$148,000	\$72,423	\$4,107,090	\$235,000	\$114,996	\$4,364,641
26	\$148,000	\$70,382	\$4,177,472	\$214,000	\$101,769	\$4,466,409
27	\$148,000	\$68,399	\$4,245,871	\$214,000	\$98,901	\$4,565,310
28	\$148,000	\$66,471	\$4,312,341	\$214,000	\$96,113	\$4,661,423
29	\$148,000	\$64,598	\$4,376,939	\$214,000	\$93,405	\$4,754,827
30	\$569,000	\$241,352	\$4,618,291	\$242,000	\$102,649	\$4,857,476

**Table B-10. PV Analysis of PRB and P&T Systems for Area 5 at
Dover AFB Assuming 20-Year Life of PRB**

Year	PRB			P&T System		
	Annual Cost	PV of Annual Cost	Cumulative PV of Annual Cost	Annual Cost	PV of Annual Cost	Cumulative PV of Annual Cost
0	\$947,000	\$947,000	\$947,000	\$502,000	\$502,000	\$502,000
1	\$148,000	\$143,829	\$1,090,829	\$214,000	\$207,969	\$709,969
2	\$148,000	\$139,775	\$1,230,604	\$214,000	\$202,108	\$912,077
3	\$148,000	\$135,836	\$1,366,441	\$214,000	\$196,412	\$1,108,489
4	\$148,000	\$132,008	\$1,498,449	\$214,000	\$190,876	\$1,299,365
5	\$148,000	\$128,288	\$1,626,736	\$235,000	\$203,700	\$1,503,065
6	\$148,000	\$124,672	\$1,751,408	\$214,000	\$180,269	\$1,683,334
7	\$148,000	\$121,159	\$1,872,567	\$214,000	\$175,189	\$1,858,523
8	\$148,000	\$117,744	\$1,990,311	\$214,000	\$170,251	\$2,028,774
9	\$148,000	\$114,426	\$2,104,737	\$214,000	\$165,453	\$2,194,228
10	\$148,000	\$111,201	\$2,215,937	\$242,000	\$181,828	\$2,376,056
11	\$148,000	\$108,067	\$2,324,004	\$214,000	\$156,259	\$2,532,315
12	\$148,000	\$105,021	\$2,429,026	\$214,000	\$151,855	\$2,684,170
13	\$148,000	\$102,061	\$2,531,087	\$214,000	\$147,575	\$2,831,745
14	\$148,000	\$99,185	\$2,630,272	\$214,000	\$143,416	\$2,975,162
15	\$148,000	\$96,390	\$2,726,662	\$235,000	\$153,051	\$3,128,213
16	\$148,000	\$93,673	\$2,820,335	\$214,000	\$135,446	\$3,263,659
17	\$148,000	\$91,033	\$2,911,369	\$214,000	\$131,629	\$3,395,289
18	\$148,000	\$88,468	\$2,999,836	\$214,000	\$127,920	\$3,523,208
19	\$148,000	\$85,974	\$3,085,811	\$214,000	\$124,314	\$3,647,523
20	\$569,000	\$321,222	\$3,407,032	\$242,000	\$136,618	\$3,784,141
21	\$148,000	\$81,197	\$3,488,229	\$242,000	\$132,768	\$3,916,908
22	\$148,000	\$78,908	\$3,567,138	\$214,000	\$114,097	\$4,031,006
23	\$148,000	\$76,685	\$3,643,822	\$214,000	\$110,882	\$4,141,887
24	\$148,000	\$74,523	\$3,718,346	\$214,000	\$107,757	\$4,249,644
25	\$148,000	\$72,423	\$3,790,769	\$235,000	\$114,996	\$4,364,641
26	\$148,000	\$70,382	\$3,861,151	\$214,000	\$101,769	\$4,466,409
27	\$148,000	\$68,399	\$3,929,549	\$214,000	\$98,901	\$4,565,310
28	\$148,000	\$66,471	\$3,996,020	\$214,000	\$96,113	\$4,661,423
29	\$148,000	\$64,598	\$4,060,618	\$214,000	\$93,405	\$4,754,827
30	\$148,000	\$62,777	\$4,123,395	\$242,000	\$102,649	\$4,857,476

**Table B-11. PV Analysis of PRB and P&T Systems for Area 5 at Dover AFB
Assuming 30-Year Life of PRB**

Year	PRB			P&T System		
	Annual Cost	PV of Annual Cost	Cumulative PV of Annual Cost	Annual Cost	PV of Annual Cost	Cumulative PV of Annual Cost
0	\$947,000	\$947,000	\$947,000	\$502,000	\$502,000	\$502,000
1	\$148,000	\$143,829	\$1,090,829	\$214,000	\$207,969	\$709,969
2	\$148,000	\$139,775	\$1,230,604	\$214,000	\$202,108	\$912,077
3	\$148,000	\$135,836	\$1,366,441	\$214,000	\$196,412	\$1,108,489
4	\$148,000	\$132,008	\$1,498,449	\$214,000	\$190,876	\$1,299,365
5	\$148,000	\$128,288	\$1,626,736	\$235,000	\$203,700	\$1,503,065
6	\$148,000	\$124,672	\$1,751,408	\$214,000	\$180,269	\$1,683,334
7	\$148,000	\$121,159	\$1,872,567	\$214,000	\$175,189	\$1,858,523
8	\$148,000	\$117,744	\$1,990,311	\$214,000	\$170,251	\$2,028,774
9	\$148,000	\$114,426	\$2,104,737	\$214,000	\$165,453	\$2,194,228
10	\$148,000	\$111,201	\$2,215,937	\$242,000	\$181,828	\$2,376,056
11	\$148,000	\$108,067	\$2,324,004	\$214,000	\$156,259	\$2,532,315
12	\$148,000	\$105,021	\$2,429,026	\$214,000	\$151,855	\$2,684,170
13	\$148,000	\$102,061	\$2,531,087	\$214,000	\$147,575	\$2,831,745
14	\$148,000	\$99,185	\$2,630,272	\$214,000	\$143,416	\$2,975,162
15	\$148,000	\$96,390	\$2,726,662	\$235,000	\$153,051	\$3,128,213
16	\$148,000	\$93,673	\$2,820,335	\$214,000	\$135,446	\$3,263,659
17	\$148,000	\$91,033	\$2,911,369	\$214,000	\$131,629	\$3,395,289
18	\$148,000	\$88,468	\$2,999,836	\$214,000	\$127,920	\$3,523,208
19	\$148,000	\$85,974	\$3,085,811	\$214,000	\$124,314	\$3,647,523
20	\$148,000	\$83,551	\$3,169,362	\$242,000	\$136,618	\$3,784,141
21	\$148,000	\$81,197	\$3,250,559	\$242,000	\$132,768	\$3,916,908
22	\$148,000	\$78,908	\$3,329,468	\$214,000	\$114,097	\$4,031,006
23	\$148,000	\$76,685	\$3,406,152	\$214,000	\$110,882	\$4,141,887
24	\$148,000	\$74,523	\$3,480,676	\$214,000	\$107,757	\$4,249,644
25	\$148,000	\$72,423	\$3,553,099	\$235,000	\$114,996	\$4,364,641
26	\$148,000	\$70,382	\$3,623,481	\$214,000	\$101,769	\$4,466,409
27	\$148,000	\$68,399	\$3,691,879	\$214,000	\$98,901	\$4,565,310
28	\$148,000	\$66,471	\$3,758,350	\$214,000	\$96,113	\$4,661,423
29	\$148,000	\$64,598	\$3,822,948	\$214,000	\$93,405	\$4,754,827
30	\$569,000	\$241,352	\$4,064,300	\$242,000	\$102,649	\$4,857,476

**Table B-12. PV Analysis of PRB and P&T Systems for Area 5 at Dover AFB
Assuming 50-Year Life of PRB**

Year	PRB			P&T System		
	Annual Cost	PV of Annual Cost	Cumulative PV of Annual Cost	Annual Cost	PV of Annual Cost	Cumulative PV of Annual Cost
0	\$947,000	\$947,000	\$947,000	\$502,000	\$502,000	\$502,000
1	\$148,000	\$143,829	\$1,090,829	\$214,000	\$207,969	\$709,969
2	\$148,000	\$139,775	\$1,230,604	\$214,000	\$202,108	\$912,077
3	\$148,000	\$135,836	\$1,366,441	\$214,000	\$196,412	\$1,108,489
4	\$148,000	\$132,008	\$1,498,449	\$214,000	\$190,876	\$1,299,365
5	\$148,000	\$128,288	\$1,626,736	\$235,000	\$203,700	\$1,503,065
6	\$148,000	\$124,672	\$1,751,408	\$214,000	\$180,269	\$1,683,334
7	\$148,000	\$121,159	\$1,872,567	\$214,000	\$175,189	\$1,858,523
8	\$148,000	\$117,744	\$1,990,311	\$214,000	\$170,251	\$2,028,774
9	\$148,000	\$114,426	\$2,104,737	\$214,000	\$165,453	\$2,194,228
10	\$148,000	\$111,201	\$2,215,937	\$242,000	\$181,828	\$2,376,056
11	\$148,000	\$108,067	\$2,324,004	\$214,000	\$156,259	\$2,532,315
12	\$148,000	\$105,021	\$2,429,026	\$214,000	\$151,855	\$2,684,170
13	\$148,000	\$102,061	\$2,531,087	\$214,000	\$147,575	\$2,831,745
14	\$148,000	\$99,185	\$2,630,272	\$214,000	\$143,416	\$2,975,162
15	\$148,000	\$96,390	\$2,726,662	\$235,000	\$153,051	\$3,128,213
16	\$148,000	\$93,673	\$2,820,335	\$214,000	\$135,446	\$3,263,659
17	\$148,000	\$91,033	\$2,911,369	\$214,000	\$131,629	\$3,395,289
18	\$148,000	\$88,468	\$2,999,836	\$214,000	\$127,920	\$3,523,208
19	\$148,000	\$85,974	\$3,085,811	\$214,000	\$124,314	\$3,647,523
20	\$148,000	\$83,551	\$3,169,362	\$242,000	\$136,618	\$3,784,141
21	\$148,000	\$81,197	\$3,250,559	\$242,000	\$132,768	\$3,916,908
22	\$148,000	\$78,908	\$3,329,468	\$214,000	\$114,097	\$4,031,006
23	\$148,000	\$76,685	\$3,406,152	\$214,000	\$110,882	\$4,141,887
24	\$148,000	\$74,523	\$3,480,676	\$214,000	\$107,757	\$4,249,644
25	\$148,000	\$72,423	\$3,553,099	\$235,000	\$114,996	\$4,364,641
26	\$148,000	\$70,382	\$3,623,481	\$214,000	\$101,769	\$4,466,409
27	\$148,000	\$68,399	\$3,691,879	\$214,000	\$98,901	\$4,565,310
28	\$148,000	\$66,471	\$3,758,350	\$214,000	\$96,113	\$4,661,423
29	\$148,000	\$64,598	\$3,822,948	\$214,000	\$93,405	\$4,754,827
30	\$569,000	\$241,352	\$4,064,300	\$242,000	\$102,649	\$4,857,476
31	\$148,000	\$61,008	\$4,125,307	\$214,000	\$88,214	\$4,945,690
32	\$148,000	\$59,288	\$4,184,596	\$214,000	\$85,728	\$5,031,418
33	\$148,000	\$57,617	\$4,242,213	\$214,000	\$83,312	\$5,114,730
34	\$148,000	\$55,994	\$4,298,207	\$214,000	\$80,964	\$5,195,694
35	\$148,000	\$54,416	\$4,352,623	\$235,000	\$86,403	\$5,282,097
36	\$148,000	\$52,882	\$4,405,505	\$214,000	\$76,465	\$5,358,561
37	\$148,000	\$51,392	\$4,456,896	\$214,000	\$74,310	\$5,432,871
38	\$148,000	\$49,943	\$4,506,840	\$214,000	\$72,215	\$5,505,086
39	\$148,000	\$48,536	\$4,555,375	\$214,000	\$70,180	\$5,575,267
40	\$148,000	\$47,168	\$4,602,543	\$242,000	\$77,126	\$5,652,392
41	\$148,000	\$45,839	\$4,648,382	\$242,000	\$74,952	\$5,727,345
42	\$148,000	\$44,547	\$4,692,929	\$214,000	\$64,412	\$5,791,757
43	\$148,000	\$43,291	\$4,736,220	\$214,000	\$62,597	\$5,854,354
44	\$148,000	\$42,071	\$4,778,291	\$214,000	\$60,833	\$5,915,187
45	\$148,000	\$40,886	\$4,819,177	\$235,000	\$64,920	\$5,980,106
46	\$148,000	\$39,733	\$4,858,910	\$214,000	\$57,452	\$6,037,558
47	\$148,000	\$38,613	\$4,897,524	\$214,000	\$55,833	\$6,093,391
48	\$148,000	\$37,525	\$4,935,049	\$214,000	\$54,259	\$6,147,651
49	\$148,000	\$36,468	\$4,971,517	\$214,000	\$52,730	\$6,200,381
50	\$148,000	\$35,440	\$5,006,956	\$242,000	\$57,949	\$6,258,330

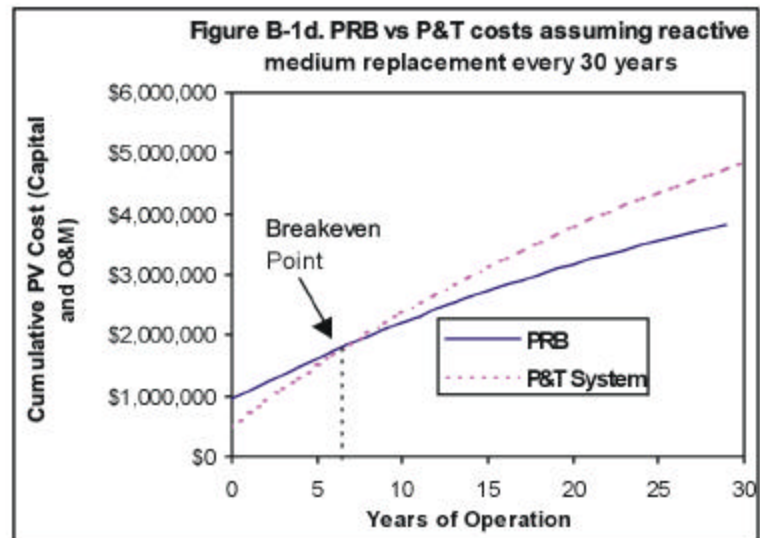
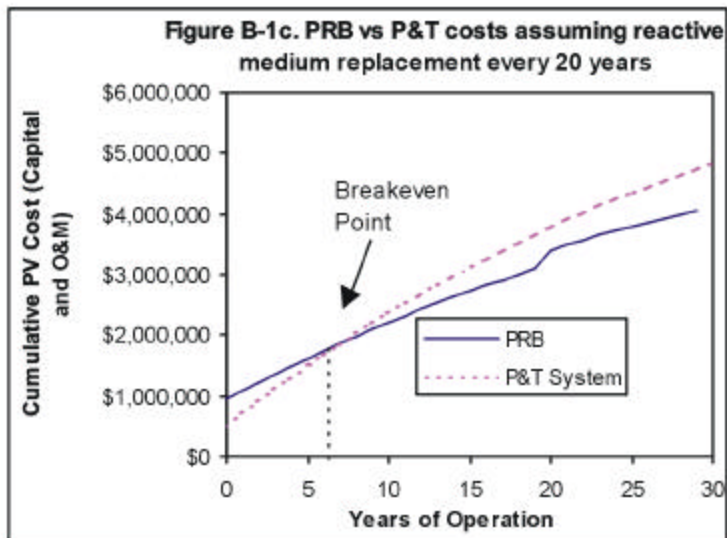
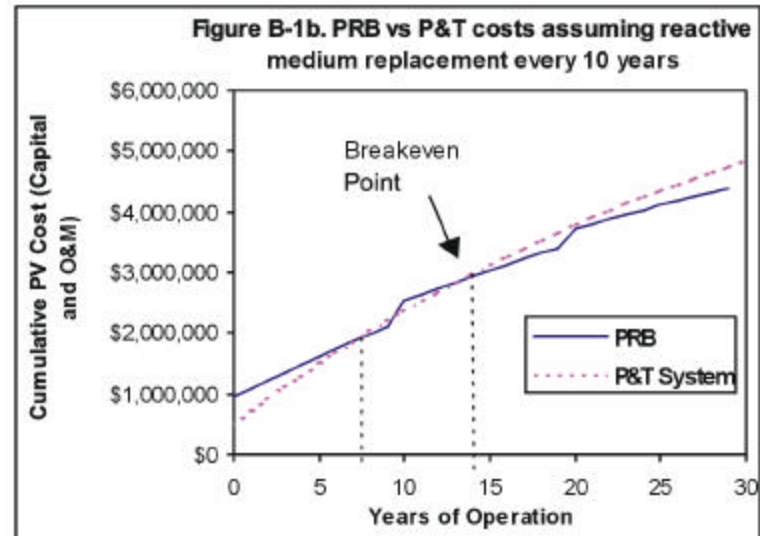
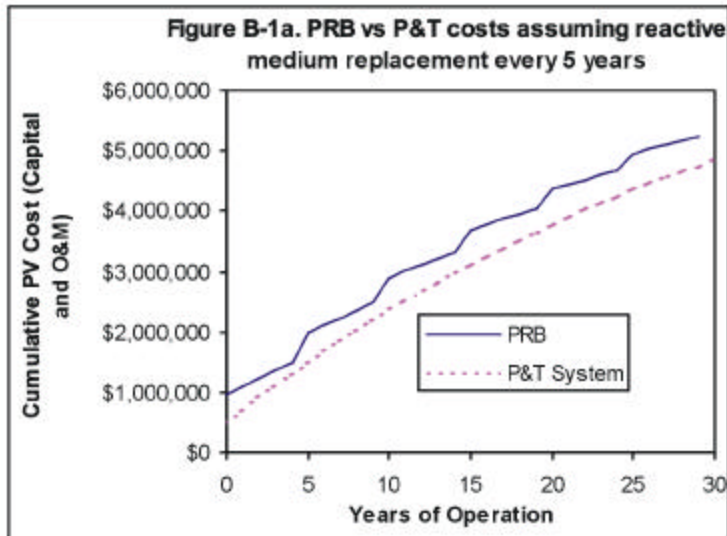


Figure B-3. Illustration of How Break-Even Point or Payback Period Varies with Expected Life of the Reactive Medium

B.5 References

Battelle. 1994. *Final Report: Crossflow Air Stripping with Catalytic Oxidation*. Prepared by Battelle, Columbus, OH for Environics Directorate, Armstrong Laboratory, Tyndall AFB, FL. September.

United States Environmental Protection Agency. 1993. Revisions to OMB Circular A-94 on Guidelines and Discount Rates for Benefit-Cost Analysis. Revised annually at <http://www.whitehouse.gov/OMB/circulars/a094/a094.html#ap-c>.

U.S. EPA, see United States Environmental Protection Agency.

Appendix C

Groundwater Flow Model Review

- C.1 Groundwater Flow Modeling Concepts**
- C.2 PRB Simulation Models**
- C.3 Previous Modeling Studies for PRB Applications**
- C.4 Hydraulic Evaluation of Funnel-and-Gate Systems**
- C.5 References**

Appendix C

Groundwater Flow Model Review

This appendix presents the general concepts of groundwater flow modeling and describes several modeling codes that may be used in designing and evaluating permeable reactive barrier (PRB) systems.

C.1 Groundwater Flow Modeling Concepts

To aid in the design of a PRB system and the interpretation of the resulting flow field, it is recommended that a groundwater flow model be constructed using the site-specific geologic and hydrogeologic data collected as part of the site characterization effort. The model can be used to assess the area of influence, optimize the design, and design the performance monitoring network for the PRB system. A complete description of groundwater flow modeling and the mathematics involved is provided in Wang and Anderson (1982) and Anderson and Woessner (1992). The steps involved in model construction and execution are discussed in the following subsections.

C.1.1 Conceptual Model Development

The first step in any modeling effort is the development of the conceptual model. The conceptual model is a three-dimensional (3-D) representation of the groundwater flow and transport system based on all available geologic, hydrogeologic, and geochemical data for the site. A complete conceptual model will include geologic and topographic maps of the site, cross sections depicting the site geology/hydrogeology, a description of the physical and chemical parameters associated with the aquifer(s), and contaminant concentration and distribution maps. The purpose of the conceptual model is the integration of the available data into a coherent representation of the flow system to be modeled. The conceptual model is used to aid in model selection, model construction, and interpretation of model results.

C.1.2 Model Selection

To be used to simulate the flow at PRBs, the groundwater flow model requires several special features/capabilities. The most important requirements derive from the need to simulate sharp hydraulic conductivity (K) contrasts at the intersection of the aquifer and the funnel walls. The specific requirements and recommendations for the PRB simulation models include the following:

- ❑ Two-dimensional (2-D) or 3-D groundwater flow models may be used to simulate the flow system of a site under consideration. A 3-D modeling approach is recommended so that the possibility of underflow or overflow and of interactions between the adjacent aquifer can be examined at the PRB and its vicinity. Vertical-flow velocities and travel times will be of critical significance in the design of systems at sites with significant vertical-flow gradients or in cases where the barriers are not keyed into the underlying confining layer.
- ❑ The groundwater flow codes should be able to simulate large contrasts in K at the funnel walls. Most of the PRB designs include a reactive cell with K higher than that of the aquifer and flanking funnel walls with extremely low permeability. The

funnels may consist of the slurry wall, which can be several feet wide, or the sheet piles, which are usually less than an inch in width. Therefore, at the intersection of the aquifer and the reactive cells, large K contrasts are developed, and many models are unable to solve these problems due to numerical instabilities. In most cases, the funnel walls are simulated by assigning a very low conductivity to the model cells representing the funnel locations. For accurate simulations, the size of the slurry walls should be the same size as the funnel walls, which will result in a very small cell size and a large number of cells in the model. However, the size of the funnel walls can reduce further if the sizes of the sheet piles (which are even thinner than the slurry walls) are taken into account. A practical compromise strategy is to simulate large areas with sufficient resolution at locations near the funnels, but to increase the cell dimensions at locations further away from the funnels. Models capable of incorporating grid blocks of variable size are recommended. Some alternative approaches have been devised to simulate the low-K funnel walls. These are discussed with the appropriate model descriptions in Section C.2, “PRB Simulation Models.”

- ❑ Many sites have significant heterogeneities, which result in the development of preferential pathways through which most of the groundwater movement occurs. The PRB design itself imparts heterogeneity to the subsurface system. The simulation of these effects requires models that can handle heterogeneity. Most general-purpose analytical models are based on the assumption of homogeneity, but most numerical models can incorporate heterogeneities.
- ❑ Many sites have features such as streams, drains, tunnels, or wells in the vicinity of the PRB sites. For example, at some sites, pump-and-treat (P&T) remediation systems may be active in the vicinity of the PRBs. These situations require the use of models that can simulate the effects of these internal sinks or sources on the PRB systems.
- ❑ The results of the model should be amenable to use with the particle-tracking programs so that the capture zones of the PRBs can be evaluated. It also should be possible to calculate volumetric flow budgets for the reactive cells.

Many groundwater flow modeling codes currently on the market meet the above requirements. A comprehensive description of nonproprietary and proprietary flow and transport modeling codes can be found in the United States Environmental Protection Agency (U.S. EPA) document titled *Compilation of Ground-Water Models* (van der Heijde and Elnawawy, 1993). Depending on the project’s needs, the designer of a PRB system may want to apply a contaminant transport code that can use the calculated hydraulic-head distribution and flow field from the flow-modeling effort. If flow and transport in the vadose zone are of concern, a coupled or uncoupled, unsaturated/saturated flow and transport model should be considered. The codes that meet most of the requirements for simulation of PRB systems are discussed in Section C.2, “PRB Simulation Models.”

C.1.3 Model Construction and Calibration

Model construction consists primarily of converting the conceptual model into the input files for the numerical model. The hydrostratigraphic units defined in the conceptual model can be used to define the physical framework or grid mesh of the numerical model. In both finite-difference

models (such as MODFLOW) and finite-element models (such as FRAC3DVS), a model grid is constructed to discretize the lateral and vertical space that the model is to represent. The different hydrostratigraphic units are represented by model layers, each of which is defined by an array of grid cells. Each grid cell is defined by hydraulic parameters (e.g., K, storativity, cell thickness, cell top, and cell bottom) that control the flow of water through the cells.

Model boundaries are simulated by specifying boundary conditions that define the head or flux of water that occurs at the model grid boundaries or edges. These boundary conditions describe the interaction between the system being modeled and its surroundings. Three types of boundary conditions generally are used to describe groundwater flow: specified-head (Dirichlet), specified-flux (Neumann), and head-dependent flux (Cauchy) (Anderson and Woessner, 1992). Internal boundaries or hydrologic stresses, such as wells, rivers, drains, and recharge, also may be simulated using these conditions. Boundary conditions are used to include the effects of the hydrogeologic system outside the area being modeled and also to make possible isolation of the desired model domain from the larger hydrogeologic system.

Calibration of a groundwater flow model refers to the demonstration that the model is capable of producing field-measured heads and flows, which are used as the calibration values or targets. Calibration is accomplished by finding a set of hydraulic parameters, boundary conditions, and stresses that can be used in the model to produce simulated heads and fluxes that match field-measured values within a preestablished range of error (Anderson and Woessner, 1992). Model calibration can be evaluated through statistical comparison of field-measured and simulated conditions.

Model calibration often is difficult because values for aquifer parameters and hydrologic stresses typically are known in relatively few locations and their estimates are influenced by uncertainty. The uncertainty in a calibrated model and its input parameters can be evaluated by performing a sensitivity analysis in which the aquifer parameters, stresses, and boundary conditions are varied within an established range. The impact of these changes on the model output (or hydraulic heads) provides a measure of the uncertainty associated with the model parameters, stresses, and boundary conditions used in the model. To ensure a reasonable representation of the natural system, it is important to calibrate with values that are consistent with the field-measured heads and hydraulic parameters. Calibration techniques and the uncertainty involved in model calibration are described in detail in Anderson and Woessner (1992).

C.1.4 Model Execution

After a model has been calibrated to observed conditions, it can be used for interpretive or predictive simulations. In a predictive simulation, the parameters determined during calibration are used to predict the response of the flow system to future events, such as the decrease in K over time or the effect of pumping in the vicinity of the PRB. The predictive requirements of the model will determine the need for either a steady-state simulation or a transient simulation, which would accommodate changing conditions and stresses through time. Model output and hydraulic heads can be interpreted through the use of a contouring package and should be applied to particle-tracking simulations in order to calculate groundwater pathways, travel times, and fluxes through the cell. Establishing travel times through the cell is a key modeling result that can be used to determine the thickness of the permeable cell.

C.2 PRB Simulation Models

This section describes the various computer simulation codes that meet the minimum requirements for simulations of groundwater flow and particle movement at PRB sites. Some of the codes already have been used at PRB sites. Nearly all are readily available from the authors or their sponsoring agencies or through resellers. Proprietary codes are included only if they have been applied at a PRB site. Not discussed are advanced programs, such as HST3D (Kipp, 1987), that can simulate the groundwater flow in the vicinity of PRBs, but which in fact are designed for simulation of more complex processes.

C.2.1 MODFLOW and Associated Programs

The perhaps most versatile, widely used, and widely accepted groundwater modeling code is the United States Geological Survey's (USGS's) modular, 3-D, finite-difference groundwater flow model, commonly referred to as MODFLOW (McDonald and Harbaugh, 1988). MODFLOW simulates 2-D and quasi- or fully 3-D, transient groundwater flow in anisotropic, heterogeneous, layered aquifer systems. MODFLOW calculates piezometric head distributions, flowrates, and water balances, and it includes modules for flow toward wells, through riverbeds, and into drains (other modules handle evapotranspiration and recharge). Various textual and graphical pre- and postprocessors are available on the market that make it easy to use the code and analyze the simulation results. These include GMS (Groundwater Modeling System) (Brigham Young University, 1996), ModelCad³⁸⁶ (Rumbaugh, 1993), Visual MODFLOW (Waterloo Hydrogeologic, Inc., 1999b), and Groundwater Vistas (Environmental Simulations, Inc., 1994).

Additional simulation modules are available through the authors and third parties. One of these is the Horizontal Flow Barrier (HFB) package (Hsieh and Freckleton, 1993). This module is especially useful in simulating the funnel-and-gate design. In normal cases, slurry walls must be simulated by very small cells of low K, which increases significantly the number of cells in the model. The HFB package permits the user to assign the sides of certain cells as planes of low K, while still using a larger cell size at the funnel walls. The low-conductivity HFB planes restrict the flow of water into the cells across the faces representing slurry walls or sheet piles. Another useful addition is the ZONEBUDGET (Harbaugh, 1990) package, which allows the user to determine the flow budget for any section of the model. This package may be used to evaluate the volumetric flow through the cell for various design scenarios.

The results from MODFLOW can be used in particle-tracking codes, such as MODPATH (Pollock, 1989) and PATH3D (Zheng, 1989), to calculate groundwater paths and travel times. MODPATH is a postprocessing package used to compute 3-D groundwater path lines based on the output from steady-state simulations obtained with the MODFLOW modeling code. MODPATH uses a semianalytical particle-tracking scheme, based on the assumption that each directional velocity component varies linearly within a grid cell in its own coordinate direction. PATH3D is a general particle-tracking program for calculating groundwater paths and travel times in transient 3-D flow fields. The program includes two major segments: a velocity interpolator, which converts hydraulic heads generated by MODFLOW into a velocity field; and a fourth-order Runge-Kutta numerical solver with automatic time-step size adjustment, which tracks the movement of fluid particles (van der Heijde and Elnawawy, 1993). A proprietary code, RWLK3D[®], developed by Battelle (Naymik and Gantos, 1995), also has been used in conjunction with MODFLOW to simulate the particle movement for the pilot-scale reactive cell

installed at former Naval Air Station (NAS) Moffett Field (Battelle, 1996) and for the PRB at Dover Air Force Base (AFB) (Battelle, 1997). This is a 3-D transport and particle-tracking code based on the Random Walk approach to solute transport simulation.

C.2.2 FLOWPATH

FLOWPATH II (Waterloo Hydrogeologic, Inc., 1999a) is a 2-D steady-state groundwater flow and pathline model. The code can simulate confined, unconfined, or leaky aquifers in heterogeneous and anisotropic media. Complex boundary conditions can be simulated. The program output includes simulated hydraulic heads, pathlines, travel times, velocities, and water balances. The funnel walls can be simulated by constructing a model grid with very small cell size in the vicinity of the permeable cells. Because of its user-friendly graphical interface, this program can be used to quickly simulate the flow fields for a number of design options. Therefore, this program has been used for several PRB sites. However, this program cannot be used if the groundwater flow at a site is very complex due to vertical fluxes or if transient flow fields are to be simulated. These situations are possible if there is a potential for vertical underflow or if the permeable wall is not keyed into the confining layer.

C.2.3 FRAC3DVS

FRAC3DVS is a 3-D, finite-element model for simulating steady-state or transient, saturated or variably saturated, groundwater flow and advective-dispersive solute transport in porous or discretely fractured porous media. The code was developed at the University of Waterloo (Therrien, 1992; Therrien and Sudicky, 1995) and is being marketed by Waterloo Hydrogeologic, Inc. The code includes preprocessors for grid mesh and input file generation, and post-processors for visualization of the simulation results. This program has many advanced features that generally are not required for simple PRB designs. However, the program is included here because the code has been used by Shikaze (1996) to simulate a hypothetical funnel-and-gate design. Further, the solute transport features of this code include the ability to simulate the multispecies transport of straight or branching decay chains. This feature may be used to simulate the reaction progress and daughter product generation in the sequential decay of chlorinated solvents in the permeable cells.

In the work by Shikaze, the impermeable cutoff walls are implemented as 2-D planes within the 3-D computational domain. This is done by adding "false nodes" wherever impermeable nodes are desired. As a consequence, at the impermeable walls, two nodes exist at the same spatial location. These two nodes are connected to elements on the opposite sides of the wall, essentially breaking the connection between two adjacent elements. The net result is an impermeable wall simulated as a 2-D plane within the 3-D domain. These simulations assume that the funnel walls are fully impermeable. This may not be a realistic assumption for very long-term simulations, especially for slurry walls.

C.2.4 GROWFLOW

GROWFLOW is an innovative PRB simulation program being developed by Applied Research Associates, Inc. (Everhart, 1996) for the United States Air Force (USAF). The program is based on the Lagrangian smooth particle hydrodynamics (SPH) concepts traditionally used in the astrophysical simulations. SPH is a continuum-dynamics solution methodology in which all hydrodynamic and history information is carried on particles. In that sense, GROWFLOW is

similar to the particle-tracking codes commonly used to display the flowpaths calculated by the numerical models. The particles in GROWFLOW are Lagrangian interpolation points that interact through the use of a smoothing kernel. The kernel defines a region of influence for each particle and permits approximations to spatial derivatives to be obtained without a mesh. The spatial derivatives are obtained from each particle using an explicit time-integration method.

GROWFLOW is a fully 3-D, saturated-unsaturated code that can handle complex geometry. The model domain and the PRB are simulated using exterior and interior flow control panels that contain and direct flow. No model grid is required. Instead, the initial particle locations serve as the integration points for spatial derivatives. The flow control panels form an impermeable boundary that restricts flow across the external model boundaries or across the internal panels that represent funnel walls. The external boundaries are simulated by assigning constant head or constant velocity source models. These source models are panels that control flow into the model domain. The flow out of the model domain is provided by a volume for the fluid to flow into; that is, the model domain is increased.

GROWFLOW input consists of the model domain parameters, the material properties, the elevation head direction, the panel locations, the saturation vs. head relationship, time-step information, the saturation vs. conductivity relationship, initial locations of all particles in the system, and particle volume. In addition, information also is needed for the smoothing length (region of influence) for the particles. The output includes a listing of the input parameters, particle locations, and heads at specified time intervals. The output can be plotted to show heads as contour maps and particle movement as pathlines.

GROWFLOW is an innovative, flexible, and versatile code for simulation and optimization of PRB systems. However, the code is experimental and several issues need to be addressed. Most importantly, the code needs to be validated against the existing analytical or numerical codes and against field data to verify its numerical accuracy. There appears to be no clear method for simulating internal sources or sinks such as wells and rivers. At many sites, these features may form a significant part of the hydrologic budgets. In addition, there appears to be no provision to check mass or volume balance in the simulations.

C.2.5 Funnel-and-Gate Design Model (FGDM)

FGDM is a multicomponent, steady-state, analytical program for funnel-and-gate design and cost-optimization. It was developed by Applied Research Associates, Inc. (Hatfield, 1996) for the USAF. Program input includes the initial concentrations and first-order reaction rates and the required water quality standards, which then are used to determine the required residence times for water in the permeable cell. The critical residence times are used with input plume-to-gate-width ratios by the program to develop several funnel-and-gate designs. Finally, the cost minimization model is used to find the minimum cost design scenario based on the input unit costs for funnel walls, gate walls, reactive media, and land. The Lagrangian cost minimization is based on a modified Newton-Raphson algorithm for solution of nonlinear equations. Because the accuracy of cost minimization is based partly on the initial estimates for the minimum cost design, it is important to have a preliminary estimate of the low-cost configuration. Additional input parameters include the funnel width, hydraulic gradient, aquifer thickness, aquifer conductivity, gate porosity, ratio of K_{aquifer} to K_{cell} , and depth of system walls. The funnel width, which

is the total width of funnel walls and the gate, is estimated in advance assuming a capture efficiency of 80%. For example, for a plume width of 80 ft, a funnel width of 100 ft is suggested. This assumption may need to be validated by further modeling or field studies. FGDM is a useful tool for a quick evaluation of several design scenarios in a simple setting. However, it cannot be used for complex settings such as heterogeneous media, or for evaluating the flow-paths through the permeable cell.

C.2.6 FLONET

FLONET (Guiguer et al., 1992) is a 2-D, steady-state flow model distributed by Waterloo Hydrogeologic, Inc. The program calculates potentials, streamlines, and velocities and can be used to generate flownets (maps showing flowlines and hydraulic heads) for heterogeneous, anisotropic aquifers. The funnel walls and the gate can be specified by assigning lower K to elements representing these features. The program was used by Starr and Cherry (1994) to evaluate several design scenarios for funnel-and-gate systems.

C.3 Previous Modeling Studies for PRB Applications

A review of the information available from PRB sites under investigation showed that MODFLOW (McDonald and Harbaugh, 1988), in conjunction with particle tracking with codes such as MODPATH (Pollock, 1989), is the code most commonly used to simulate PRB technology. Other programs such as FLONET (Guiguer et al., 1992), FRAC3DVS (Therrien and Sudicky, 1995), FLOWPATH (Waterloo Hydrogeologic, Inc., 1996), and RWLK3D[®] (Naymik and Gantos, 1995) also have been used at some sites. Two new codes, GROWFLOW (Everhart, 1996) and FGDM (Hatfield, 1996), have been developed recently for the USAF to simulate and optimize the funnel-and-gate systems. However, these new codes have not been applied at any sites to date. The sites that used MODFLOW include Dover AFB; the Sunnyvale, CA site, former NAS Moffett Field, CA (PRC, 1996; Battelle, 1996); the Sommersworth Sanitary Land-fill, NH; an industrial facility in Kansas; and General Electric Co. Appliances, WI. FLOWPATH has been used to evaluate the design at Belfast, Northern Ireland; Fairchild AFB, WA; and the United States Department of Energy (DOE) Kansas City, KS site. General modeling evaluations of PRB technology are those by Gupta and Fox (1999), Starr and Cherry (1994), and Shikaze (1996). These papers evaluate the effects of various parameters on the design and performance of typical funnel-and-gate configurations, although some of the conclusions are applicable to continuous reactive barriers as well.

Starr and Cherry (1994) used FLONET (Guiguer et al., 1992) to illustrate the effects of funnel-and-gate geometry (design) and reactive cell hydraulic conductivity (K_{cell}) on the size and shape of capture zone, the discharge groundwater flow volume through the gate, and the residence time in the reactive cell. Only the configurations with barriers keyed into the underlying confining layer were simulated. The hanging wall systems were not simulated using FLONET because 3-D simulations describe them best. The simulated system had properties similar to those of the surficial aquifer at Canadian Forces Base Borden, Ontario, Canada. The simulated aquifer was isotropic, with a homogeneous aquifer hydraulic conductivity (K_{aquifer}) of 28.3 ft/day and a hydraulic gradient of 0.005. The funnel walls were assumed to be 1-m- (3.28-ft-) thick slurry walls, with a K equal to 0.0028 ft/day. The K of the reactive cell was 283 ft/day, the maximum laboratory-measured value for 100% iron, in the base case. The range of values for K_{cell}

indicates differences in the source of granular iron, as well as variability of the K measurement itself. A porosity of 0.33 was used for all materials.

The following conclusions were made based on the simulation of several scenarios.

- ❑ For systems with funnel walls at 180 degrees (straight funnel), the discharge through the gate and the hydraulic capture zone width increases as the funnel width increases. However, the increase in discharge is not directly proportional to funnel width. In fact, the relative discharge (ratio of discharge through the aquifer with PRB versus discharge with no PRB) through the gate decreases dramatically as the funnel width increases.
- ❑ For a constant funnel width, the absolute and relative discharge through the gate (and the capture zone width) increase with an increase in gate width. Therefore, it is desirable to have a gate as wide as is practical.
- ❑ For a given funnel-and-gate design, the discharge through the gate increases with increase in K_{cell} relative to the K_{aquifer} . However, there is relatively little increase in discharge when the K_{cell} is more than 10 times higher than the K_{aquifer} . This result implies that, although a reactive cell conductivity higher than the K_{aquifer} is desirable, K_{cell} does not have to be much higher than K_{aquifer} . This is a useful result, because the large grain sizes required for very high- K_{cell} values would result in a low total surface area for reactions and lower residence times.
- ❑ For all orientations to the regional flow gradient, the maximum absolute discharge occurs at apex angles (the angles between the two funnel walls) of 180 degrees (straight barrier). However, for apex angles between 127 and 233 degrees, there is little effect on discharge. Outside this range, the discharge drops rapidly. This result implies that there is no significant advantage of a slightly angled funnel-and-gate system over a straight barrier (and vice versa).
- ❑ For all apex angles, the maximum discharge occurs when the funnel is perpendicular to the regional flow gradient.
- ❑ The groundwater flow models can be used effectively to design the funnel-and-gate systems at sites with special design requirements due to complex flow fields, seasonal fluctuations, or access restrictions. These may include systems with angled funnels, multiple gates, asymmetrical funnels, or U-shaped funnel-and-gates.
- ❑ A balance between maximizing the capture zone of the gate and maximizing the residence times of contaminated water in the gate should be achieved. The discharge and residence times are inversely proportional. The residence time generally can be increased without affecting the capture zone by increasing the width of the gate.

Shikaze (1996) used the FRAC3DVS code to examine 3-D groundwater flow in the vicinity of a partially penetrating (hanging wall) funnel-and-gate system for 16 different combinations of parameters. All simulations were for steady-state, fully saturated groundwater flow. The 16 simulations consisted of variations in four dimensionless parameters: the ratio of K_{cell} to

K_{aquifer} ; the ratio of width of a single funnel wall to the depth of the funnel-and-gate; the ratio of total funnel wall width to the gate width; and the hydraulic gradient. The following conclusions were drawn from these simulations:

- ❑ Absolute discharge through the gate increases as the hydraulic gradient increases. However, there is almost no effect of hydraulic gradient on the relative discharge or on the size of the relative capture zone (hydraulic capture zone width/total width of funnel-and-gate).
- ❑ For higher values of K_{cell} vs. K_{aquifer} , there is an increase in absolute and relative discharge through the gate as well as in the relative size of the capture zone. Thus, a higher K_{cell} tends to draw more flow toward the gate.
- ❑ Higher values for the ratio of width of the single funnel wall (one wing) to the depth of the funnel-and-gate system result in lower absolute and relative discharge, and in smaller capture zones. This is because, for cases of wide but shallow funnel walls, there is an increase in the flow component that is diverted under the barrier rather than through the gate.
- ❑ Higher values for the ratio of total funnel wall width to the width of the gate result in higher absolute discharge but lower relative discharge and smaller hydraulic capture zones. This result implies that, for wider funnel walls, the increase in the discharge through the gate is not proportional to the increase in the funnel wall area.

C.4 Hydraulic Evaluation of Funnel-and-Gate Systems

The section includes a detailed hydraulic evaluation of a typical funnel-and-gate configuration in a homogeneous setting. It also illustrates a modeling approach that may be used to design the location, configuration, and dimensions of such a PRB and determine the appropriate monitoring configuration. MODFLOW can be used to develop a steady-state numerical approximation of the groundwater flow field and to calculate flow budgets through the gate. Particle tracking techniques under advective flow conditions only can be used to delineate capture zones and travel times in the vicinity of the funnel-and-gate. RWLK3D[®] (Prickett et al., 1981) or any similar particle-tracking code could be used to simulate particle pathways. The model simulations can be performed to aid in both the design phase and the evaluation phase of PRB systems for the containment and remediation of contaminated groundwater. These simulations can build upon previous modeling efforts conducted by Starr and Cherry (1994). Specific objectives can include determining how changes in gate conductivity over time affected capture zone width, retention times for groundwater moving through the reactive cell, and flow volumes through the gate.

The model domain and grid size typically is determined based on the site-specific conditions. The primary criteria are that the domain should be large enough so that the boundary conditions do not affect flow in the vicinity of the PRB. Further, the model cell size in the vicinity of the PRB should be small enough to provide sufficient resolution for retention time calculations. The funnel-and-gate configuration modeled in this illustration is the pilot-scale PRB at former NAS Moffett Field (see Figure C-1). The funnel consists of two 20-ft lengths of sheet piling oriented perpendicular to flow on either side of a 10-ft by 10-ft reactive cell representing the gate. The reactive cell is bounded on its sides by 10-ft lengths of sheet piling. The gate itself consists of

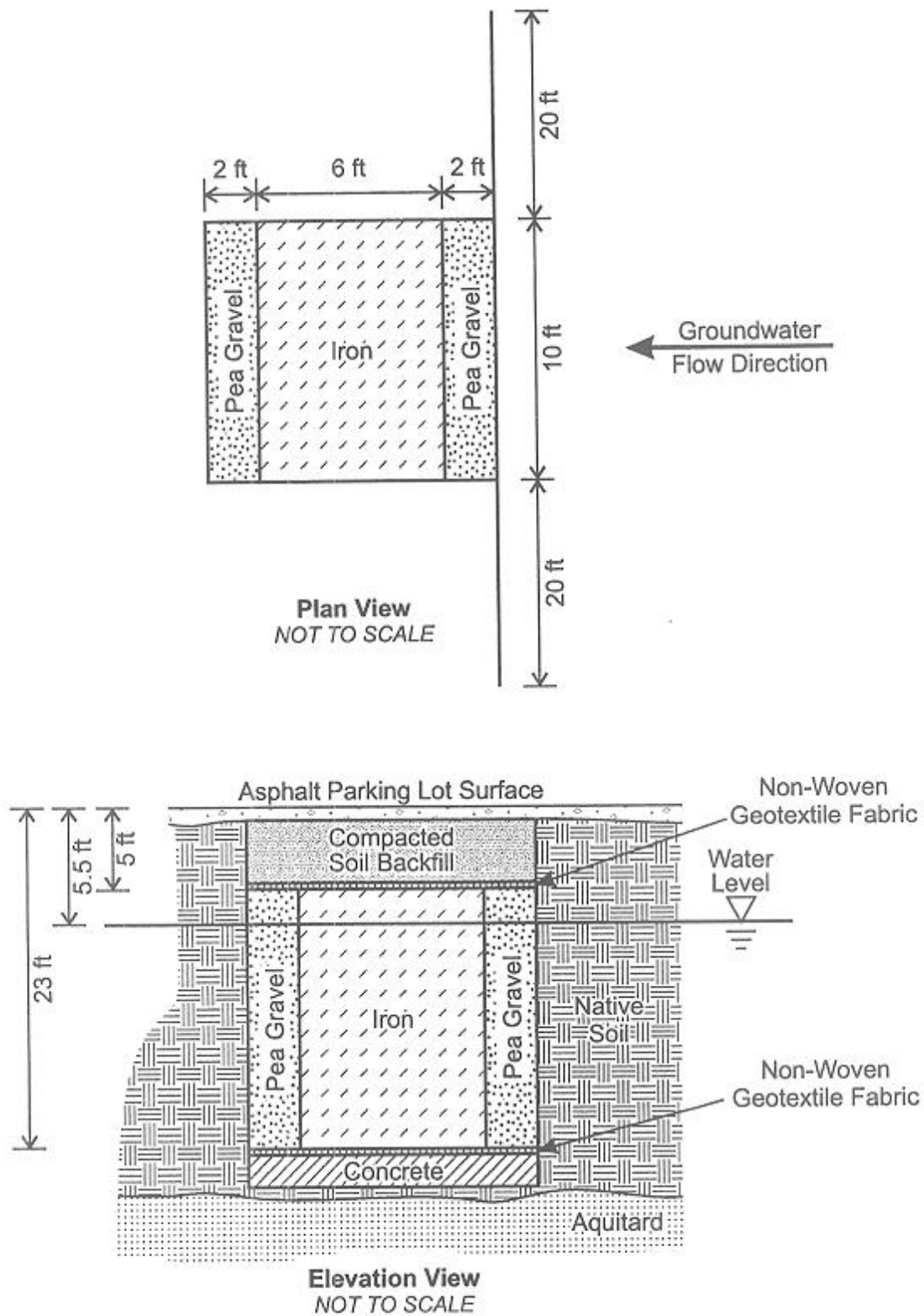


Figure C-1. Pilot-Scale Funnel-and-Gate System Installed at Former NAS Moffett Field, CA (Courtesy of PRC, 1996)

2 ft of ¾-inch pea gravel located on both the upgradient and downgradient ends of the reactive cell, which has a 6-ft flowthrough thickness of iron.

For this model of a funnel-and-gate system, the domain consisted of a single layer that is 500 ft long and 300 ft wide. The grid had 98 rows and 106 columns, resulting in a total of 10,388 nodes. Grid nodes were 10 ft by 10 ft at their maximum (in the general domain area) and 0.5 ft by 0.5 ft in the region of the gate itself. Specified head nodes were set along the first and last rows of the model to establish a gradient of 0.006. No flow conditions were set along the first and last columns of the model.

The funnel (sheet piling) was simulated as a horizontal flow barrier having a K of 2.0×10^{-6} ft/day. For the continuous reactive barrier configuration, the funnel may be excluded from the model. The pea gravel was assigned a K of 2,830 ft/d. The reactive cell consisting of granular iron was assigned a K of 283 ft/d, the maximum laboratory-measured value for 100% iron. It should be noted that in some modeling studies (e.g., Thomas et al., 1995), a reactive cell with K of 142 ft/d has been used for 100% iron. In general, the K value for the reactive medium should be determined from laboratory permeability testing. Porosity was held constant at 0.30 for all materials in each of the simulations.

For this illustration, simulated K_{aquifer} was varied among 0.5, 1, 2, 5, 10, 20, 50, and 100 ft/d to represent low- and high-permeability aquifers. Once this base scenario was established, simulations were conducted to evaluate reductions in K_{cell} over time that could potentially be caused by buildup of precipitates. To determine the effects of decreased permeability of the gate over a period of operation, K_{cell} was reduced in 10% increments from the initial 283 ft/d to 28.3 ft/d for each value of K_{aquifer} . An additional set of simulations was performed with K_{cell} reduced by 95% to 14.15 ft/d, resulting in a total of 11 simulations for each value of K_{aquifer} . For each individual simulation, a single value for K_{aquifer} was used. The effects of geologic heterogeneities were not considered in these simulations. The results from the 88 simulations were used to evaluate the impact of variations in K_{cell} and K_{aquifer} on capture zone width, flow volumes, and travel times through (retention times in) the reactive cell.

Table C-1 lists the model run number, reactive cell conductivity, aquifer conductivity, ratio of reactive cell to aquifer conductivity, capture zone width, residence time within the reactive cell, and groundwater discharge through the reactive cell. Capture zone width in each of the simulations was determined by tracking particles forward through the reactive cell. Two hundred particles (1 particle every 0.5 ft) were initiated along a 100-ft-long line source upgradient from the PRB. The location of the flow divides between particles passing through the reactive cell and those passing around the ends of the funnel were used to determine capture zone width. Residence time within the reactive cell for each simulation was determined from the length of time required for the particles to pass through it. Figure C-2 illustrates the determination of flow divides and travel times for simulation number 57, which had an aquifer conductivity of 20 ft/d and a reactive cell conductivity of 283 ft/d. Particle pathlines have been overlain onto the calculated water-table surface. Particle pathlines and intermediate time steps within the reactive cell are also shown. In some cases, there may be significant variation in residence times at the edges of the reactive cell and at its center. For example, Vogan et al. (1994) showed that

Table C-1. Summary of Funnel-and-Gate Model Runs

Run #	K_{cell} (ft/day)	K_{aquifer} (ft/day)	Ratio of K_{cell}· K_{aquifer}	Capture Width (ft)	Discharge (ft³/day)	Residence Time (days)	Relative Discharge
1	283	0.1	2,830.00	NA	NA	NA	NA
2	283	0.5	566.00	34	2.356	219.0	1.000
3	255	0.5	509.40	NA	2.356	220.0	1.000
4	226	0.5	452.80	NA	2.355	218.0	1.000
5	198	0.5	396.20	NA	2.355	219.0	1.000
6	170	0.5	339.60	NA	2.354	220.0	0.999
7	142	0.5	283.00	NA	2.354	219.0	0.999
8	113	0.5	226.40	NA	2.353	218.0	0.999
9	85	0.5	169.80	NA	2.352	220.0	0.998
10	57	0.5	113.20	NA	2.350	220.0	0.998
11	28	0.5	56.60	NA	2.344	220.0	0.995
12	14	0.5	28.30	NA	2.334	NA	0.991
13	283	1	283.00	32.75	4.732	107.0	1.000
14	255	1	254.70	NA	4.732	107.5	1.000
15	226	1	226.40	NA	4.730	107.5	1.000
16	198	1	198.10	NA	4.729	107.5	0.999
17	170	1	169.80	NA	4.727	107.5	0.999
18	142	1	141.50	NA	4.725	107.5	0.998
19	113	1	113.20	NA	4.721	107.5	0.998
20	85	1	84.90	NA	4.716	107.5	0.997
21	57	1	56.60	NA	4.705	108.0	0.994
22	28	1	28.30	NA	4.672	108.5	0.987
23	14	1	14.15	NA	4.603	110.0	0.973
24	283	2	141.50	NA	9.475	52.5	1.000
25	255	2	127.35	NA	9.472	52.5	1.000
26	226	2	113.20	NA	9.468	52.5	0.999
27	198	2	99.05	NA	9.462	52.5	0.999
28	170	2	84.90	NA	9.455	52.5	0.998
29	142	2	70.75	NA	9.446	52.5	0.997
30	113	2	56.60	NA	9.432	53.0	0.995
31	85	2	42.45	NA	9.408	53.0	0.993
32	57	2	28.30	NA	9.362	53.5	0.988
33	28	2	14.15	NA	9.223	54.5	0.973
34	14	2	7.08	NA	8.954	56.0	0.945
35	283	5	56.60	32.17	23.613	21.0	1.000
36	255	5	50.94	NA	23.593	20.9	0.999
37	226	5	45.28	NA	23.568	21.0	0.998
38	198	5	39.62	NA	23.535	21.1	0.997
39	170	5	33.96	NA	23.493	21.1	0.995
40	142	5	28.30	NA	23.432	21.1	0.992
41	113	5	22.64	NA	23.344	21.3	0.989
42	85	5	16.98	NA	23.197	21.4	0.982

Table C-1. Summary of Funnel-and-Gate Model Runs (Continued)

Run #	K_{cell} (ft/day)	K_{aquifer} (ft/day)	Ratio of K_{cell}· K_{aquifer}	Capture Width (ft)	Discharge (ft³/day)	Residence Time (days)	Relative Discharge
43	57	5	11.32	NA	22.909	21.6	0.970
44	28	5	5.66	NA	22.082	22.6	0.935
45	14	5	2.83	NA	20.597	24.0	0.872
46	283	10	28.30	32.17	46.407	10.6	1.000
47	255	10	25.47	32.17	46.328	10.6	0.998
48	226	10	22.64	32.17	46.169	10.8	0.995
49	198	10	19.81	32.33	46.040	10.7	0.992
50	170	10	16.98	32.33	45.870	10.9	0.988
51	142	10	14.15	32.5	45.628	10.9	0.983
52	113	10	11.32	31.5	45.274	11.0	0.976
53	85	10	8.49	31.67	44.763	11.0	0.965
54	57	10	5.66	31.83	43.566	11.4	0.939
55	28	10	2.83	32.17	40.562	12.3	0.874
56	14	10	1.42	NA	35.630	13.9	0.768
57	283	20	14.15	31.81	91.493	5.4	1.000
58	255	20	12.74	NA	91.239	5.4	0.997
59	226	20	11.32	NA	91.331	5.5	0.998
60	198	20	9.91	NA	89.890	5.6	0.982
61	170	20	8.49	NA	89.262	5.6	0.976
62	142	20	7.08	NA	88.379	5.6	0.966
63	113	20	5.66	NA	86.708	5.7	0.948
64	85	20	4.25	NA	84.126	5.8	0.919
65	57	20	2.83	NA	78.681	6.3	0.860
66	28	20	1.42	NA	73.403	6.7	0.802
67	14	20	0.71	NA	59.502	8.3	0.650
68	283	50	5.66	31.5	221.445	2.3	1.000
69	255	50	5.09	NA	219.770	2.3	0.992
70	226	50	4.53	NA	217.730	2.3	0.983
71	198	50	3.96	NA	215.185	2.4	0.972
72	170	50	3.40	NA	211.925	2.4	0.957
73	142	50	2.83	NA	207.005	2.4	0.935
74	113	50	2.26	NA	200.755	2.5	0.907
75	85	50	1.70	NA	190.560	2.6	0.861
76	57	50	1.13	NA	173.695	2.9	0.784
77	28	50	0.57	NA	136.155	3.7	0.615
78	14	50	0.28	NA	94.409	5.8	0.426
79	283	100	2.83	30.38	410.105	1.3	1.000
80	255	100	2.55	NA	404.240	1.2	0.986
81	226	100	2.26	NA	397.135	1.2	0.968
82	198	100	1.98	NA	388.355	1.3	0.947
83	170	100	1.70	NA	377.240	1.3	0.920
84	142	100	1.42	NA	362.735	1.4	0.884

Table C-1. Summary of Funnel-and-Gate Model Runs (Continued)

Run #	K_{cell} (ft/day)	K_{aquifer} (ft/day)	Ratio of K_{cell}· K_{aquifer}	Capture Width (ft)	Discharge (ft³/day)	Residence Time (days)	Relative Discharge
85	113	100	1.13	NA	343.060	1.5	0.837
86	85	100	0.85	NA	314.455	1.6	0.767
87	57	100	0.57	NA	268.935	1.8	0.656
88	28	100	0.28	NA	188.075	2.7	0.459
89	14	100	0.14	NA	116.935	4.2	0.285
90	283	200	1.42	NA	NA	NA	NA

NA = Not applicable.

simulated residence times in a funnel-and-gate system (with caisson gates) varied from 29 hours at the edges to 82 hours in the center of the reactive cell.

Discharge through the reactive cell was determined from the MODFLOW-calculated, cell-by-cell flow file using the MODUTILITY code zone budget (Harbaugh, 1990). Correlation between K_{aquifer} and K_{cell}, retention time, discharge, and capture zone width were determined by plotting the results of the 88 simulations against one another. Some basic relationships are readily apparent.

Figure C-3 illustrates the correlation between K_{aquifer}, retention time, and discharge through the gate. There is an inverse relationship between K_{aquifer} and retention time. As aquifer conductivity increases, the retention time within the reactive cell decreases. As aquifer conductivity increases, the total discharge through the gate increases. Finally, Figure C-3 shows a very strong inverse correlation between the total discharge through the gate and the retention time within the reactive cell. Therefore, aquifers having high hydraulic conductivities may require a greater reactive cell flowthrough thickness to meet residence time requirements so that contaminant levels can be reduced to regulatory limits.

The conductivities of both the aquifer and the reactive cell were plotted against capture zone width. A general correlation exists between an increase in K (and discharge through the gate) and capture-zone width. As K increased, the capture-zone width generally increased. However, the capture zone width appeared to be more sensitive to the length of the funnel walls and was generally observed to occur at just over half of the funnel wall length on either side of the gate. Capture zone widths ranged from roughly 0.2 to 2 ft beyond the midpoint of the funnel wall. Figure C-4 is a plot showing the reduction in discharge (due to potential buildup of precipitate) through the gate that results from decreasing K_{cell} at aquifer conductivities of 0.5, 10, and 100 ft/d. In each of the plots shown in Figure C-4, K_{cell} decreases from 283 ft/d to 14.15 ft/d. Reductions in K_{cell} were simulated to represent the potential clogging of the reactive cell by precipitation. The percent decline in discharge through the gate was determined for each decline in K_{cell}. When aquifer conductivity is 0.5 ft/d, the reactive cell conductivity is much greater than the aquifer conductivity for each of the 11 simulations performed, and the percent decline in discharge through the gate is very small. Decreasing reactive cell conductivity from 283 ft/d to

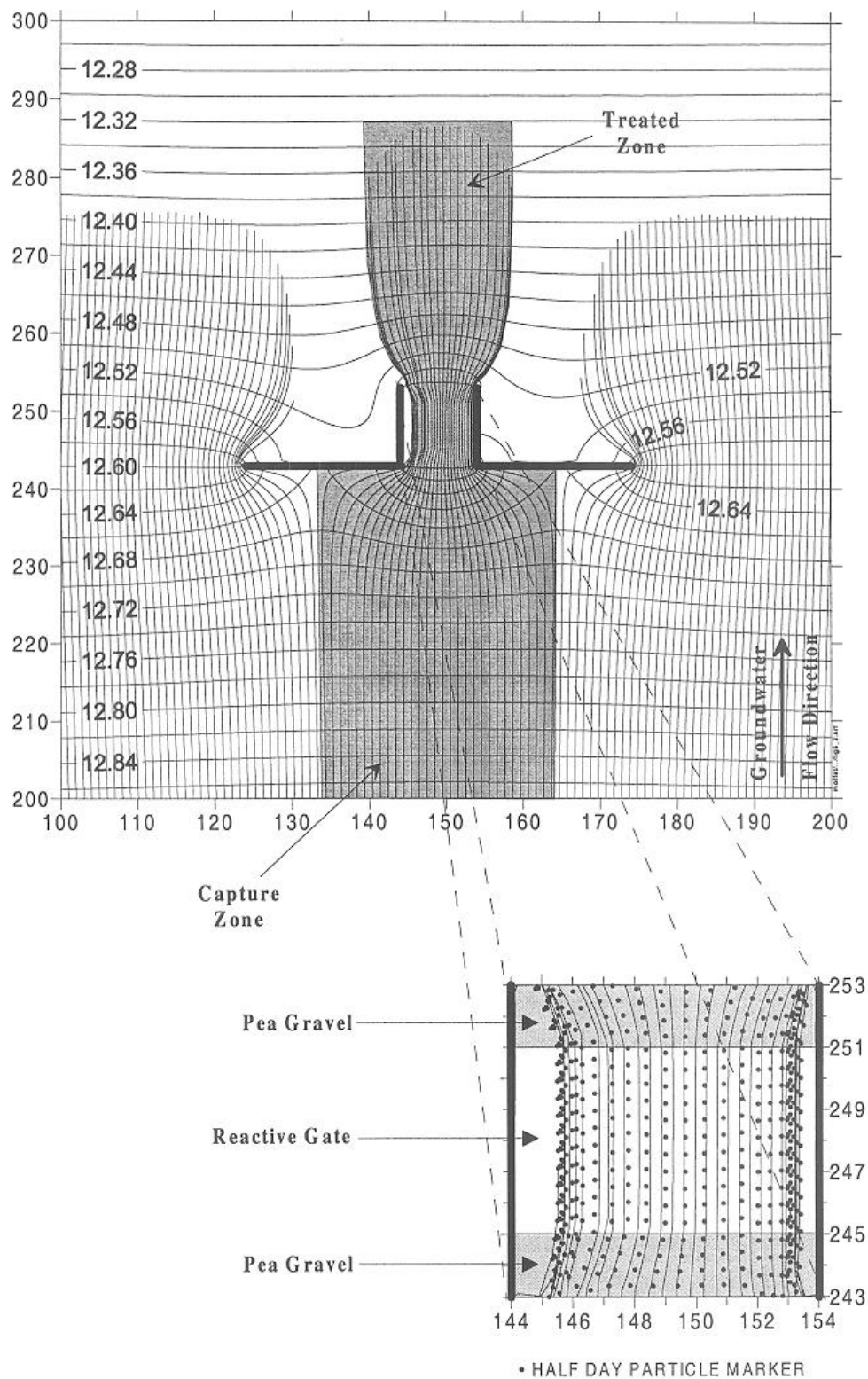
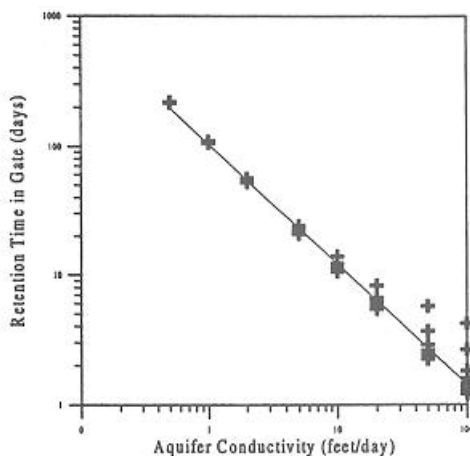
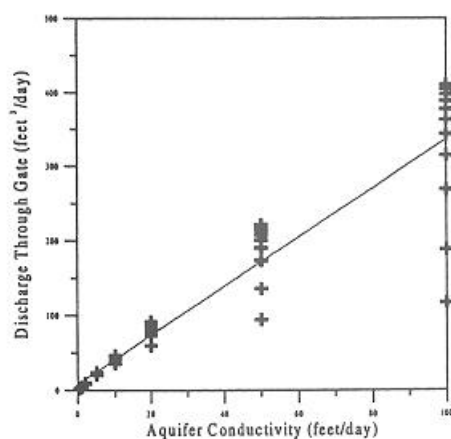


Figure C-2. Simulated Particle Pathlines Overlain upon Water Table Including Zoomed in View of Gate Area

(a) K_{aquifer} versus retention time



(b) K_{aquifer} versus discharge



(c) Retention time versus discharge

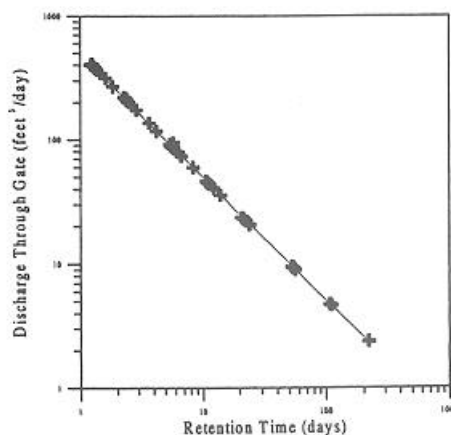


Figure C-3. Correlation Between K_{aquifer} , Discharge, and Travel Time Through the Gate for a Homogeneous, One-Layer Scenario

14.15 ft/d resulted in only a 1% decline in the discharge through the gate. As aquifer conductivity was increased, a larger reduction in discharge through the gate occurred as the reactive cell conductivity decreased. For aquifer conductivities of 10 and 100 ft/d, discharge through the gate decreased by roughly 27 and 71%, respectively, over the same decline in gate conductivity. In

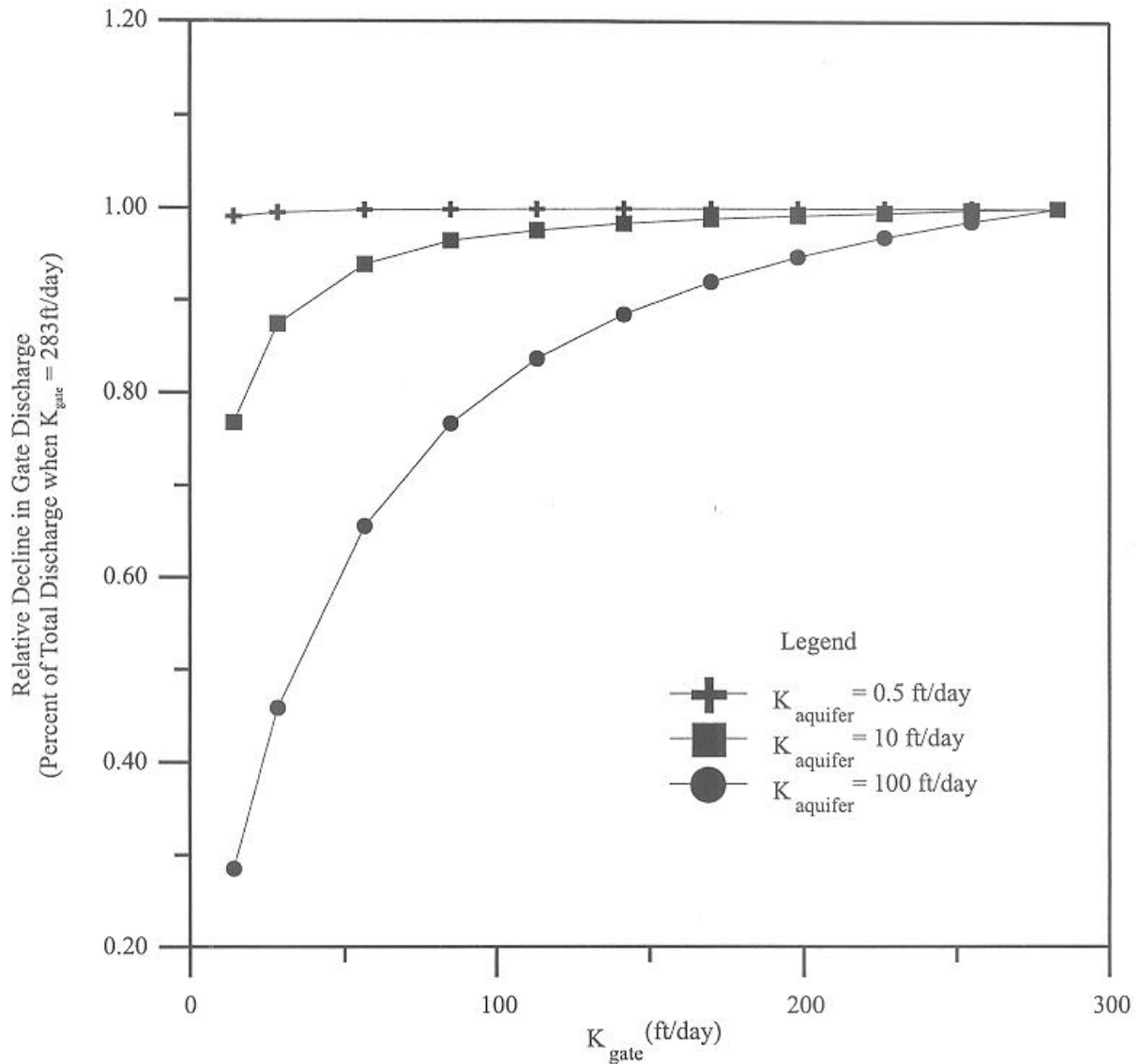


Figure C-4. Correlation Between K_{cell} and Discharge at $K_{aquifer}$ of 0.5, 10, and 100 ft per day K_{cell} Varied Between 283 and 14.15 ft per day

both cases, the ratio of K_{cell} to $K_{aquifer}$ approaches or becomes less than 1 as K_{cell} decreases. Therefore, the effects of precipitate buildup in the reactive cell are likely to be felt earlier in high-permeability aquifers. However, as discussed below, there is considerable leeway before such effects are noticed.

Figure C-5 is a plot of the ratio of K_{cell} to $K_{aquifer}$ versus discharge through the gate for the 88 simulations. The plot indicates that declines in reactive cell conductivity due to clogging have very little influence on the volume of groundwater passing through the gate as long as the reactive cell conductivity is roughly 5 times the conductivity of the aquifer. In these instances, discharge through the gate remained at roughly 95% of the simulated discharge when the gate

conductivity was 283 ft/d. Because discharge is relatively unaffected, residence times and capture zone width will remain relatively unchanged for a given aquifer conductivity. As the ratio between K_{cell} and K_{aquifer} declines below 5, the relative decrease in discharge becomes greater and results in decreased capture zone widths and increased retention times. Thus, as long as the hydraulic conductivity of a freshly installed reactive cell is designed to be one or two orders of magnitude greater than the hydraulic conductivity of the aquifer, there is considerable flexibility for precipitates to build up without significantly affecting the hydraulic capture zone.

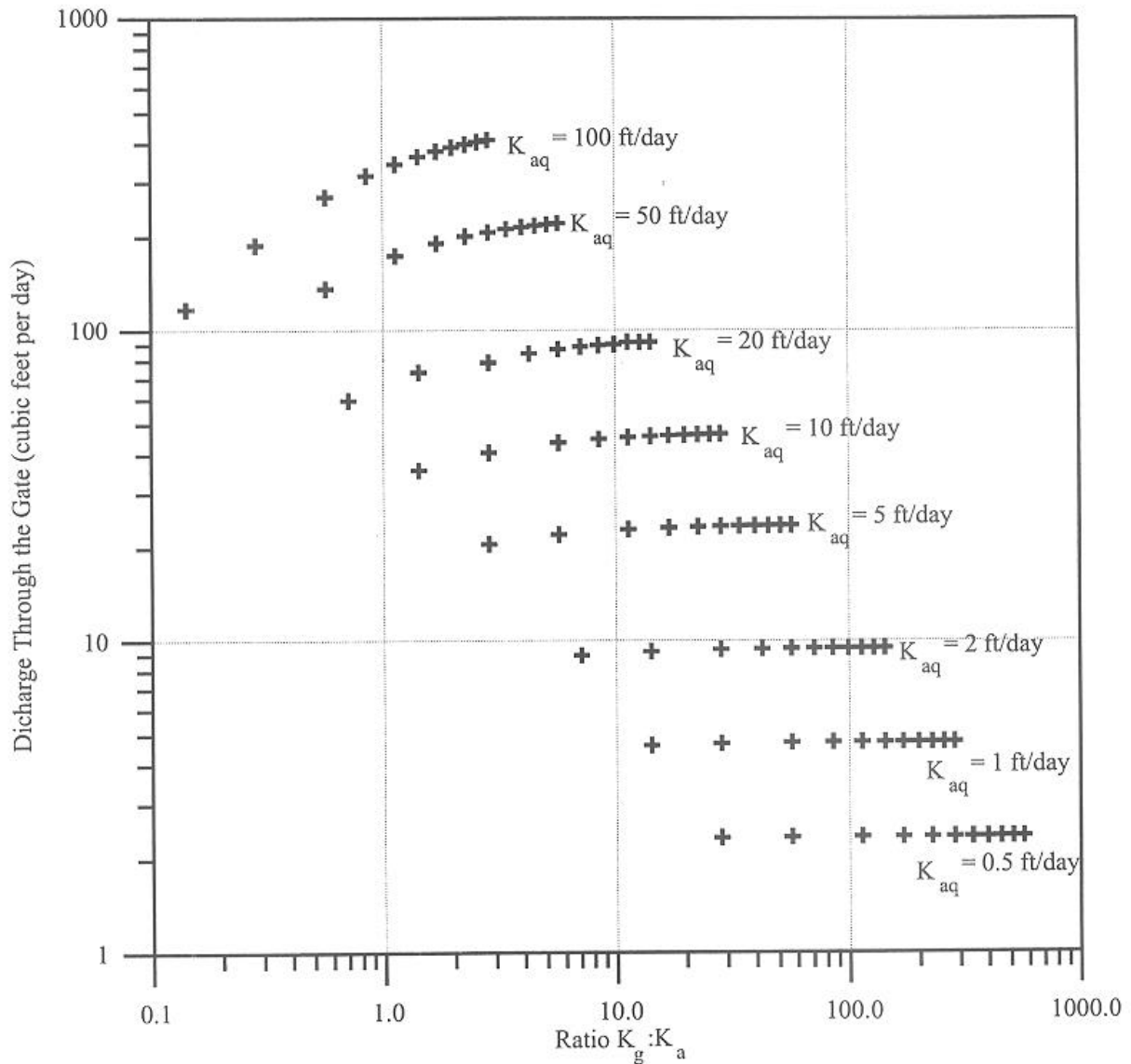


Figure C-5. Correlation Between Ratio of K_{cell} to K_{aquifer} Versus Discharge Through the Gate for a Homogeneous, One-Layer Scenario

C.5 References

Anderson, M.P. and W.W. Woessner. 1992. *Applied Groundwater Modeling: Simulation of Flow and Advective Transport*. Academic Press, NY.

Battelle. 1996. *Draft Evaluation of Funnel-and-Gate Pilot Study at Moffett Federal Airfield with Groundwater Modeling*. Prepared for the U.S. Department of Defense, Environmental Security Technology Certification Program and Naval Facilities Engineering Services Center, Port Hueneme, CA. September 11.

Battelle. 1997. *Design/Test Plan: Permeable Barrier Demonstration at Area 5, Dover AFB*. Prepared for Air Force Research Laboratory, Tyndall AFB. November 14.

Brigham Young University. 1996. *GMS: Department of Defense Groundwater Modeling System*, Version 2.0.

Environmental Simulations, Inc. 1996. *Groundwater Vistas*.

Everhart, D. 1996. *Theoretical Foundations of GROWFLOW*. ARA-TR-96-5286-3. Prepared by Applied Research Associates, Inc. for U.S. Air Force, Tyndall Air Force Base. April.

Guiguer, N., J. Molson, E.O. Frind, and T. Franz. 1992. *FLONET—Equipotential and Streamlines Simulation Package*. Waterloo Hydrogeologic Software and the Waterloo Center for Groundwater Research, Waterloo, Ontario.

Gupta, N., and T.C. Fox. 1999. "Hydrogeologic Modeling for Permeable Reactive Barriers." *Journal of Hazardous Materials*, 68: 19-39.

Harbaugh, A.W. 1990. *A Computer Program for Calculating Subregional Water Budgets Using Results from the U.S. Geological Survey Modular Three-Dimensional Finite-Difference Ground-Water Flow Model*. United States Geological Survey Open-File Report 90-392.

Hatfield, K. 1996. *Funnel-and-Gate Design Model*. ARA-TR-96-5286-4. Prepared by Applied Research Associates, Inc. for U.S. Air Force, Tyndall Air Force Base. April.

Hsieh, P.A., and J.R. Freckleton. 1993. *Documentation of a Computer Program to Simulate Horizontal-Flow Barriers Using the U.S. Geological Survey Modular Three-Dimensional Finite-Difference Ground-Water Flow Model*. United States Geological Survey Open-File Report 92-477.

Kipp, Jr., K.L. 1987. *HST3D: A Computer Code for Simulation of Heat and Solute Transport in Three-Dimensional Groundwater Flow Systems*. WRI 86-4095. United States Geological Survey, Denver, CO.

McDonald, M.G., and A.W. Harbaugh. 1988. *A Modular Three-Dimensional Finite-Difference Ground-Water Flow Model: Techniques of Water-Resources Investigations of the United States Geological Survey*. Book 6.

Naymik, T.G., and N.J. Gantos. 1995. Solute Transport Code Verification Report for RWLK3D, Internal Draft. Battelle Memorial Institute, Columbus, OH.

Pollock, D.W. 1989. *Documentation of Computer Programs to Compute and Display Pathlines Using Results from the U.S. Geological Survey Modular Three-Dimensional Finite-Difference Ground-Water Flow Model*. United States Geological Survey Open-File Report 89-381.

PRC, see PRC Environmental Management, Inc.

PRC Environmental Management, Inc. 1996. *Naval Air Station Moffett Field, California, Iron Curtain Area Groundwater Flow Model*. June.

Prickett, T.A., T.G. Naymik, and C.G. Lounquist. 1981. *A "Random Walk" Solute Transport Model for Selected Groundwater Quality Evaluations*. Illinois Department of Energy and Natural Resources, Illinois State Water Survey, Bulletin 65.

Rumbaugh, J.O., III. 1993. ModelCad³⁸⁶: *Computer-Aided Design Software for Groundwater Modeling, Version 2.0*. Geraghty & Miller, Inc., Reston, VA.

Shikaze, S. 1996. *3D Numerical Modeling of Groundwater Flow in the Vicinity of Funnel-and-Gate Systems*. ARA-TR-96-5286-1. Prepared by Applied Research Associates, Inc. for U.S. Air Force, Tyndall Air Force Base. April.

Starr, R.C., and J.A. Cherry. 1994. "In Situ Remediation of Contaminated Ground Water: The Funnel-and-Gate System." *Groundwater*, 32(3): 465-476.

Therrien, R. 1992. "Three-Dimensional Analysis of Variably-Saturated Flow and Solute Transport in Discretely-Fractured Porous Media." Ph.D. thesis, Dept. of Earth Science, University of Waterloo, Ontario, Canada.

Therrien, R., and E. Sudicky. 1995. "Three-Dimensional Analysis of Variably-Saturated Flow and Solute Transport in Discretely-Fractured Porous Media." *Jour. of Contaminant Hydrology*, 23: 1-44.

Thomas, A.O., D.M. Drury, G. Norris, S.F. O'Hannesin, and J.L. Vogan. 1995. "The In-Situ Treatment of Trichloroethene-Contaminated Groundwater Using a Reactive Barrier-Result of Laboratory Feasibility Studies and Preliminary Design Considerations." In Brink, Bosman, and Arendt (Eds.), *Contaminated Soil '95*, pp. 1083-1091. Kluwer Academic Publishers.

van der Heijde, P.K.M., and O.A. Elnawawy. 1993. *Compilation of Groundwater Models*. EPA/600/2-93/118. U.S. EPA's R.S. Kerr Environmental Research Laboratory, Ada, OK.

Vogan, J.L., J.K. Seaberg, B.G. Gnabasik, and S. O'Hannesin. 1994. "Evaluation of In-Situ Groundwater Remediation by Metal Enhanced Reductive Dehalogenation Laboratory Column Studies and Groundwater Flow Modeling." 87th Annual Meeting and Exhibition of the Air and Waste Association, Cincinnati, OH, June 19-24, 1994.

Wang, H.F., and M.P. Anderson. 1982. *Introduction to Groundwater Modeling: Finite Difference and Finite Element Methods*. W.H. Freeman and Company, NY.

Waterloo Hydrogeologic, Inc. 1999a. *FLOWPATH II for Windows 95/NT*.

Waterloo Hydrogeologic, Inc. 1999b. *Visual MODFLOW User's Manual*.

Zheng, C. 1989. *PATH3D*. S.S. Papadopoulos and Assoc., Rockville, MD.

Appendix D

Geochemical Modeling

D.1 Equilibrium Modeling

D.2 Forward Equilibrium Modeling

D.3 Inverse Modeling

D.4 References

Appendix D

Geochemical Modeling

D.1 Equilibrium Modeling

Equilibrium modeling can be conducted using only site characterization data; influent and effluent analysis of groundwater from a column test is not required. Equilibrium geochemical modeling has been used in a few cases to make predictions about mineral precipitation in PRBs at former Naval Air Station (NAS) Moffett Field, CA; Dover Air Force Base (AFB), DE; and former Lowry AFB, CO (Battelle, 1998; Battelle, 1999; Sass and Gavaskar, 1999). The primary disadvantage of equilibrium modeling is that reaction kinetics and nonequilibrium behavior are not taken into account. Therefore, although equilibrium modeling may serve as a qualitative tool to indicate the type of precipitates that may form in a given system, the results should not be taken as a quantitative assessment of all the processes that would be occurring inside a PRB.

Reaction path modeling is one form of equilibrium modeling that can serve a useful predictive purpose when one of the components is not in equilibrium with the system. (It is assumed that the other components reach equilibrium at each step of the reaction.) The geochemical modeling code PHREEQC (Parkhurst 1995) was used to conduct these simulations. Thermodynamic data were obtained from the MINTEQ database (Allison et al., 1991). Selected equilibrium constants that are relevant to this study are shown in Table D-1. To illustrate this approach, a simulation was run using native groundwater near the former NAS Moffett Field PRB. The groundwater was allowed to react incrementally with pure iron until equilibrium was reached. This approach was used because iron is unlikely to react completely with the groundwater and the extent of reaction cannot be determined *a priori* (i.e., without experimental data for a particular type of iron under site-specific conditions). Results of the reaction path model are shown in Figures D-1 to D-4.

Figure D-1 shows that pH increases until a plateau is reached at about pH 11.2. This plateau begins after approximately 1 gram of iron has dissolved per liter of pore water (g Fe/L). The plateau continues to about 2.7 g Fe/L have dissolved, at which point the pH increases somewhat further. Equilibrium is reached with respect to the iron after approximately 3.4 g Fe/L have dissolved. Also shown in Figure D-1 is the trend in redox potential (Eh), which is symmetrical to the pH behavior. At the plateau region, Eh is approximately -520 millivolts (mV). At equilibrium, the Eh decreases to almost -700 mV. It should be emphasized that true equilibrium with respect to the iron may not actually be reached in a real system. The kinetics of the iron reaction may be affected by the groundwater constituents, some of which may cause the iron surface to become passivated.

Figure D-2 shows that a number of iron-rich solids may precipitate, and in some cases dissolve, as the iron continues to react with the groundwater. The first phases to form are ferrous siderite (FeCO_3) and marcasite (FeS_2). As the reaction progresses, marcasite becomes unstable and is replaced by mackinawite (FeS), which contains a more reduced form of sulfur. Also, siderite later dissolves and the ferric compounds $\text{Fe}(\text{OH})_3$ and “green rust” form. In this example, green rust appears to account for a small loss of Cl ions. Note that $\text{Fe}(\text{OH})_2$ does not form during any of the quasi-equilibrium steps, which is a result that contrasts with the expected appearance of

Table D-1. Mineral Equilibrium Reactions Used in Geochemical Modeling Calculations

Mineral	Reaction	Log K	delta H (kcal/mol)
Anhydrite	$\text{CaSO}_4 \rightleftharpoons \text{Ca}^{+2} + \text{SO}_4^{-2}$	-4.637	-3.769
Aragonite	$\text{CaCO}_3 \rightleftharpoons \text{Ca}^{+2} + \text{CO}_3^{-2}$	-8.36	-2.615
Brucite	$\text{Mg}(\text{OH})_2 + 2\text{H}^+ \rightleftharpoons \text{Mg}^{+2} + 2\text{H}_2\text{O}$	16.792	-25.84
Calcite	$\text{CaCO}_3 \rightleftharpoons \text{Ca}^{+2} + \text{CO}_3^{-2}$	-8.475	-2.585
Dolomite	$\text{CaMg}(\text{CO}_3)_2 \rightleftharpoons \text{Ca}^{+2} + \text{Mg}^{+2} + 2\text{CO}_3^{-2}$	-17.0	-8.29
Fe metal	$\text{Fe} \rightleftharpoons \text{Fe}^{+2} + 2\text{e}^-$	15.114	-21.3
Ferrihydrite	$\text{Fe}(\text{OH})_3 + 3\text{H}^+ \rightleftharpoons \text{Fe}^{+3} + 3\text{H}_2\text{O}$	4.891	0.0
Goethite	$\text{FeOOH} + 3\text{H}^+ \rightleftharpoons \text{Fe}^{+3} + 2\text{H}_2\text{O}$	0.5	-14.48
Green Rust	$\text{Fe}(\text{OH})_{2.7}\text{Cl}_{0.3} + 2.7\text{H}^+ \rightleftharpoons \text{Fe}^{+3} + 2.7\text{H}_2\text{O} + 0.3\text{Cl}^-$	-3.04	0.0
Gypsum	$\text{CaSO}_4 \cdot 2\text{H}_2\text{O} \rightleftharpoons \text{Ca}^{+2} + \text{SO}_4^{-2} + 2\text{H}_2\text{O}$	-4.848	0.261
Mackinawite	$\text{FeS} + \text{H}^+ \rightleftharpoons \text{Fe}^{+2} + \text{HS}^-$	-4.648	0.0
Magnesite	$\text{MgCO}_3 \rightleftharpoons \text{Mg}^{+2} + \text{CO}_3^{-2}$	-8.029	-6.169
Marcasite	$\text{FeS}_2 + 2\text{H}^+ + 2\text{e}^- \rightleftharpoons \text{Fe}^{+2} + 2\text{HS}^-$	-18.177	11.1
Melanterite	$\text{FeSO}_4 \cdot 7\text{H}_2\text{O} \rightleftharpoons \text{Fe}^{+2} + \text{SO}_4^{-2} + 7\text{H}_2\text{O}$	-2.47	2.86
Portlandite	$\text{Ca}(\text{OH})_2 + 2\text{H}^+ \rightleftharpoons \text{Ca}^{+2} + 2\text{H}_2\text{O}$	22.675	-30.69
Siderite	$\text{FeCO}_3 \rightleftharpoons \text{Fe}^{+2} + \text{CO}_3^{-2}$	-10.55	-5.328

Source: Allison et al. (1991).

$\text{Fe}(\text{OH})_2$ during column testing (Mackenzie et al., 1999). Research conducted at the University of Waterloo and at EnviroMetal Technologies, Inc. (ETI) also suggests that noncarbonate iron precipitates in granular iron are composed mostly of $\text{Fe}(\text{OH})_2$ which is converted over time to magnetite (Odziemkowski et al., 1998). However, the presence of sulfate in former NAS Moffett Field groundwater, which becomes converted to sulfide, is probably the reason that $\text{Fe}(\text{OH})_2$ has no stability region in this water.

Figure D-3 shows the precipitation trends for non-ferrous phases. Note that the predicted order of precipitation is aragonite (or calcite), followed by magnesite, then brucite. The CaCO_3 phase remains stable until about 3.0 g Fe/L have dissolved. Magnesite is stable for only a portion of the reaction, and then dissolves and allows brucite to predominate. Figure D-4 shows the concentrations of various species that form at different pH values. In this figure, pH is dependent on the reaction steps illustrated in Figure D-1.

Another form of equilibrium modeling known as inverse modeling also can be used to evaluate the types and degree of precipitation, and is described in Section D.3. Inverse modeling can be conducted with column test data as well, but may be more suitable for evaluating monitoring data from a field PRB system.

D.2 Forward Equilibrium Modeling

In general, forward equilibrium modeling involves calculating speciation of dissolved constituents and saturation relative to minerals that can exist in the chemical system defined by the input parameters (field parameters and elemental concentrations). The speciation routine simply

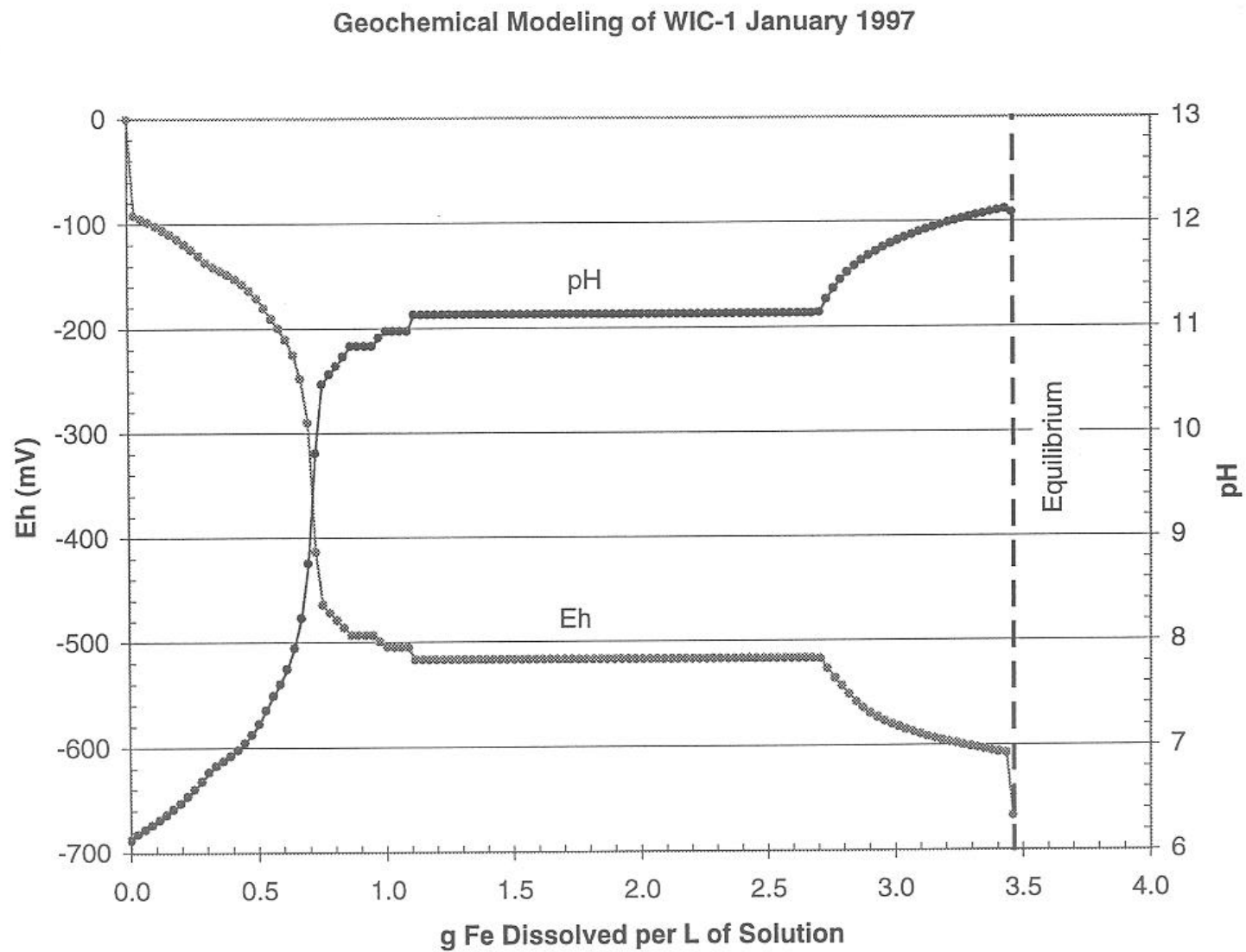


Figure D-1. pH and Eh Results from Reaction Path Modeling for the Former NAS Moffett Field PRB

Geochemical Modeling of WIC-1 January 1997

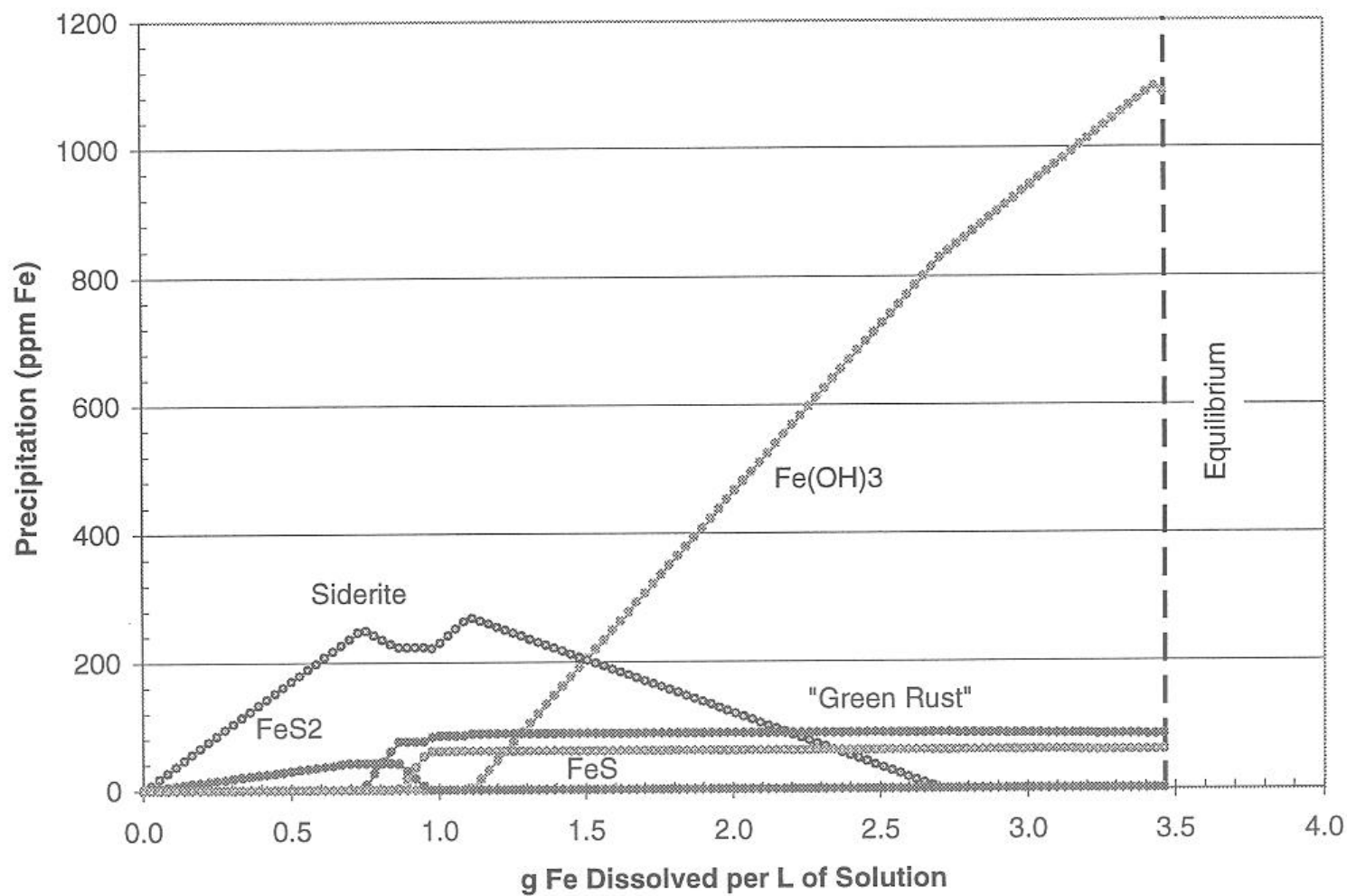


Figure D-2. Precipitation Trends for Ferrous Solids Determined from Reaction Path Modeling for the Former NAS Moffett Field PRB

Geochemical Modeling of WIC-1 January 1997

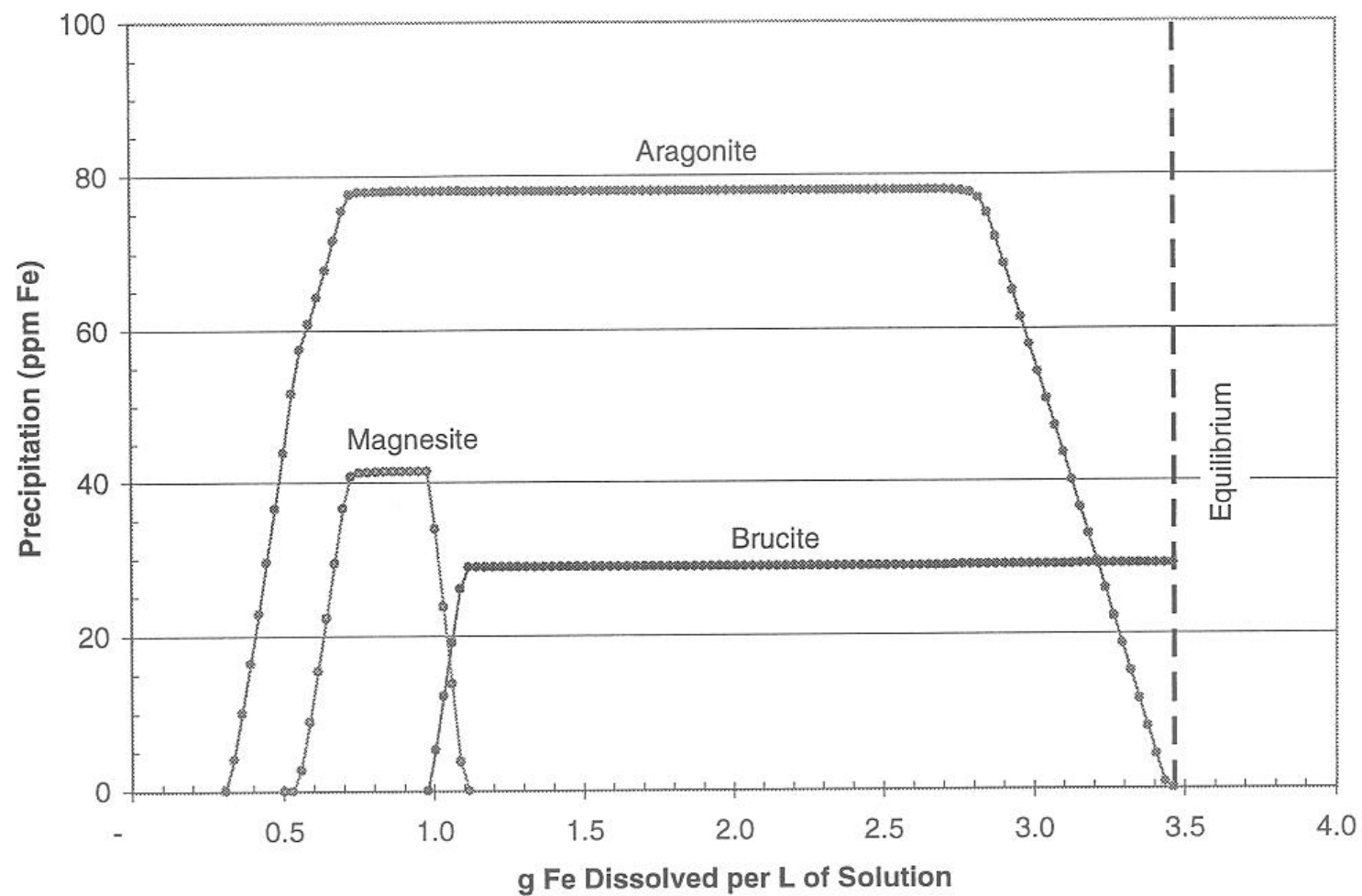


Figure D-3. Precipitation Trends for Non-Ferrous Solids Determined from Reaction Path Modeling for the Former NAS Moffett Field PRB

Geochemical Modeling of WIC-1 January 1997

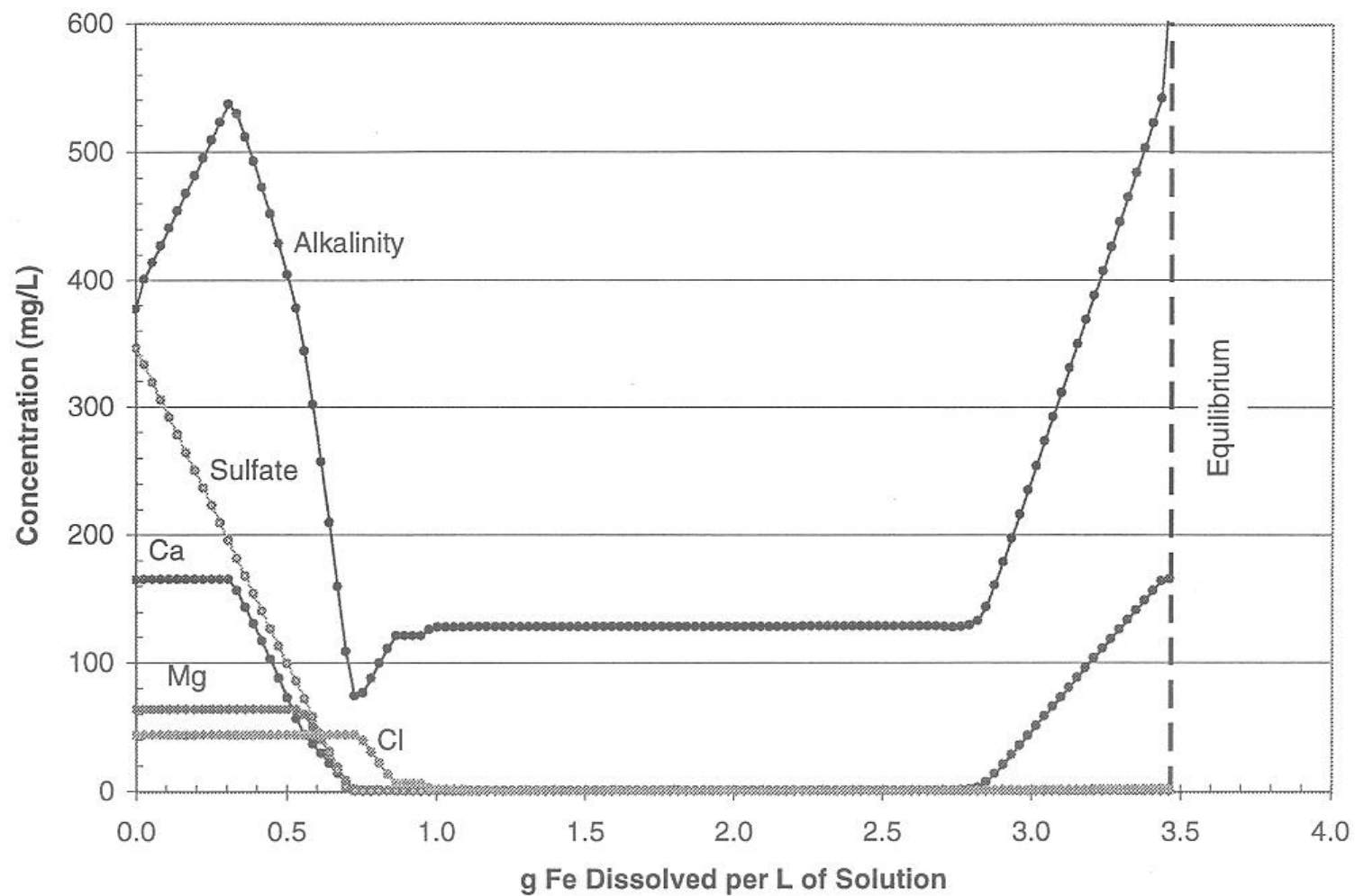


Figure D-4. Inorganic Indicator Parameter Results from Reaction Path Modeling for the Former NAS Moffett Field PRB

calculates concentrations of all aqueous complexes for which the model has thermodynamic data. Mineral saturation is defined by a saturation index (SI) given by $SI = \log (IAP/K)$, where IAP is ion activity product and K is the thermodynamic equilibrium constant for a mineralogical reaction. When $SI = 0$, the mineral and groundwater are considered to be in equilibrium; negative values imply undersaturation of the mineral phase and positive values imply oversaturation. In practice, mineral equilibrium may be assumed when $SI = \pm 0.20$.

An example of forward equilibrium modeling is described here using monitoring data from former NAS Moffett Field collected in April 1997 (see Table D-2 for a partial list of input data). Calculations of mineral saturation indices were made using the geochemical modeling code PHREEQC (Parkhurst, 1995), and are presented in Table D-3. Values greater than -0.20 in Table D-2 are bolded, indicating probable saturation or oversaturation with respect to the mineral phase.

The data in Table D-3 indicate that saturation indices vary spatially for most minerals within the former NAS Moffett Field PRB. For example, calcite (CaCO_3) is close to equilibrium in the upgradient aquifer and upgradient pea gravel. Calcite becomes slightly oversaturated in the upgradient portion of the reactive cell, then rapidly falls below saturation in the downgradient portion of the reactive cell, as shown in Figure D-5. The horizontal lines in the figure at $SI = \pm 0.20$ indicate a typical saturation range. Aragonite, which has a similar trend of SI values, is metastable with respect to calcite in groundwater environments, but has been observed to precipitate in column tests during prior research. These transitions probably arise due to the abrupt change in pH after the groundwater enters the reactive cell. The SI calculations suggest that water becomes oversaturated with respect to calcite (or aragonite) in the first one or two feet of the reactive cell. The transition to undersaturation indicates that alkalinity or calcium content of the water (or both) decreases to such an extent that CaCO_3 becomes unstable. In other words, when the $SI < 0.2$, insufficient Ca^{+2} and CO_3^{-2} is available to precipitate a solid. This instability could arise because CaCO_3 and other carbonate or calcic minerals have precipitated inside the transition zone.

It may be significant that the transition zone appears to exist a foot or two downgradient of the pea gravel-iron interface, rather than at the interface itself. Because water is flowing through the cell, the apparent lag time suggests that reaction kinetics for precipitation are slow relative to residence time inside the reactive cell (i.e., time-scale is in days). Thus, filling of pore space by precipitates may be distributed over some range in the cell, rather than concentrated along the upgradient face of the reactive cell. Distributing the precipitate buildup over a longer distance may delay the eventual decline in permeability caused by clogging of the pore space.

Magnesite (MgCO_3) and brucite [$\text{Mg}(\text{OH})_2$] show similar trends as calcite: both are undersaturated in the aquifer and upgradient pea gravel, then become oversaturated in the upgradient portion of the reactive cell and undersaturated further downgradient (see Figures D-6 and D-7). Figure D-6 shows that there are no data points in the magnesite stability field, suggesting that magnesite either is oversaturated or undersaturated, but may never actually precipitate. Brucite, on the other hand, does seem to be stable in the upgradient portion of the PRB, like calcite (SI between -0.2 and 0.2), and for this reason may precipitate (see Figure D-7).

Table D-2. Selected Results of Field Parameter Measurements at the Former NAS Moffett Field PRB (April 1997)

Well ID	pH	Temp (°C)	ORP (mV)^(a)	Eh (mV)^(b)	Deep DO (mg/L)^(c)	Shallow DO (mg/L)^(d)
<i>Upgradient A1 Aquifer Zone Wells</i>						
WIC-1	6.8	19.9	177.2	374.2	< 0.1	< 0.1
5	7.1	20.2	144.3	341.3	< 0.1	8.8
6	8.8	20.2	92.2	289.2	< 0.1	4.3
7	7.0	20.1	155.5	352.5	< 0.1	0.5
8	7.1	20.1	157.8	354.8	< 0.1	0.7
<i>Upgradient Pea Gravel Wells</i>						
WW-7A	7.1	20.6	101.6	298.6	0.3	2.2
7B	7.1	20.7	122.5	319.5	< 0.1	0.7
7C	7.1	20.5	117.1	314.1	< 0.1	1.8
7D	7.4	20.3	110.4	307.4	< 0.1	1.1
<i>Reactive Cell Wells</i>						
WW-8A	10.2	20.8	-343.4	-146.4	< 0.1	0.3
8B	10.2	20.9	-327.5	-130.5	< 0.1	0.3
8C	9.9	20.4	-309.0	-112.0	< 0.1	0.8
8D	11.2	20.4	-359.3	-162.3	< 0.1	0.7
WW-9A	10.4	20.9	-626.2	-429.2	< 0.1	0.2
9B	10.4	21.1	-634.8	-437.8	< 0.1	0.3
9C	10.3	21.1	-507.6	-310.6	< 0.1	0.2
9D	11.3	20.8	-665.6	-468.6	< 0.1	0.3
<i>Downgradient Pea Gravel Wells</i>						
WW-10A	9.9	20.9	-554.6	-357.6	< 0.1	< 0.1
10B	9.0	20.8	-433.8	-236.8	< 0.1	0.3
10C	9.0	20.6	-351.9	-154.9	< 0.1	0.3
10D	10.5	20.7	-364.5	-167.5	< 0.1	1.0
<i>Downgradient A1 Aquifer Zone Wells</i>						
WIC-3	6.9	20.1	62.1	259.1	< 0.1	1.8
9	7.1	20.4	-16.4	180.6	0.2	8.6
10	8.4	20.4	-149.7	47.3	< 0.1	0.1
11	12.0	20.3	-245.0	-48.0	< 0.1	4.5
12	7.0	20.2	9.6	206.6	< 0.1	1.0
<i>Downgradient A2 Aquifer Zone Well</i>						
WIC-4	7.1	19.9	85.1	282.1	< 0.1	4.6

(a) In situ oxidation-reduction potential (ORP) measured against Ag/AgCl reference electrode.

(b) Eh calculated by adding 197 mV to the ORP measurement.

(c) Dissolved oxygen (DO) measurement at mid-screen or 15 ft below ground surface (bgs).

(d) DO measurement just below water level (~6 ft bgs).

Table D-3. Results of PHREEQC Calculation of Groundwater Saturation Indices^(a)

Well ID	Anhydrite	Aragonite	Brucite	Calcite	Dolomite	Fe(OH) ₃	Goethite	Gypsum	Melanterite	Portlandite	Siderite
<i>Upgradient A1 Aquifer Zone Wells</i>											
WIC-1	! 1.17	! 1.14	! 7.85	! 1.00	! 2.13	! 5.83	0.01	! 0.93	! 6.86	! 13.67	! 2.22
WIC-5	! 1.13	! 3.06	! 11.33	! 2.91	! 6.00	! 10.07	! 4.21	! 0.90	! 7.22	! 17.08	! 4.50
WIC-6	! 1.29	1.88	0.02	2.03	4.06	0.92	6.78	! 1.06	! 16.65	! 5.87	! 8.82
WIC-8	! 1.21	! 2.39	! 10.24	! 2.25	! 4.62	! 8.72	! 2.86	! 0.97	! 7.43	! 16.04	! 3.98
<i>Upgradient A2 Aquifer Zone Well</i>											
WIC-2	! 1.24	! 0.61	! 6.54	! 0.46	! 1.12	! 3.27	2.58	! 1.01	! 6.61	! 12.29	! 1.35
<i>Upgradient Pea Gravel Wells</i>											
WW-2	! 1.16	! 0.21	! 5.98	! 0.06	! 0.24	! 5.49	0.36	! 0.92	! 7.44	! 11.80	! 1.85
WW-7A	! 1.19	! 0.03	! 5.57	0.12	0.14	! 2.64	3.21	! 0.95	! 7.02	! 11.42	! 1.23
WW-7B	! 1.17	! 0.32	! 6.17	! 0.17	! 0.44	! 4.52	1.33	! 0.94	! 7.41	! 11.98	! 1.91
WW-7C	! 1.19	! 0.31	! 5.93	! 0.16	! 0.41	1.23	7.10	! 0.96	! 7.37	! 11.74	! 1.83
WW-7D	! 2.70	! 1.55	! 5.00	! 1.41	! 1.66	! 3.76	2.10	! 2.47	! 7.82	! 12.06	! 2.03
WW-11	! 1.20	! 0.21	! 5.92	! 0.06	! 0.22	! 3.30	2.56	! 0.96	! 6.65	! 11.73	! 1.01
WW-16A	! 1.31	! 0.58	! 6.28	! 0.43	! 0.88	! 3.39	2.46	! 1.07	! 6.79	! 12.20	! 1.43
WW-16B	! 1.23	! 0.40	! 6.29	! 0.25	! 0.59	! 3.27	2.58	! 0.99	! 6.66	! 12.14	! 1.20
WW-16C	! 1.20	! 0.08	! 5.69	0.07	0.02	! 2.35	3.51	! 0.96	! 6.42	! 11.51	! 0.67
WW-16D	! 1.18	0.39	! 4.68	0.54	0.98	! 2.10	3.76	! 0.95	! 6.79	! 10.50	! 0.57
<i>Reactive Cell Wells</i>											
WW-1B	! 1.62	! 0.45	! 0.57	! 0.31	! 0.65	! 2.99	2.85	! 1.38	! 7.56	! 6.49	! 1.77
WW-1C	! 2.49	! 0.94	! 0.72	! 0.80	! 0.63	! 2.14	3.71	! 2.25	! 7.54	! 7.62	! 1.36
WW-3	! 2.68	! 0.17	! 1.09	! 0.02	1.23	! 0.85	5.01	! 2.44	! 6.74	! 8.29	0.41
WW-4A	! 2.12	! 0.94	! 3.26	! 0.79	! 0.93	! 4.54	1.31	! 1.88	! 7.15	! 9.87	! 1.35
WW-4B	! 2.46	! 0.53	! 2.37	! 0.38	0.16	! 2.77	3.08	! 2.22	! 7.45	! 9.22	! 0.89
WW-4C	! 2.94	! 1.15	! 3.47	! 1.01	! 0.69	! 5.25	0.61	! 2.70	! 7.46	! 10.71	! 1.04
WW-4D	! 1.18	1.17	! 3.08	1.31	2.53	! 5.23	0.63	! 0.94	! 7.72	! 8.90	! 0.73
WW-5	! 2.57	! 1.05	! 3.11	! 0.90	! 1.02	! 4.49	1.37	! 2.33	! 7.81	! 9.81	! 1.65
WW-8A	! 2.12	! 0.31	! 2.54	! 0.16	0.49	! 2.85	3.00	! 1.89	! 6.81	! 9.28	! 0.36
WW-8B	! 2.48	0.05	! 1.24	0.20	1.51	! 1.28	4.57	! 2.24	! 7.10	! 8.28	0.06
WW-8C	! 2.75	! 0.37	! 1.94	! 0.22	0.86	! 0.66	5.21	! 2.52	! 7.03	! 9.14	0.01
WW-8D	! 2.28	0.29	0.61	0.43	1.41	! 0.38	5.48	! 2.04	! 8.28	! 5.85	! 1.08
WW-9A	! 1.91	! 0.84	! 2.64	! 0.69	! 0.93	! 4.56	1.29	! 1.68	! 7.02	! 9.02	! 1.32
WW-9B	! 2.78	! 0.94	! 2.14	! 0.79	! 1.00	! 4.09	1.76	! 2.54	! 6.88	! 8.69	! 0.43

Table D-3. Results of PHREEQC Calculation of Groundwater Saturation Indices (Continued)

Well ID	Anhydrite	Aragonite	Brucite	Calcite	Dolomite	Fe(OH) ₃	Goethite	Gypsum	Melanterite	Portlandite	Siderite
<i>Reactive Cell Wells (continued)</i>											
WW-9C	! 2.71	! 1.02	! 1.37	! 0.87	! 0.73	! 2.71	3.14	! 2.47	! 7.48	! 8.33	! 1.16
WW-9D	! 1.31	1.02	! 2.88	1.17	1.26	! 5.27	0.59	! 1.07	! 7.95	! 7.72	! 0.98
WW-12	! 2.15	! 1.71	! 6.06	! 1.57	! 2.30	! 2.14	3.71	! 1.92	! 5.81	! 12.83	! 0.75
WW-13A	! 2.11	! 2.56	! 6.12	! 2.42	! 4.14	! 3.29	2.56	! 1.87	! 6.86	! 12.76	! 2.69
WW-13B	! 2.25	! 0.60	! 1.83	! 0.45	! 0.09	! 4.71	1.13	! 2.01	! 7.52	! 8.60	! 1.25
WW-13C	! 2.95	! 0.97	! 1.37	! 0.82	! 0.48	! 3.53	2.32	! 2.72	! 7.59	! 8.45	! 0.96
WW-14	! 2.05	! 0.49	! 1.12	! 0.34	! 0.21	! 1.98	3.87	! 1.81	! 6.62	! 7.52	! 0.42
WW-17A	! 2.21	! 0.19	! 1.60	! 0.05	0.76	! 3.75	2.10	! 1.98	! 7.83	! 8.39	! 1.18
WW-17B	! 2.42	! 2.28	! 6.18	! 2.13	! 3.40	! 3.36	2.48	! 2.18	! 7.03	! 12.99	! 2.27
WW-17C	! 2.84	! 0.56	! 0.78	! 0.41	0.20	! 2.62	3.24	! 2.60	! 7.74	! 7.72	! 0.82
WW-17D	! 1.94	! 1.96	! 6.55	! 1.81	! 3.61	! 3.54	2.31	! 1.70	! 7.19	! 12.50	! 2.59
<i>Downgradient Pea Gravel Zone Wells</i>											
WW-10A	! 1.57	! 0.39	! 2.37	! 0.25	! 0.47	1.50	7.34	! 1.33	! 7.97	! 8.34	! 2.18
WW-10B	! 1.71	! 1.45	! 5.22	! 1.30	! 3.03	! 6.39	! 0.54	! 1.47	! 7.54	! 10.74	! 2.66
WW-10C	! 1.64	! 1.96	! 6.23	! 1.82	! 4.04	! 2.79	3.05	! 1.41	! 7.00	! 11.77	! 2.70
WW-10D	! 1.63	! 1.83	! 5.86	! 1.69	! 3.71	! 7.23	! 1.37	! 1.40	! 7.61	! 11.44	! 3.16
WW-15	! 1.98	! 2.41	! 6.66	! 2.27	! 4.68	! 8.21	! 2.35	! 1.74	! 7.77	! 12.42	! 3.56
WW-18A	! 1.66	! 0.77	! 3.31	! 0.62	! 1.29	! 4.53	1.32	! 1.43	! 6.67	! 9.21	! 1.15
WW-18B	! 1.55	! 0.07	! 2.11	0.08	! 0.45	! 2.97	2.88	! 1.31	! 6.99	! 7.43	! 0.87
WW-18C	! 1.95	1.49	0.29	1.64	1.68	! 0.65	5.21	! 1.72	! 12.05	! 4.03	! 3.96
WW-18D	! 1.43	0.92	! 1.40	1.06	! 1.15	! 1.13	4.73	! 1.19	! 9.04	! 4.05	! 2.05
<i>Downgradient A1 Aquifer Zone Wells</i>											
WIC-3	! 1.17	! 0.31	! 6.12	! 0.16	! 0.47	! 2.81	3.04	! 0.94	! 6.83	! 11.91	! 1.33
WIC-9	! 1.62	! 0.87	! 6.42	! 0.72	! 1.64	! 3.99	1.86	! 1.38	! 7.84	! 12.16	! 2.46
WIC-10	! 1.63	! 1.02	! 4.80	! 0.88	! 2.39	0.68	6.53	! 1.40	! 8.03	! 10.11	! 2.80
WIC-12	! 1.26	! 0.40	! 5.90	! 0.25	! 0.68	! 3.58	2.28	! 1.02	! 7.48	! 11.64	! 1.98
<i>Downgradient A2 Aquifer Zone Well</i>											
WIC-4	! 1.27	! 0.32	! 5.92	! 0.17	! 0.54	! 2.39	3.45	! 1.03	! 6.76	! 11.67	! 1.19

(a) Bold values are nonnegative, indicating saturation or oversaturation with respect to the referenced mineral phase.

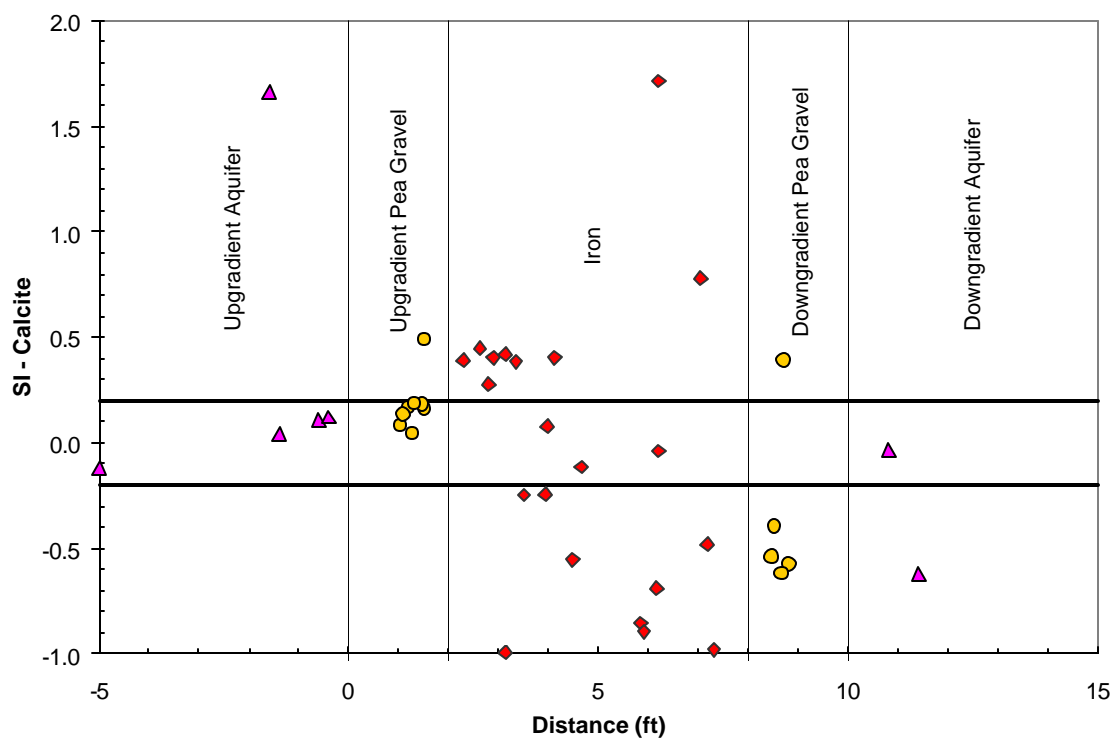


Figure D-5. Calcite Saturation Indices in Former NAS Moffett Field PRB

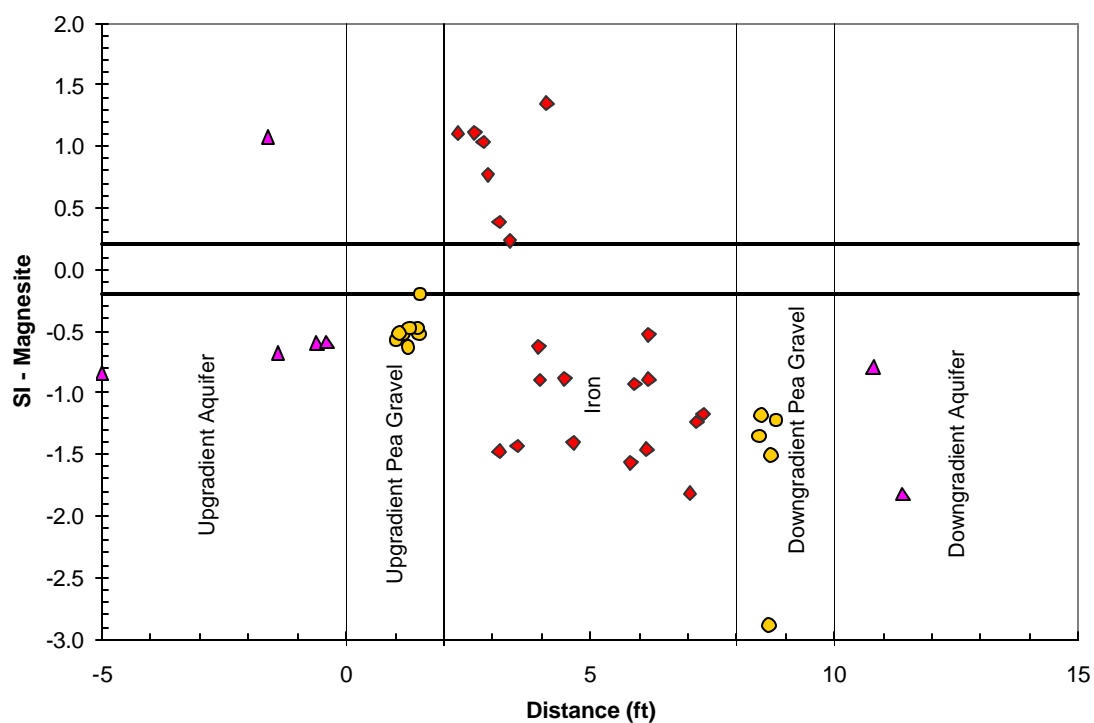


Figure D-6. Saturation Indices for Magnesite in Former NAS Moffett Field PRB

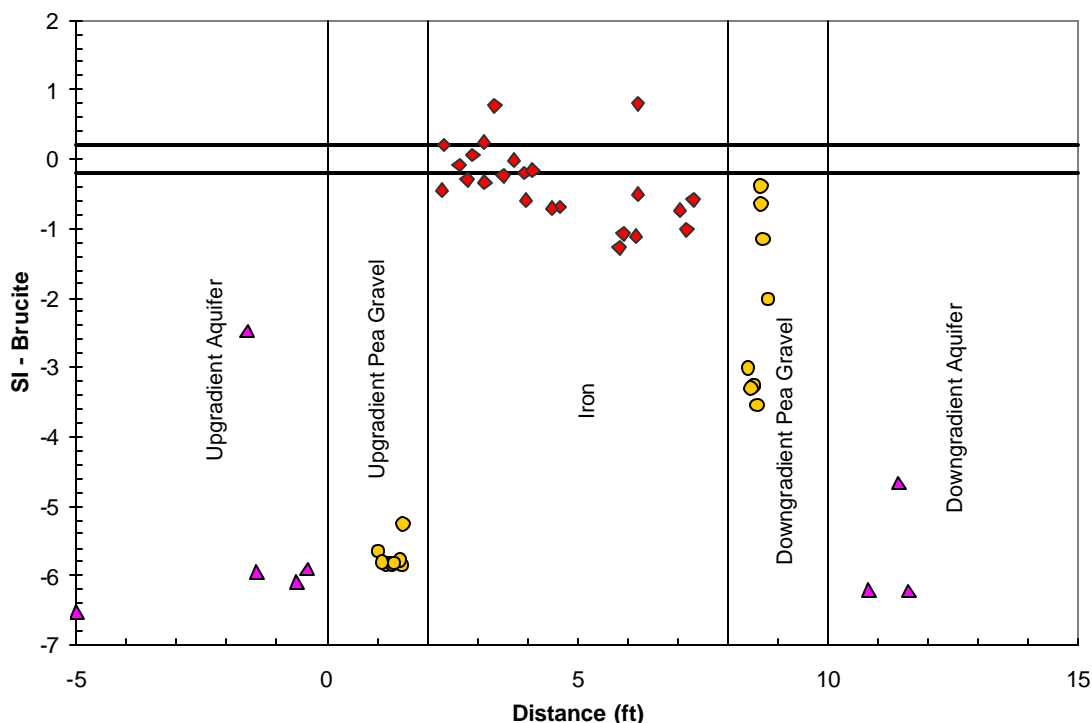


Figure D-7. Brucite Saturation Indices in Former NAS Moffett Field PRB

Siderite (FeCO_3), a ferrous carbonate mineral, is below saturation throughout most of the PRB (see Table D-3). However, data for iron are rather scant due to difficulty in detecting low concentrations (see Table D-2). Another ferrous mineral, melanterite ($\text{FeSO}_4 \cdot 7\text{H}_2\text{O}$), also was evaluated and determined to be undersaturated at all locations in the PRB. The stabilities of three ferric minerals were evaluated in a few cases where sufficient data for soluble iron are available. Goethite ($\alpha\text{-FeOOH}$) and “green rust” (not shown in Table D-3) tend to be oversaturated throughout the PRB, and amorphous ferric hydroxide [$\text{Fe}(\text{OH})_3$] tends to be undersaturated. Intermediate SI values between amorphous and crystalline phases may indicate that $\text{Fe}(\text{OH})_3$ is transforming to goethite over time.

Both gypsum ($\text{CaSO}_4 \cdot 2\text{H}_2\text{O}$) and melanterite are undersaturated at all locations, which suggests that the decline in sulfate levels in the reactive cell are not due to precipitation of sulfate minerals. A more likely explanation is that sulfate is reduced to sulfide due to low Eh. Additional calculations show that water in the reactive cell could be in equilibrium with marcasite (FeS_2) or mackinawite (FeS). SI calculations for sulfides could not be performed because sulfide was below detection in nearly all water samples.

D.3 Inverse Modeling

Equilibrium modeling indicates the type of precipitates that may form in the reactive medium. What is not known from field investigations is (1) how much of these precipitates are formed given the residence time (kinetics) of the groundwater in the reactive medium, and (2) how much of the precipitates formed stay in the reactive cell, as opposed to being transported away by the

flow. Inverse modeling attempts to answer the first question on how much of each type of precipitate is likely to be formed at the geochemical and flow (kinetic) conditions at a given PRB site. Inverse modeling conducted at the design stage requires both site characterization and column test data (i.e., inorganic parameter levels in column influent and effluent). Inverse modeling also may be conducted to interpret groundwater monitoring data for inorganic parameters (influent and effluent to the PRB) after the PRB is constructed.

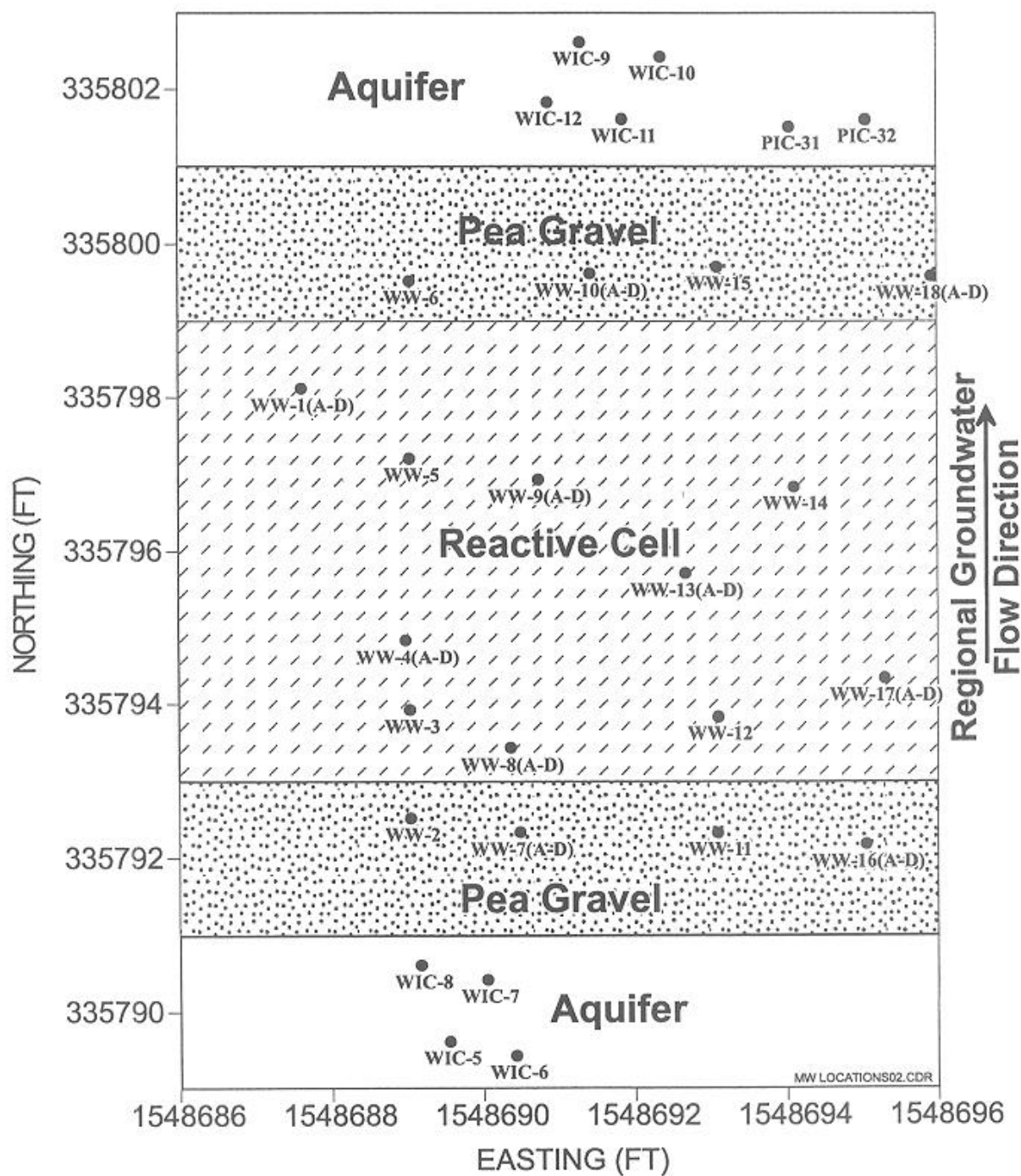
PHREEQC (Parkhurst, 1995) was selected for inverse modeling because it contains a large set of mass-balance equations, allows redox processes to be modeled, and accounts for uncertainties in the analytical data. One mode of operation finds the minimum number of inverse models needed to satisfy all of the constraints. Another mode of operation finds all sets of minerals that can satisfy the constraints, even if they are not minimal. Optionally, for each inverse model, minimum and maximum mole transfers that are consistent with the uncertainties are computed individually for each mineral in the inverse model.

In general usage, a flowpath is assumed to exist between two wells where concentration measurements would be taken (Plummer and Back, 1980). The water at the upgradient end of the flowpath is assumed to react with minerals, or in this case metallic iron, to produce the observed composition in the downgradient water. Using the difference in elemental concentrations between the two aqueous solutions, the model calculates the amounts of minerals, and in some cases gases, that either dissolved or precipitated along the flowpath.

Based on results of water-level measurements, downhole groundwater velocity measurements, and tracer tests at former NAS Moffett Field, water flows continuously from south to north (see Figure D-8). Although there may be localized flow patterns in individual wells, which may vary over time, it is assumed that on a time average water flows through the reactive cell in a south to north direction. Therefore, inverse models were run for two wells that are aligned along the flow direction. The wells selected for inverse modeling were located along the center line of the PRB. The upgradient pea gravel was represented by WW-7C and the reactive cell was represented by WW-8C, which is located approximately 0.5 ft into the iron zone (see Figure D-8). The elevations of both wells were the same (3.5 ft above mean sea level) for consistency.

The input parameters for wells WW-7C and WW-8C are given in Table D-2. Allowed phase transfers are listed in Table D-4. Note that zero-valent iron is only allowed to dissolve while all other phases are only allowed to precipitate. Methane is included as a sink for reduced-carbonate carbon. Chemical reduction of carbonate species to methane may not occur to a significant extent under the conditions that exist inside a PRB (i.e., without methanogenic bacteria present) (Drever, 1997). However, methane was considered as a possible sink because it was detected in some of the groundwater samples. In addition, other phases could have been included in the model runs, but were excluded to simplify the output.

Modeling results presented in Table D-5 indicate that four independent scenarios (i.e., models) could explain the data equally well. All four models are minimum sets which contain the fewest number of compounds needed to perform the calculations. Model 1 calls for dissolving 368 mg Fe/L of groundwater (mean value; see Table D-5 for minimum and maximum calculations).



* Easting and Northing coordinates correspond to the California State Plane Coordinate System for zone 403.

Figure D-8. Locations of Monitoring Wells Within and Near the Former NAS Moffett Field PRB

Table D-4. Phase Transfers Allowed in Inverse Modeling Run

Phase	Allowed Transfer
Fe Metal	dissolve
Fe(OH) ₃	precipitate
Siderite	precipitate
Marcasite	precipitate
Brucite	precipitate
Aragonite	precipitate
Magnesite	precipitate
CH ₄	precipitate

Table D-5. Results of Inverse Modeling Along a Flowpath Between the Pretreatment Zone and the Interface with the Reactive Cell at the Former NAS Moffett Field PRB

Mineral	Fe Metal	Ferric Hydroxide	Siderite	Marcasite	Brucite	Aragonite	Magnesite	Methane
Formula	Fe	Fe(OH) ₃	FeCO ₃	FeS ₂	Mg(OH) ₂	CaCO ₃	MgCO ₃	CH ₄
Model 1								
Mean	368	-299	-306	-137	-62	-367	NA	NA
Minimum	348	-336	-325	-137	-67	-371	NA	NA
Maximum	371	-267	-247	-131	-62	-366	NA	NA
Model 2								
Mean	348	-375	-183	-137	NA	-367	-89	NA
Minimum	328	-412	-202	-137	NA	-371	-98	NA
Maximum	351	-343	-124	-131	NA	-366	-89	NA
Model 3								
Mean	554	-939	NA	-137	NA	-367	-90	-25
Minimum	478	-986	NA	-137	NA	-371	-98	-28
Maximum	579	-793	NA	-131	NA	-367	-89	-17
Model 4								
Mean	713	-1,242	NA	-137	-62	-367	NA	-42
Minimum	636	-1,289	NA	-137	-68	-371	NA	-45
Maximum	737	-1,095	NA	-131	-62	-367	NA	-34

NA = not applicable, because the species was not considered in the model.

Concentrations are in mg/L.

Positive numbers imply dissolution; negative numbers imply precipitation.

Concomitant to dissolution and oxidation of the iron, different amounts of ferric hydroxide, siderite, marcasite, brucite, and aragonite precipitate. The relationship between the amount of iron dissolved and the total amount of iron present can be calculated if values for porosity and density of iron are known. Using an estimated porosity of 0.65 and density of 8 g/mL, the fraction of dissolved iron in Model 1 (368 mg Fe/L) is equivalent to 85 mg Fe dissolved per kilogram iron metal (i.e., 85 ppm).

The other three models differ by substitutions with one or two compounds. Model 2 requires magnesite to precipitate instead of brucite and consumes slightly less iron than Model 1. Model 3 does not require either siderite or brucite to precipitate, but calls for formation of methane. Similarly, Model 4 also forms methane, but differs from Model 3 by precipitating brucite instead of magnesite. Siderite is absent in both Model 3 and Model 4. Normally, the model chosen as the “most correct” would be based on actual observations of precipitates in core samples. In reducing environments, analysis of methane in water samples also would be an indicator. Due to the low abundance of precipitates in the core samples, the analyses do not definitively confirm or refute several predictions invoked by inverse modeling. First, corrosion of the iron is not obvious from microscopic inspection of the iron grains. Also, iron oxides (or oxyhydroxides) are ubiquitous in the core samples as well as in the virgin iron and therefore it is difficult to confirm whether precipitation of ferric hydroxide has occurred. In a few samples, $\text{Fe}(\text{OH})_3$ and FeOOH were suspected. Sulfur compounds thought to be present in reduced form such as FeS_2 were suspected in the upgradient iron. Aragonite was confirmed by x-ray diffraction. However, siderite, brucite, and magnesite were not confirmed by any analysis methods. Magnesium was believed to be associated with calcium, which could imply precipitation of high-Mg calcite along with pure calcium-aragonite. Methane was detected in the reactive cell, but concentrations did not tend to exceed 2 mg/L, which is substantially below the values predicted in Models 3 and 4 (25 mg/L and 42 mg/L, respectively; see Table D-5). It should be noted that the solubility limit of methane in water is 25 mg/L (at 1 atm partial pressure). Therefore, Model 4 can be rejected on the grounds that the methane generated would exceed saturation and such high levels are not borne out by field measurements. Results from the forward modeling (Section D.2) tend to support the possibility of aragonite (or calcite), brucite, magnesite, and methane. Due to the paucity of iron data, forward modeling was not able to calculate saturation indices for any of the iron compounds. Because none of the predicted species shown in Table D-5 can be ruled out, it must be assumed that Models 1, 2, and 3 provide plausible explanations for the evolution of groundwater inside the reactive cell.

In addition to the kinds of minerals that potentially precipitate within the reactive cell, it is useful to predict the impact that precipitation would have on the porosity of the granular iron. Table D-6 shows the results of volume calculations based on the mass balance calculations in Table D-5. The net porosity change is a loss of approximately 0.028% based on Models 1 and 2, and a porosity loss of approximately 0.035%, based on Model 3. These porosity changes are based on one pore volume of water. To estimate the total accumulation of particulate inside the PRB over time, the recharge rate within the precipitation zone must be calculated. (It is assumed that the precipitation takes place within the first 0.5 ft of the reactive cell.) Groundwater flow-rate in the PRB was estimated to be between 0.2 and 0.5 ft/d (Battelle, 1998). Therefore, this zone takes between 1 day and 2.5 days to recharge. If the precipitation rate is 0.030% of the initial pore volume per recharge period, then the loss of pore space is between 4 and 11% per year. In contrast, core sampling at former NAS Moffett Field after 16 months of operation did not reveal very significant levels of precipitation. The amount of aragonite precipitated was calculated to be 0.2% during the operational period (Battelle, 1998). Because mineral matter did not seem to be accumulating in the iron, it is possible that colloidal-size precipitates are either migrating downgradient with the flow, or gravity-settling within the PRB. If the level of precipitate accumulation were to be as high as predicted by inverse modeling, the effect on hydraulic

Table D-6. Results of Inverse Modeling Along a Flowpath Between the Pretreatment Zone and the Interface with the Reactive Cell at the Former NAS Moffett Field PRB

Mineral	Fe Metal	Ferric Hydroxide	Siderite	Marcasite	Brucite	Aragonite	Magnesite	Net Change in Porosity
Density (g/mL)	8	~4	3.96	4.89	2.39	2.95	3.0	NA
<i>Model 1</i>								
Mean	46	-75	-77	-28	-26	-125	NA	-0.028%
Minimum	43	-84	-82	-28	-28	-126	NA	-0.030%
Maximum	46	-67	-62	-27	-26	-124	NA	-0.026%
<i>Model 2</i>								
Mean	44	-94	-46	-28	NA	-125	-30	-0.028%
Minimum	41	-103	-51	-28	NA	-126	-33	-0.030%
Maximum	44	-86	-31	-27	NA	-124	-30	-0.025%
<i>Model 3</i>								
Mean	69	-235	NA	-28	NA	-125	-30	-0.035%
Minimum	60	-246	NA	-28	NA	-126	-33	-0.037%
Maximum	72	-198	NA	-27	NA	-124	-30	-0.031%

NA = not applicable, because the species was not considered in the model.

Concentrations are in μL per liter of pore space, or parts per million by volume (ppmv).

Positive numbers imply dissolution (increased pore space); negative numbers imply precipitation (loss of pore space).

conductivity could be measurable. Hydrologic modeling has shown that hydraulic conductivity of the reactive cell has to reduce by more than half before any significant hydrologic change occurs (Battelle, 1998).

The rate of iron corrosion calculated by the inverse model also can be compared directly to experimental work by Reardon (1995). In Reardon's study, corrosion rates were measured by monitoring hydrogen pressure increases inside sealed vessels containing granular iron (Master Builders), water, and several salts. After an initial rise in hydrogen pressure, steady state rates began to develop, which were found to depend on the solution composition. Average long-term corrosion rates were close to 0.5 mmol/kg/d, or 30 mg/kg/d. For comparison, Model 1 in this study predicts that 85 mg/kg are corroded along a flowpath in the former NAS Moffett Field reactive cell. If it is again assumed that the groundwater flowrate is between 0.2 and 0.5 ft/d in the reactive cell, then the corrosion rate predicted by inverse modeling is between 34 and 85 mg/kg/d. Thus, the modeling results in this section and Reardon's experimental data agree at the lower flowrate estimate. However, there are a number of differences between the conditions in the former NAS Moffett Field PRB and the Reardon experiment that may make this agreement coincidental. Most notable is that the PRB at former NAS Moffett Field contains Peerless iron, whereas Master Builders iron was used in Reardon's (1995) study. In addition, particle sizes of the iron were somewhat different and solution temperature and composition were different. Nevertheless, the fact that corrosion rates determined by modeling field data and the experimental study are close could suggest that the fundamental corrosion processes affecting each study are related.

Inverse modeling thus is able to provide a method for quantification of how much precipitate is likely to be formed in the reactive medium over time. The question that still remains unanswered is how much of this precipitate stays in the reactive cell and how much is carried away with the groundwater flow. Additional research is required in this area to be able to make accurate longevity predictions for a PRB system.

D.4 References

Allison, J.D., D.S. Brown, and K.J. Novo-Gradac. 1991. *MINTEQA2/PRODEFA2, A Geochemical Assessment Model for Environmental Systems: Version 3.0 User's Manual*. EPA/600/3-91/021. U.S. Environmental Protection Agency, Office of Research and Development, Washington, DC. 106 pp.

Battelle. 1998. *Performance Evaluation of a Pilot-Scale Permeable Reactive Barrier at Former Naval Air Station Moffett Field, Mountain View, California*. Prepared for Naval Facilities Engineering Service Center, Port Hueneme, CA. November 20.

Battelle. 1999. *Draft Final Report: Design, Construction, and Monitoring of the Permeable Reactive Barrier in Area 5 at Dover Air Force Base*. Prepared for Tyndall Air Force Base, FL. November 8.

Drever, J.I. 1997. *The Geochemistry of Natural Waters: Surface and Groundwater Environments*, 3rd ed. Prentice-Hall, Inc., New York, NY.

Mackenzie, P.D., D.P. Horney, and T.M. Sivavec. 1999. "Mineral Precipitation and Porosity Losses in Granular Iron Columns." *Journal of Hazardous Materials*, 68: 1-17.

Odziemkowski, M.S., T.T. Schuhmacher, R.W. Gillham, and E.J. Reardon. 1998. "Mechanism of Oxide Film Formation on Iron in Simulating Groundwater Solutions: Raman Spectral Studies." *Corrosion Studies*, 40(2/3): 371-389.

Parkhurst, D.L. 1995. *User's Guide to PHREEQC - A Computer Program for Speciation, Reaction-Path, Advective-Transport, and Inverse Geochemical Calculations*. USGS 95-4227 Lakewood, CO.

Plummer, L.N., and W. Back. 1980. "The Mass Balance Approach: Applications to Interpreting the Chemical Evolution of Hydrologic Systems." *American Journal of Science*, 280: 130-142.

Reardon, E.J. 1995. "Anaerobic Corrosion of Granular Iron: Measurement and Interpretation of Hydrogen Evolution Rates." *Environ. Sci. Technol.*, 29(12): 2936-2945.

Sass, B., and A. Gavaskar. 1999. "Evaluation of Longevity Factors at Three Permeable Barrier Sites Based on Geochemical Characteristics." Abstract for the *Second International Conference on Remediation of Chlorinated and Recalcitrant Compounds*. Monterey, CA, May 22-25, 2000. Abstract submitted August 9.